Effective and Adaptive Energy Restoration in WRSNs by a Mobile Robot

by

Osama Ismail Aloqaily

Thesis submitted to the University of Ottawa

In partial fulfillment of the requirements For the

Ph.D. degree in Electrical and Computer Engineering

School of Electrical Engineering and Computer Science

Faculty of Engineering

University of Ottawa

⋆ The Ph.D Program is a joint program with Carleton University, administered by Ottawa-Carleton Institute for Electrical and Computer Engineering

Abstract

The use of a mobile charger ($\mathcal{MC}$) is a popular method to restore energy in wireless rechargeable sensor networks(WRSN), whose effectiveness depends critically on the recharging strategy employed by the $\mathcal{MC}$. In this thesis, we propose a novel on-line recharging mechanism strategy, called *Continuous Local Learning* (**CLL**), which predicts the current energy level of the sensor nodes and dynamically updates the schedule to visit the nodes before their batteries get depleted. The strategy is based on simple computations done by the $\mathcal{MC}$ with little memory requirements, and the communication is strictly local (between the $\mathcal{MC}$ and neighbouring nodes).

In spite of its simplicity, this strategy was experimentally shown to be highly *effective* in keeping the network perpetually operating, ensuring that the number of sensing holes (i.e., non-operational sensors due to battery depletion) and their duration are very small at any time, and achieving immortality (i.e., no node ever becoming non-operational) under many settings even in large networks.

We also studied the *flexibility* of **CLL** under a variety of network parameters, showing its applicability in various contexts. We particularly focused on network size, data rate, sensors' battery-capacity, and speed of the $\mathcal{MC}$, and studied their impact on operational size and disconnection time under a wide range of values. The experiments indicate the fact that the effectiveness of **CLL** holds under all considered settings.

We then compared the proposed solution with the popular class of *static* strategies since they share with **CLL** the features of simplicity, strict local communication

and small memory and computational requirements. Experimental results showed that **CLL** outperforms these strategies in effectiveness. Not only is the number of sensors that are operational at any time higher under **CLL**, but the average duration of a sensing hole is also significantly lower.

Finally, we studied the *adaptability* of **CLL** to a network's sudden changes, in particular changes in data rate, which we call spikes. We studied the impact of spikes parameters on the performance of **CLL**. Experimental results showed that **CLL** is capable of reacting and adapting to these sudden changes with only a slight increase in non-operational size and disconnection time.

Acknowledgements

All praises and glory be to **Allah** who helped me to achieve this work.
Prophet Mohammad(Peace be upon him) said **" *He who does not thank the people is not thankful to Allah*"**.
My first and most thanks go to my supervisors Prof.Nicola Santoro and Prof.Paola Flocchini. Thank you for all the great opportunities and experiences that I have received throughout the journey of the Ph.D. I am in debt to you. *It was an honor both to be taught by and work with two of the most senior scientists in the field.*

Special thanks to my mother. Your guidance, support, supplications, and prayers throughout my life are greatly appreciated, and I honestly would not have been able to do this without you. If it were not for your unwavering faith in me, I would not have never come this far. I can't thank you enough for that. This success has been possible because of you!!

I owe a huge debt of gratitude and indebtedness to my brothers, my family in-law and friends, I am delighted to have you in my life, and my success is your success!!

To little miss Reem, Ayoub, Mohammad, and Auwn, thank you for being the joy and bright light since you came into my life.. I am breathing because of you.

Last but not least, to my beloved wife, Ala, I don't have enough words, and I don't

think I can ever be grateful enough for everything you have done over the past years. You never questioned my decisions; you always believed in me when things were tough, and you were always there to provide sanity and lift my spirits.

DEDICATION

This Thesis is dedicated

To the soul of my father, may Allah shower his soul with mercy and forgiveness.

To my mother, may Allah give her long life.

To my beloved wife and children,

Auwn, Mohammad, Ayoub , and Reem.

With all my love...

Osama

Contents

List of Figures

List of Tables

List of Symbols

BS	Base Station
$d_{i,j}$	Distance between sensor s_i and sensor s_j
Dis	Average Disconnection Duration
E_{max}	Sensor Battery Capacity
E_{MC}	$\mathcal{MC}$ Battery Capacity
h	Number of Sensing Holes
J	Joules
kJ	kilo-Joule
m/s	Meter per Second
$\mathcal{MC}$	Mobile Charger
min	Minutes
n	Network Size (Number of Sensors)
P	Energy Consumption Rate
W	Watts(Joule/second)

$\mathcal{S}$	Set of Sensors
$S_{Exp}(s,t)$	Expected State of Charge of sensor (s) at time (t)
SS	Service Station
$T_{E_{max}}$	Sensor's battery life time
ν	$\mathcal{MC}$ velocity
Δ	Recharging Rate
δ	Expected Consumption Rate
ϵ	Energy Consumption Constant
η	Charging Efficiency
θ	Maximum Charging Threshold
λ	Data Rate
τ	Non-operational Threshold

Chapter 1

Introduction

1.1 Energy Restoration Problem

Wireless sensor networks (WSNs) consist of small devices, called *nodes*, deployed in a targeted area to monitor, collect, and report information on the surrounding environment. They have been used in a wide variety of industrial, military, and civilian applications (e.g., see [1,2]). Due to their versatility and low cost, WSNs represent the best candidate for many applications including smart-city applications [3–5], health applications [6,7], environment applications [8,9], localization and target tracking applications [10,11], intruder tracking applications [12,13], and barrier monitoring applications [14,15].

The main problem with WSNs is their limited lifetime. The network devices are mainly powered by batteries of limited (usually small) capacity. As each (sensing and communication) operation performed by a node consumes energy, its battery eventually becomes depleted and the node stops being operational, creating a *sensing hole* in the network and possibly a *coverage hole* in the monitored area. Thus, unless remedial action is taken, the coverage decreases until the entire network ceases to function.

This power consumption problem, whose existence is seen as a major obstacle to the use of WSNs in a wide range of applications [16], has been long known in the sensor network community, and many approaches have been studied and proposed to alleviate it if not solve it.

The earliest approaches to extend the WSN lifetime focused on techniques aimed at improving energy conservation and efficiency (e.g., duty cycling, low-cost communication, etc.) so as to reduce the energy consumption of the sensors and prolong the network lifetime (e.g., [17, 18]); these approaches however only delay the inevitable demise of the network.

To prolong the life of the network almost indefinitely it is indeed necessary to restore the depleted energy in the network. Various approaches to energy restorations have been considered in the literature.

The first type suggests the enhancement of each node with additional capabilities so as to render it able to recharge its own battery. An example of such approach, which we shall call *endogenous*, is the proposal to provide the sensors with *energy harvesting* equipment, enabling them to collect energy from surrounding resources (e.g., [19, 20]). Another example of endogenous approach is the proposal to equip each node with *mobility* and location capabilities so that it can move to a recharging station when the battery level becomes too low (e.g., [21, 22]). Both endogenous approaches require sensor nodes of substantially increased complexity (and thus cost); this fact severely limits their feasibility and applicability.

An important popular alternative is an approach that does not require more complex sensors but rather relies on an *exogenous* (i.e., external) element. More precisely, this approach proposes the use of a robot or vehicle to act as a *mobile charger* ($\mathcal{MC}$) and move around the WSN area to replenish the energy of sensors in need. This exogenous approach, intensively studied from a theoretical point of view, is quite important also from a practical point of view due to the recent developments in non-radiative *wireless*

energy transfer technology (e.g., [23–26]); once this technology is fully developed, the $\mathcal{MC}$ should be able to recharge a node battery without the need for wires and plugs, with energy efficiently generated elsewhere. Not surprisingly, *wireless rechargeable sensor network* (WRSN) represents the emerging technology of WSN (e.g., see [27]).

The idea behind this approach is simple: the mobile charger, provided with access to an unlimited source of energy[1], moves continuously through the network, wirelessly recharging nodes if found to be in need.

This approach can provide perpetual operation of the WSN since even depleted (non-operational) node will be operational again, after a time of disconnection. Clearly, the goal of this approach is both to maintain a large number of the nodes operational at any time and to ensure that, whenever a node becomes inactive because of battery depletion, the state of inactivity (i.e., the sensing hole) lasts for a very short time. How well this goal is achieved in a network can thus be measured in terms of the (average) number of active nodes at a given time, called *operational size*, and the (average) duration of a sensing hole, called *disconnection time*.

These two measures and, hence, the *effectiveness* of the approach, depend critically on the *recharging strategy* employed to decide which node should be serviced next by the $\mathcal{MC}$ and the amount and type of information required for making such decisions. Indeed, with an appropriate strategy, it is possible to maintain a substantial part of the network operational at all times, with possibly different nodes operational at each time (e.g., [28–32]). Under some special conditions, it is even possible to totally remove the occurrence of sensing holes: each node will always have an energy level above a minimum threshold so that the network remains fully operational at all times; this ideal or optimal level of effectiveness is also referred to as *immortality* [33, 34].

There is a large variety of recharging strategies proposed and investigated in the literature. Despite their differences, they can all be classified as either *static* or *dynamic*.

[1] e.g., though a recharging station, or provided with renewable energy resources, etc.

In a *static* strategy, the recharging order is predetermined, typically pre-computed at the base station, and the $\mathcal{MC}$ always visits the nodes (recharging the battery if needed) periodically according to this order (e.g., [30, 33, 35, 36]). Because of their nature, these strategies are also called *periodic protocols*. Except for the initial pre-computation of this order, no other global computation is performed, hence these strategies are simple, highly scalable, and require very limited (or no) global communication. Furthermore, the $\mathcal{MC}$ needs to have only very simple computational power and memory; hence these strategies can be implemented using very weak (computation and communication wise) robots. On the other hand, the recharging order never changes regardless of the energy consumption pattern; in other words, these strategies are "blind" to future changes.

A *dynamic* strategy (e.g., [32, 37–47]), on the other hand, is one that continuously modifies the recharging order to adapt to changes in the energy consumption of the sensors. The clear advantages of dynamic strategies is their adaptability; the typical disadvantage is the continuous intensive communication usually involved.

There exists a very extensive literature on energy restoration in WRSN proposing both static and dynamic strategies developed under a wide variety of assumptions on the network conditions.

The initial investigations have mainly been *offline* studies (e.g., [34, 48–52]); i.e., they investigate in a centralized way (TSP-like) optimization problems involving (and hence requiring) global information about the network in its entire lifetime. These investigations are mainly of mathematical interest. From a practical point of view, in addition to requiring communication overhead and intensive computation capabilities, their results on the performance of the proposed strategies are valid only if the assumed system conditions persist in the future. In other words, they have a basic lack of adaptability, and could suffer substantial performance degradation in case of changes in the network conditions [53].

Of a different nature are *on-line* methods (e.g., [28, 32, 37–47, 54]), i.e., techniques

that do not require complete global a-priori knowledge, and where decisions are made based solely on the past and the current network status. Hence on-line strategies could be potentially used in real systems. The on-line recharging strategies proposed and examined in the literature typically fall into two classes.

In the strategies of the first class, the nodes report their energy levels periodically (e.g., [32, 37, 39, 43]) or when the battery level reaches a certain threshold, as in the case of *on demand* policies (e.g., [31, 40, 44, 45, 55–60]). This information is sent to the base station which will compute the order in which nodes should be recharged and communicate it to the mobile charger (e.g., [55, 57]), or to the (moving) mobile charger directly (e.g., [31, 32, 39, 40, 44, 45, 58, 60, 61]). The need to (periodically or on-demand) report information to the base station noticeably increases the communication costs [28]. These communication overheads may be even greater when the information has to be sent directly to the mobile charger: since it is moving, this would require flooding or tracking its location [62], the latter being a complex and expensive operation. We refer to these strategies[2] as *global on-line protocols*. Clearly, they require high amounts of communication, making them quite unpractical even in medium-sized sensor networks [29]. Also, they usually need to compute the solution of complex optimization problems on an ongoing basis.

The other class of on-line strategies is the one where the decision requires only local interaction between the $\mathcal{MC}$ and nodes in close proximity. These *local* (or, *distributed* [63]) *on-line protocols* have been much less investigated. Moreover, the few existing studies consider only specific network arrangements (e.g., linear [64] or circular [29, 65]) or do not examine perpetual recharging (e.g., focus on the time elapsed until the first node depletes its battery [54]).

The current state of research on on-line dynamic recharging strategies raises important questions.

Clearly, the acquisition of real-time energy data is extremely useful regarding the

[2] These strategies are called “global knowledge protocols" in [28].

effectiveness of the recharging strategy. At the same time, the large communication overhead incurred by global on-line protocols makes scalability impossible. Hence, a natural research question is as follows: Can a highly effective strategy (e.g., leading to immortality) be devised where the acquisition of energy data is done without long distance communication, in a fully localized way? In other words, can a local (i.e. distributed) on-line strategy achieve such a goal?

The extreme simplicity of static strategies offers a multitude of advantages, including highly scalability, very limited (or no) communication, $\mathcal{MC}$ with very simple computational power and memory. They also have been shown to be rather effective in some settings. Hence, a natural research question: Is it possible to improve upon the effectiveness of static strategies while keeping the advantages they offer?

In this thesis, we provide a positive answer to these questions.

1.2 Methodology

In this thesis we used the following methodology. First, we studied the literature related to the problem and determined a gap in the proposed solutions. Second, we designed an online strategy that would fill that gap. Third, we verified the effectiveness of the proposed strategy using a discrete event simulator developed in MATLAB. Fourth, we analyzed the results to show the effectiveness, flexibility and adaptability of **CLL**. Finally, we assessed the advantages of **CLL** with respect to the class of static strategies by comparing its effectiveness and adaptability with the static strategy of minimum travel cost.

1.3 Contributions

We propose a novel local on-line dynamic strategy for energy restoration, called *Continuous Local Learning* (**CLL**); unlike the existing local on-line strategies, it provides perennial functioning of a WRSN regardless of its topology. This strategy operates under dynamic network conditions without any a-priori knowledge of the network, uses low-complexity computations by the mobile charger with little memory requirements, and requires only local communications between the $\mathcal{MC}$ and neighbouring nodes. In other words, while not static, it shares all the advantages of the static strategies.

We experimentally studied the effectiveness, flexibility and adaptability of the proposed recharging strategy. Our results show that this strategy is flexible, adaptive and highly effective; it reaches immortality in a large variety of settings and outperforming the static strategies in effectiveness.

In the proposed strategy, instead of letting the nodes request recharge when in need or periodically report their energy levels (directly or through a base station), the $\mathcal{MC}$ gathers the battery energy levels of the neighbouring nodes as it moves through the network. This eliminates long distance communications between the $\mathcal{MC}$ and the nodes, and works without the need for clustering, cluster management, and cluster-head elections.

The collected data are used by the $\mathcal{MC}$ to determine online the dynamics of the network nodes and to build a fully dynamic recharging schedule. More precisely, the data are used by the $\mathcal{MC}$ to *predict* the time when a node's battery would need recharging, and this information is used to determine, with a simple heuristic, which node should be recharged next. It is during the movement that the $\mathcal{MC}$ updates the data from the nodes it comes in contact with. This mechanism provides a continuous local gathering of energy information and, in turn, a dynamic energy depletion prediction.

Our strategy does not require any a-priori knowledge of the network. Initially, the $\mathcal{MC}$ explores the network in a preliminary phase, collecting data from the encountered nodes and their neighbours, and servicing those that need recharging. At the end of this phase, the $\mathcal{MC}$ prediction starts taking place.

This predictive strategy offers many advantages (fully distributed, local communication, local learning, simple heuristic). Our interest is obviously to determine how effective this simple strategy is.

The main contributions include the following.

- We studied the effectiveness of **CLL** and showed that it is highly effective in keeping the network perpetually operating, often achieving immortality or near-immortality. In particular, the experimental results indicate that, under the same parameter values where immortality has been examined in the literature, the system becomes *immortal* even in networks of considerably larger size.

- We studied the flexibility of **CLL** under a variety of network parameters, showing its applicability to various contexts. We particularly focused on four parameters, network size, data rate, sensors' battery-capacity, and speed of mobile charger, and studied their impact on operational size and disconnection time under a wide range of values. The experiments indicate the fact that the effectiveness of **CLL** holds under all considered settings.

- We compared the effectiveness of our strategy with those of static strategies under the same parameters. The comparison was performed by focusing on the static strategy, denoted by **H**, that consumes the minimal amount of travelling energy.

  In all settings, **CLL** outperforms **H** in effectiveness. Not only the number of sensors that are operational at any time is higher under **CLL**, but also the average duration of a sensing hole is also significantly lower.

  Moreover, we performed the comparison of **CLL** and **H** in situations where, for

a group of sensors located around the Base Station (BS), the energy consumption rate is much higher than the rest. We showed that, in all cases, **CLL** outperforms **H** , and it does so more and more significantly as the difference between the energy consumption of the two groups grows.

- We examined the effectiveness and adaptiveness of **CLL** to situations when the number of sensing, receiving and transmitting operations unexpectedly and suddenly increase, creating a spike in the network energy consumption. The experiments have shown that **CLL** is able to cope with the sudden changes in data rates with minimal loss of effectiveness (e.g., in the worst spike setting, only 0.76% more nodes might be non-operational). Moreover, we compared the impact of the occurrence of spikes on **CLL** with respect to that it has on the static recharging strategy **H** ; the experiments indicated that **CLL** outperforms **H** also in presence of spikes.

1.4 Organization of the Thesis

The thesis is organized as follows:

- In Chapter 2, we present the literature review of the research efforts to solve the energy restoration problem in WSN.
- In Chapter 3, we describe the energy restoration problem, the proposed system model, the simulation environment and the performance metrics.
- In Chapter 4, we introduce the Continuous Local Learning Strategy, which is online, fully distributed, uses only local communication between the $\mathcal{MC}$ and neighbouring nodes, operates under dynamic network conditions without any a-priori knowledge of the network, is based on simple computations by the $\mathcal{MC}$ with little memory requirements, and is highly effective in keeping the network

perpetually operating and achieving immortality even in large networks. A paper containing part of these results appeared in [66].

- In Chapter 5, we study the flexibility of the Continuous Local Learning Strategy under a wide variety of ranges of the network parameters, showing its applicability to various contexts. The focus of the chapter is, in particular, on four parameters that distinguish the applications, network size (number of sensors), data rate, sensor's battery-capacity, and speed of mobile charger used to replenish energy. A paper containing part of these results appeared in [67].

- In Chapter 6, we compare the Continuous Local Learning Strategy and one of the classical periodic recharging strategies, based on the Hamiltonian Cycle. The effectiveness of the Continuous Local Learning solution and that of the Hamiltonian solution are analyzed under a range of settings, where we consider homogeneous sensors that have the same range of data rates. In addition, we compare **CLL** and **H** when the sensors have heterogeneous consumption, that is, the sensors have variable data rates based on their location in the network. We study two scenarios: The first scenario is when the data rate of the sensors around the BS is double the data rate of the other sensors. The second scenario is when the data rate of the sensors around the BS is 5 times higher than the data rate of the others.

- In Chapter 7, we study the effectiveness and adaptiveness of the Continuous Local Learning strategy to cope with sudden changes in the sensors' data rates, spikes. We describe the spike parameters (occurrence, intensity, spread, and duration) and discuss the impact of each one of these parameters on the performance of **CLL**. We also compare the performance of **CLL** with that of **H** in presence of spikes.

- In Chapter 8, we summarize the thesis contributions and discuss the future directions of this research.

Chapter 2

Related Work

In this chapter, we review the existing approaches to solving the energy problem in wireless sensor networks. We start with a brief overview of earlier research on energy saving and conservation. We then review the existing energy restoration techniques, both endogenous (i.e., endowing each node with additional capabilities) and exogenous (i.e., using an external element). In particular, we give a comprehensive overview of the research on exogenous energy restoration by wireless recharging using a mobile charger ($\mathcal{MC}$). In Figure 2.1, the classification of energy restoration strategies is shown.

2.1 Energy Saving

The study of the energy problem of sensors and its impact on sensor lifetime began early after the introduction of Wireless Sensor Networks(WSNs). Earlier work focused on saving energy by one of two approaches: scheduling operational times, and finding efficient routing protocols and transmission mechanisms [68, 69]. These approaches reduce the energy consumption and prolong WSN lifetime; however, they cannot save the WSN from inevitable demise. We will briefly discuss those energy-saving approaches.

The first approach in [70–73] suggested the activation and deactivation of the sensors over time alternatively. In particular, [70] introduced dynamic sleep scheduling based on Analytical Hierarchy Process (AHP) to improve the network's lifetime; they considered three factors, residual energy, coverage of sensing area, and distance to cluster-head to decide which node is to sleep. Wu et al. [71] formulated a non-convex optimization problem to reduce the expected energy consumption using sleep/wake schedule. The authors proposed a sleep scheduling scheme based on a hierarchy process to balance energy consumption in battery-powered nodes. In [72], the authors proposed algorithm to find the number of sensors required to achieve the best coverage; sensors uses the algorithm to alternate between sleep and active mode, thus prolonging the sensor's lifetime and preserving the coverage level.

In the second approach, the authors of [68, 69, 74–78] proposed hierarchy routing protocols and communication mechanisms to reduce energy consumption in WSN. In [68,69,74], they suggested the selection of a Cluster Head (CH) randomly in [68], based on residual energy and transmission cost in [69], or in a centralized way at the Base Station (BS) in [74]. The CH is an intermediary between the BS and the sensors in the cluster, and it is responsible for transmitting data to the BS. The authors of [75, 76] suggested the use of a structure for transmission routes between sensors and the BS, [75] suggested a chain structure, while [76] proposed a tree structure where each node sends only to its parent node.

In [79], the authors proposed the combination of sleep scheduling and tree based clustering to save WSN energy. Each node sends only to one node, (the parent), toward the cluster head. Nodes in this technique sleep for a time, and when they wake up, they transmit only to the parent.

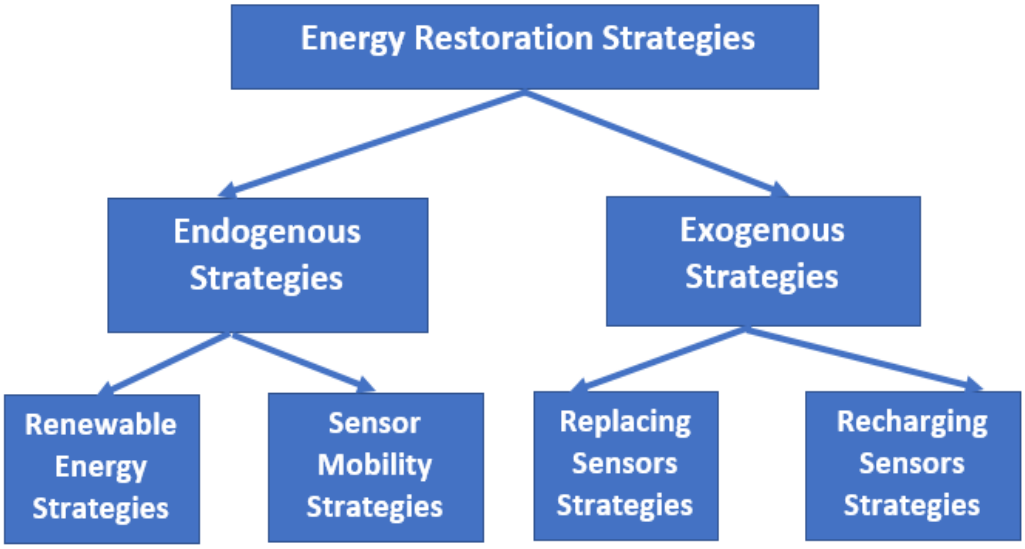

Figure 2.1: Classification of energy restoration strategies.

2.2 Endogenous Restoration

This section describes the literature where the energy restoration problem is solved by enhancing the capabilities of the sensors, which then become responsible for solving the problem themselves. Those enhancements include energy harvesting equipment, and mobility.

2.2.1 Restoration by Energy Harvesting

Many works in the literature address energy restoration problems in WSNs, either using a single renewable energy resource or combining renewable energy resources with other energy restoration methods. In this section, we introduce both strategies in different subsections.

2.2.1.1 Single Renewable Resource

Energy restoration using renewable resources has been studied in the literature intensively. For example, in [80–85] the authors suggested the use of various renewable resources to sustain the WSN with the required energy. In particular, the authors of [83] proposed the use of solar energy to power the WSN in water surface monitoring application.

In [80] various possible renewable energy resources were reviewed, particularly solar energy, radio energy, thermal energy, and wind energy. The paper considers wind energy as a potential candidate for full or partial powering of WSN applications to monitor oil and gas lines, as well as bridges structural health. The author suggested combining wind resources with solar or thermal resources to reduce resource fluctuations.

Bai et al [81] proposed the use of vibration or thermoelectric energy resources to power WSN. The WSN is installed in aircraft engines to collect information about the aircraft engine's health and performance. Their model involves four modules: a specific routing module, a sensor positioning module, a network membership module, and a media access module. Sensors in this model have the means to harvest energy from vibration or thermoelectric resources in aircraft engines and communicate the collected data to monitor the aircraft engine's performance. Various resources of renewable energy shown in Figure 2.2.

The authors of [82, 84–86] proposed prolonging the WSN lifetime using harvested energy and introducing power-aware topology or rout construction, in other words to route the packets based on the residual power of the neighbours.

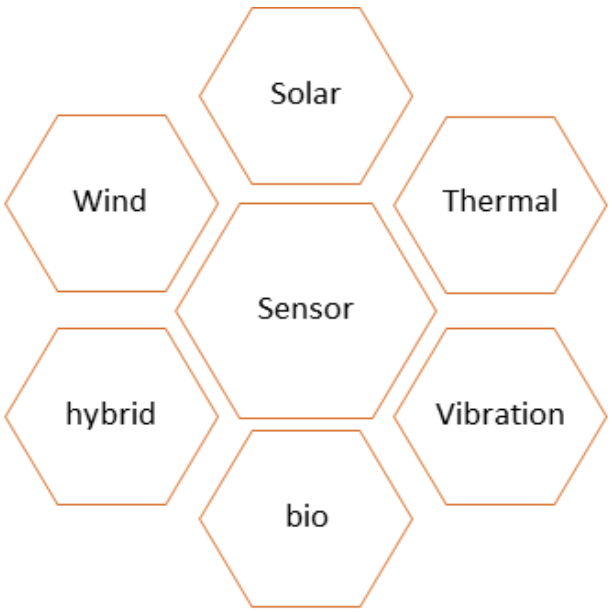

Figure 2.2: Renewable resources for WSN.

2.2.1.2 Multi-Sources Energy Harvesting

To create a sustainable system, several works in the literature proposed the combination of renewable resources with other recharging methods, since renewable resources experience a fluctuation in energy quantity and require extra storage and hardware.

Zhou et al. [87] suggested the combination of wind, solar, and wireless charger to power WSN. The authors proposed following the weather-cast to determine the locations of wind turbines and solar cells and the use of wireless chargers for the uncovered area. They suggested deploying extra energy storage to restore energy from high peak harvesting periods to be used in low harvesting periods to achieve sustainability.

Wang et al. [88] proposed combining solar energy and wireless recharging to guarantee network sustainability. They suggested using solar energy to power cluster-heads and mobile chargers to provide energy for other nodes. For the purpose of data gathering, they assumed that the mobile charger's route is formulated as a disk, with possible shortcuts to power cluster-heads if weather is not appropriate. Moreover, they initially perform full recharging and if the energy demands are high they allow partial

recharging. To simplify the problem, they divide it into three levels: how to deploy solar-powered cluster-heads, maintain energy balance in wireless recharging nodes, and combine wireless recharging with data collection.

2.2.2 Restoration via Sensor Mobility

Many authors [21, 22, 89, 90] proposed providing the sensors with a means to travel to the recharging station, refill their batteries and return to their original positions. In this section, we briefly discuss some ideas in this area.

The authors of [21] suggested proactive solutions based on local knowledge; the mobile sensor decides to recharge its battery and whether to swap with a neighbour or not. In this approach, mobile sensors monitor their energy levels; when the energy level reaches a threshold, they explore the neighbour's residual energy to find the best candidates to swap with them to maximize the network coverage, moving toward the recharging station in several swapping operations.

The authors of [89] proposed having mobile nodes that move in the field with constant velocity, stop at predefined locations to compute residual energy and find the closest recharging station (energy bank). In moving toward the charging station, a node takes a random step and computes its residual energy again, if the residual energy is enough the node continues communication, but if it is not enough the node moves directly to the charging station.

In [22], the authors propose the use of fixed and mobile wireless chargers to recharge mobile sensors. Fixed chargers invite the mobile sensors to travel to them to refill their batteries, while mobile chargers are used in case of emergency to recharge critical sensors. Moreover, reinforcement learning (RL) is used to optimize charging cost.

He et al. [91] proposed a mobile to mobile charging strategy. In this strategy, mobile robots report their residual energy to a mobile charger. The mobile charger

rendezvous with in-need robots to replenish their batteries. The authors proposed a tree-based recharging schedule to minimize the charger's travel distance. They looked at the problem as a shortest-path problem and employed a queue-based solution based on a predefined energy threshold for the sensors.

2.3 Exogenous Restoration

An important popular alternative to endogenous restoration is the use of an *exogenous* (i.e., external) element. More precisely, rather than adding complexity to the senors, this approach uses a *mobile charger* ($\mathcal{MC}$) that moves around the WSN area to recharge or replace the depleted batteries (or replace the sensors) in the field. (see Figure 2.3).

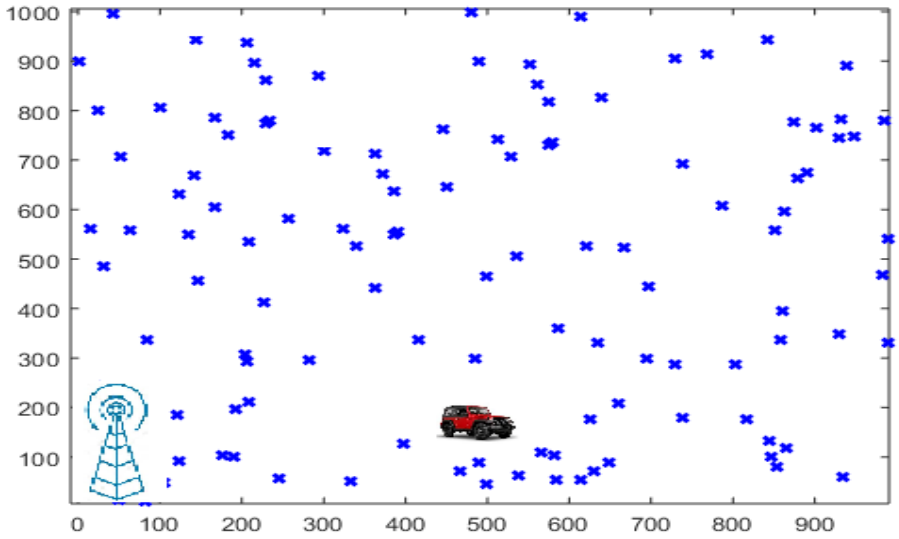

Figure 2.3: Mobile charger and wireless sensor network.

Although the means by which energy is restored to the nodes are very different, the replacement and recharging strategies follow essentially the same principles, and are practically interchangeable. In both replacement and recharging solutions, the mobile charger is required to find the depleted sensors and replace/recharge their batteries. This must be done according to some replacement/recharging schedule, whose goal is

to maximize the network coverage at any point in time. Thus, the effectiveness of both replacement and recharging strategies depend on finding an efficient schedule to visit and replace or recharge the sensor while the network coverage is maximal.

Because of advances in wireless recharging technology, the recharging option has become more attractive and more feasible, and most of the work focus on recharging strategies.

In the following subsection, we review the existing work on replacement; we describe an essential difference in the existing work on recharging, and provide a detailed review of the existing recharging strategies.

2.4 Exogenous Restoration by Replacement

Most of the literature on replacement strategies were developed in the context of handling failures; hence, most solutions use a mobile robot to replace the entire sensor (not just its battery). In this context, the robot does not carry new sensors to replace faulty ones, but rather finds a new “spare" sensor whenever needed from a set of redundant sensors already deployed in the network.

In [92], the authors proposed the use of two types of robots in the system; the robots might be a manager robot or a maintainer robot. Once a node fails, the neighbours detect and report the failures to the manager robot, which issues a replacement order to one of the maintainer robots. The authors proposed three algorithms to divide the work between the robots: a centralized algorithm that has one manager robot and multiple maintainer robots, one for each group of nodes; a fixed algorithm that divides the network area into sub-regions with one robot serving the region as manager and maintainer robot; a dynamic algorithm where nodes are dynamically divided among the robots.

A different approach is used in [93], where the mobile robot traverse the network looking for low or depleted sensors, picks them up, replaces them with new ones, and brings them to a recharging station.

The authors of [94] proposed the replacement of damaged sensors by spare passive sensors gathered from the field. They proposed a Max-Min ant system trajectory since the optimal reallocation trajectory is NP-hard. They studied the performance of six heuristic functions based on Ant Colony Optimization.

In [63], the authors classified the literature into centralized and distributed solutions. Next, they proposed centralized and distributed strategies and studied the performance of two approaches, a battery recharging approach and a battery replacing approach, before drawing the limitations and advantages of each approach. They modelled a test-bed system to compare the approaches considering four metrics for comparison purposes: sustainability ratio, the time during which all sensors are kept alive; network lifetime, the time from the beginning until the battery depletion of the first sensor; percentage of dead nodes; movement energy, the energy spent by the mobile charger while moving.

2.5 Exogenous Restoration by Recharging

There exists a very extensive literature on energy restoration in WRSN proposing recharging strategies developed under a wide variety of assumptions on the network conditions.

The initial investigations have mainly been *offline* studies, investigating and solving in a centralized way optimization (TSP-like) problems involving (and hence requiring) global information about the network conditions in its lifetime.

Of a different nature are *on-line* studies where recharging decisions are made on an ongoing basis relying solely on the past and the current network status; depending on

how the needed information is acquired, they can be further classified as *global* or *local*.

We shall call the recharging strategies proposed in those studies *offline* and *on-line* strategies (or protocols) accordingly.

Despite their differences, recharging strategies can all also be classified as either *static* or *dynamic*.

In a *static* strategy, the recharging order is predetermined, and the $\mathcal{MC}$ visits the nodes (recharging their batteries, if needed) periodically according to this order. Typically, the strategies developed by off-line studies are static. This class is particularly relevant to our study due to the fact that, once the order is computed (on-line or off-line), they are simple and require minimal communication and computation.

A *dynamic* strategy is one that continuously modifies the recharging order to adapt to changes in the energy consumption of the sensors. Typically, the strategies developed by online studies are dynamic.

In the following subsections, we briefly review the offline strategies, and examine both the global and local sub-classes of on-line strategies. Finally, we review the static ones.

2.5.1 Offline Recharging Strategies

Obviously, all offline strategies are centralized, since the base station (or the $\mathcal{MC}$) computes the recharging order based on the full information about the system's entire life time. Those information include the location, the level of energy, and consumption rate, required to compute the recharging order.

Offline strategies have many shortcomings; they require global knowledge about the whole life of network and extra communication overhead. In addition, offline solutions need extra computation capabilities and produce fixed recharging orders, making the solutions not to be flexible [38]. Moreover, offline strategies are vulnerable to changes

in the network conditions, show a lack of adaptability, and suffer from substantial performance degradation [53].

In [34], the authors proposed a periodic recharging strategy. First, they partition the network into subsets. Each subset will have a set of nodes that are selected randomly for the first time and does not overlap with other sets. They aimed to maintain the network operational by decreasing the node's energy consumption. They formulated the recharging schedule problem as TSP that connects each set of nodes in addition to the BS. Moreover, they tested their strategy on a small network of 100 sensors.

In [48], sensors report their energy information to the BS, which computes the recharging order. The authors aimed to find an optimal recharging schedule for a small size network. They suggested two heuristics to prolong the WSN lifetime and implemented their solution on a few sensors. They reported low efficiency in recharging large scale networks and acceptable efficiency for small scale networks to prolong the sensor's lifetime.

Dai et al. [95] Proposed a recharging strategy for a Point of Interest (POI) oriented WRSN, where multiple sensors monitor each POI; thus, an activation schedule that coordinates the sensors' active time is required. Moreover, they suggested optimizing the charging order problem based on that activation schedule. To maximize WSN services' quality, the mobile charger periodically visits and recharges the sensors that maximize the total network coverage of the POIs. The authors assumed that the mobile charger travel time and its energy consumption are negligible to simplify the problem. Furthermore, they assumed that the mobile charger uses a fixed recharging schedule.

In [49], the authors proposed a periodic recharging schedule based on the Hamiltonian cycle. They employed a dynamic optimization model to maximize the $\mathcal{MC}$ vocational time. To do so, they divided the network area into clusters, periodically visit each cluster, and recharge the cluster nodes simultaneously.

Authors of [50] looked at the problem in two points: they formulate the recharging

path as TSP to minimize the $\mathcal{MC}$ travel time, and used the Lambert function to find optimal charging time. Further, they adopted a multi-sensor charging scenario to reduce total recharging time.

It is worth to mentioning that many offline strategies [96, 97] proposed the use of multiple chargers. The authors of [96], for example, focusing on minimizing the chargers' travel-distances, formulated the problem as a travel salesman problem. To solve the problem complexity, they suggested using fixed consumption rates. In [97], the authors addressed the issue of finding the minimum number of chargers to satisfy the energy requirements of the WSN.

2.5.2 Online Recharging Strategies

Online strategies in the literature can be classified based on real-time energy data acquisition into *global* and *local* protocols. In *global* protocols, the $\mathcal{MC}$ or the BS decides on the recharging order based on the node energy information that is continuously sent to the mobile charger or base station. In *local* protocols, the $\mathcal{MC}$ interacts only with nodes within its proximity to decide on recharging order.

2.5.2.1 Global Protocols

In [37], the authors proposed that the base station collects charging requests and generates a list of needy sensors and recharging schedule based on Simulated Annealing. The authors used sensors' demands, the distance between the charger and the sensors, and the charger's level of energy, to generate the recharging schedule. The recharging path is updated every recharging round to reach the neediest sensors and to reduce recharging time. The algorithm's performance was evaluated in small area networks, $100m \times 100m$, and small network sizes (50 to 100 nodes).

The authors of [38] reformulate the problem as a reward collection problem. Sensor

nodes report their energy consumption to the BS, which computes the recharging order and communicates it to the mobile charger. The mobile charger follows this recharging order, and all new recharging requests are queued for the next tour. The authors aimed to maximize the collected reward in both full and partial recharging, and the mobile charger gains more rewards once it visits the sensors in need.

In [39], the authors proposed the combination of an energy sensitive routing protocol with the recharging process. They demanded the sensors to periodically send residual energy information, which helps the mobile charger to maintain a map of the global network energy. After that, the mobile charger chooses a set of nodes to recharge. On the sensors side, they compute routing costs and choose the routes that minimize the cost, which eventually reduces consumed energy significantly.

In [40], the authors divided needy sensors into primary and passer-by sensors. The recharging schedule includes all primary (local and global) sensors in addition to local passer-by sensors. Initially, sensors demand to be charged, and the mobile charger collects the requests and sorts them into primary and passer-by requests. The mobile charger charges the nearby needy sensors (local ones) and only charges the nearby non-needy sensors if there are no requests from sensors further away (global ones). The primary passer-by strategy achieved good coverage in terms of quality of monitoring [95].

The authors of [32, 42–45] looked at the problem from the network utility point of view. Once a sensor's energy reaches a predefined threshold, it sends a charging request to the mobile charger, which computes the route for the most in need sensors. The authors assumed that the length of the recharging route is bounded by a predefined quantity. In addition, they propose an algorithm to compute a set of anchor points for data gathering. Those anchor points are sensors with the least residual energy. They employed a vehicle to move around the network, recharge the selected sensors and gather data from surrounding sensors in a multi-hop fashion before transmitting the collected data to the base station.

The authors of [41] proposed that the mobile charger receives and collects charging requests and groups them into clusters based on spatial criteria; then it chooses one of the clusters to serve a set of sensor nodes in that cluster. The authors proposed the generation of a recharging schedule based on the travel salesman problem, which minimizes the travel distance for each recharging trip.

In [59], the mobile charger waits for a specific time to receive, as much as possible, charging requests from the sensors, having more requests from the same “cluster" of the sensors making the recharging process performance better. The authors assumed that the $\mathcal{MC}$ could charge multiple sensors once it stops at any location. The waiting time before dispatching a new recharging tour is variable and depends on the received charging requests. The mobile charger waits until the time is up, and if only one sensor is listed for that recharging trip, the mobile charger starts the tour. Preemption of recharging trips is not allowed to guarantee fairness among the sensors.

He et al. [46, 47] proposed an online strategy, Nearest-Job-Next with Preemption (NJNP), where the mobile charger collects charging requests, stores them in a pool, and computes a recharging schedule based on temporal and spatial properties of incoming charging request. During the recharging tour, the mobile charger continue to receive charging requests. If a sensor node is very close to the mobile charger’s position and its energy level is very low, the mobile charger disrupts the current recharging operation and moves to the new sensor node to charge it. However, the NJNP solution does not guarantee recharging the nodes prior to their energy depletion [98].

In [99], the authors studied the optimistic and pessimistic options of finding a periodic recharging schedule for WSN. They assumed that the mobile charger has an Oracle of all the sensors’ energy consumption rates. Based on those consumption rates, a mobile charger determines a set of sensor nodes to be charged in a fixed charging scheme based on Hamiltonian cycle. The optimistic scenario comes if the predictions match the real consumption; if not, the pessimistic scenario occurs.

The authors of [100] employed charging drones, and suggested using machine learning (ESN-ANN)to predict the consumption of the sensors and the best stop positions for the drone to charge the sensors in the range. The authors combined two energy sources: the drone charger and static tower charger. Drones moves in periodic way to charge sensors far away from the towers, while towers provide energy to charge all sensors in the range. To cluster the sensors, they suggested using the k-means algorithm. Drone and towers replenished energy using radio frequencies. The authors proposed the use of Mean-field Approximation to reduce the interference between the various frequencies. They tested their proposal in a very dense network made of 400 sensors deployed in an area of $50m \times 50m$.

In [101], the authors used ARIMA (Autoregressive Integrated Moving Average Model) and GRNN (Generalized Regression Neural Network) hybrid model to predict the remaining life time of the sensors. The remaining life time and distance between the $\mathcal{MC}$ and the sensors were used to determine the set of nodes to be recharged. Next, they computed the Hamiltonian path that connects the selected nodes. The $\mathcal{MC}$ starts the charging tour from the BS and return back to the BS to recharge its battery.

2.5.2.2 Local Protocols

The authors of [65, 102] considered a ring network and proposed that the $\mathcal{MC}$ traverses it in the counter-clockwise direction (when aware of an existing need) to recharge depleted sensors. Every node is allowed to communicate locally with its clock-wise neighbour. If in need, it will send a recharge request to that neighbour; the request will be forwarded along the ring until it reaches either the $\mathcal{MC}$ or a node that already sent the request. Note that this mechanism ensures that there is no need to send nodes' locations or IDs.

In [64], the authors considered a linear sensor network. Sensors in need send a recharging request to the next neighbour; the request will be forwarded along the line

until reaching either the $\mathcal{MC}$ or a node that already sent the request.

In [63], the authors assumed that the $\mathcal{MC}$ uses past information to decide the recharging schedule. The $\mathcal{MC}$ traverses the nodes in three methods: randomly, based on minimum energy, and based on minimum expected life-time. They did not report how they collected the past information initially to use it later when determining the scheduling.

These strategies are designed to compute and modify recharging order for each recharging cycle. In [29, 54], the authors tested many routing protocols and trajectories to maximize the network lifetime. In [54], the authors examined the impact of different routing protocols on sensors' residual-energy. They proposed a limited reporting protocol, where one of the nodes is elected in each neighbourhood to collect energy information from neighbours and report those numbers to the mobile charger. In [29], the authors proposed that the network has limited energy and investigated the optimal ratio of energy assigned to the mobile charger relative to energy assigned to the sensors. Also, they tested full recharging versus partial recharging. Finally, they tested their hypothesis under several trajectories. In one of those trajectories, the authors assumed that the $\mathcal{MC}$ traverse the nodes in a circular trajectory around the sink, this trajectory consists of concentric circles. They assumed that the $\mathcal{MC}$ changes the radii of the circle based on the energy level of the sensors. However, they did not report how the energy information of the outer circle that the $\mathcal{MC}$ has not traversed yet was acquired.

2.5.3 Static Strategies

The authors of [30,33,36] aimed to maximize the $\mathcal{MC}$'s inactive time over the active time (i.e., the recharging time). Thus, they propose a periodic recharging schedule based on a Hamiltonian cycle computed with a-priori global knowledge of the network. They employed a mobile charger that processes the received charging requests from small

scale network (50 sensors in [30] and 100 sensors in [33]), and generates a recharging schedule based on Hamiltonian cycle. The mobile charger periodically visits the sensors, in the same order, to fully recharge them. The proposed solution shows that the network might reach immortal level using a single charger for small WSNs. However, the study did not considers network scalability and the impact of network changes on the performance of the proposed strategy.

The authors of [35] proposed two static energy restoration strategies based on a fixed circular and linear order of the nodes employing multiple chargers.

In [103, 104], the authors considered a charger with a global knowledge of the network and proposed dividing the network area into adjacent hexagonal cells. The mobile charger stops at the center of each cell to charge all node in the cell. The distance between the charger and the sensors is controlled and the energy reception rate for every sensor is calculated. They optimized the problem to find the best path to visit all cells. The authors suggested using the Reformulation-Linearization Technique (RLT). They tested the proposal for networks of 100 sensors, and found that good results might be achieved in terms of travel distance and working time to vacation time. Visiting the cell's center rather than visiting its nodes reduces the travelling distance, which explains their results.

2.6 Additional Issues and Extensions

2.6.1 Charging Multiple Sensors

The idea of this approach is that all sensors around the wireless charger and within the electromagnetic field can harvest energy in different quantities. Many proposals in the literature suggest using this idea to decrease the network's recharging time. Further, clustering the nodes reduces the communication overhead significantly. Thus, several

studies propose the division of the network area into clusters, and all the sensors in a cluster harvest energy simultaneously, despite the fact that the distance between the charger's coil and the sensor's coil significantly impacts the amount of energy replenished to the remote sensors. In the following paragraphs, we will discuss those techniques and algorithms. Although communication overhead reduces noticeably in cluster-based energy restoration strategies, recharging efficiency decreases significantly because of the increase in the distance between the charger and sensors, which clearly reduces the recharging efficiency and the recharging time in the suggested works.

Wang et al. [105] proposed a greedy algorithm to divide the network area into several clusters. The authors optimize another algorithm for travelling and recharging costs based on TSP. Thus, the mobile charger stops at different locations every recharging round. The mobile charger stops only once for each cluster and stays until all sensors in the cluster are fully charged. Since they proposed charging all the sensors in the cluster fully, the time might be longer than usual.

In [106], the authors aimed to maximize the sensors' lifetime by minimizing the recharging tour length and maximizing the recharging utility gain; at the same time, the mobile charger receives a reward for every successful recharging process. They assumed that the mobile charger has finite energy and the maximum number of served requests are limited.

The authors of [107, 108] aimed to minimize the number of the $\mathcal{MC}$ stops and the recharging duration in the network. Thus, they divided the network area, using the k-means clustering algorithm, into clusters. They found that to reduce the recharging delay, the charger needs to stop in more locations. For example, in a network of 200 sensors deployed in an area of $100m \times 100m$, which is considered a dense network, the mobile charger should stop 159 times to minimize the recharging delay. Thus, they demanded that system users suggest a performance degradation ratio to reduce the number of stops.

Lai et al. [109] also aimed to minimize the recharging time by reducing the number of recharging stops. They use an integer linear programming model to achieve this goal. After dividing the network area into cliques, each clique will have a number of the recharging stops relative to the number of sensors: at least three recharging stops are required. Again, the authors use the sensors' locations and recharging time to schedule the recharging round.

Fu et al. [110] suggested the use of the k-Vertex Disjoint Path to let the sensors join one of the clusters based on the residual energy in its neighbours, which lead to one of the cluster-heads in the network area. They used the same principle to connect the cluster-heads with the base-station. This algorithm aims to maximize the network coverage by minimizing the nodes' failure in the network. The authors reported a significant decrease in communication overhead.

The authors of [111] looked at the problem from the coverage point of view; they aim to maximize the network coverage by giving each sensor a weight. First, they divide the network into clusters; each sensor in a cluster was assigned a colour (Red, Yellow, Green) based on its residual energy. Second, each colour zone follows a different recharging strategy. Sensors with higher coverage contribution toward their cluster are in the red zone and are charged more frequently.

2.6.2 Partial Recharging vs Full Recharging

The recharging process takes a long time, especially if the charger has a long list of sensors to charge. Most of the works in literature adopts full recharging (i.e., when the charger reaches a node in need, it fully replenishes its battery before proceeding to the next). In some strategies, the authors introduced predefined recharging thresholds and once the mobile charger reaches the threshold (which could be partial), it moves to the next sensors on the list. This is the case for [29, 38, 112–114].

The authors of [112, 113] studied a partial recharging strategy to maximize the network lifetime. The mobile charger replenishes a sufficient amount of energy to a sensor to keep it alive until the next visit. In the meantime, it visits other nodes on the list providing them with enough energy to power themselves. Then, the mobile charger revisits the partially recharged nodes to recharge them fully. Finally, the mobile charger generates a new list of to-be charged nodes using the same technique. The authors of [113] reported longer travelling distances commuted by the charger. To solve the problem, they proposed another strategy that minimize travel distance reducing network coverage.

In [114], the authors proposed recharging the nodes partially to reduce non-operational time, and they selected a set of nodes to be charged based on their residual energy. Meanwhile, they proposed removing nodes that are not directly influencing the network coverage from the selected set of nodes. For every cycle, they chose different set of sensors, which makes it a dynamic strategy.

In [29], the authors tested partial and full recharging from another aspect. They considered that the network energy is one unit, and they studied how to divide the network energy between nodes and the mobile charger.

Both [29, 113] reported longer travel distances for the charger, thus introducing wasted energy and wasted time, which imply long waiting time for other nodes in the network and vulnerability to functionality loss.

Liang et al. [38] examined partial recharging versus full recharging strategies and concluded that partial recharging causes more wasted energy on travelling, which is obvious since the mobile charger travels forward and backward between nodes, which causes more energy to be consumed.

2.6.3 Multiple Chargers

Several authors [98, 115–119] proposed the idea of using multiple chargers to charge a large number of sensors or to charge sensors in a large area. Sensors send a charging request to the base station, and the base station forwards the request to one of the chargers based on spatial and temporal criteria. Thus, all the works are considered on-demand and centralized strategies, which require additional coordination and communications.

In [115, 116], the authors found that one charger is not sufficient to cover a vast area network or a dynamic one. They proposed employing Named Data Networking (NDN) for real-time energy information gathering, coordination between chargers, and efficient energy replenishment, which eventually reduced the communication overhead in the network. Authors of [98,117] proposed an algorithm to find the minimum number of chargers needed to cover vast area networks.

Lin et al. [118] suggested the designation of a charger for each sub-area based on the temporal and spatial correlation of charging requests. The authors of [119] proposed to having one mobile vehicle loaded with multiple static chargers. The vehicle visits the sensors in need and leaves one of the chargers to charge that node. After sufficient time, the vehicle comes back to collect the chargers.

The authors of [120] aimed to minimize the wasted energy used in travelling. They proposed dividing the network area using the k-means algorithm and employing a mobile charger for each partition. They formulated the problem of having multiple chargers to find the minimum number of chargers that maximizes the network lifetime and minimize the wasted energy for long-distance travelling. They did not study the coordination between various chargers.

The authors of [121] proposed using two types of chargers: those that recharge the sensors and those that recharge the first type of chargers. The goal is to have the first

type work without interruptions. The only problem is the coordination between the two types of chargers.

A multiple charger approach has several problems because of its nature, such as the coordination between various chargers and the communication overhead for coordination purposes. Moreover, using multiple chargers is expensive in terms of cost and communication overhead, especially in the case of vast networks.

Chapter 3

Model

In this chapter, we introduce the basic definitions and terminology.

3.1 The Sensors

Let $\mathcal{S} = \{s_1 \ldots, s_n\}$ be a set of n *sensor nodes* (or, simply *nodes*), randomly distributed over a square two-dimensional area of size $A \times A$. Each node has sensory equipment that allows it to monitor its surroundings; it also has provision for wireless communication. The purpose of a sensor node is to sense its surrounding and, when needed, communicate the results to a fixed *base station* (BS), located within the area. Multi-hop data routing is employed for forwarding data by the sensor nodes to the base station, which is the sink node for all data generated by all sensor nodes.

The nodes are homogeneous (i.e., with the same capabilities), and each is powered by a wirelessly-rechargeable on-board battery. All batteries have the same capacity, E_{max}.

All sensing, processing and communication activities of a node consume energy.

Energy consumption for sensing and processing data is considered negligible compared with the power consumed for communication (e.g., [33, 34, 122–124]). As for communication, including both reception and transmission of data, we assumed that the power consumption of node $s \in \mathcal{S}$ at time t is

$$P(s,t) = \epsilon \times \lambda(s,t) \tag{3.1}$$

where ϵ is a factor that depends on the radio communication model; $\lambda(s,t)$, called *data rate* of s at time t, is the total amount of received and transmitted data by s at time t. Such a data rate $\lambda(s,t)$ is a random value following a Poisson distribution. Subsequently, we will denote the average power consumption per time unit by P.

Depending on the frequency and type of activities, nodes might consume energy differently, thus depleting their batteries at different rates.

For a node s, we denote the energy level of the battery of node s at time t by $S(s,t)$, and refer to it as its *state of charge*; when no ambiguity arises, we denote the current state of charge by $S(s)$.

If the state of charge of a node's battery falls below a predefined threshold τ, the sensor becomes *non-operational*: it stops its sensing activities, thus creating a *sensing hole* in the network, and it uses its remaining energy only for the limited local communication required for recharge.

3.2 The Mobile Charger

The Mobile charger $\mathcal{MC}$ is a special mobile entity, a robot or a vehicle, deployed in the system to recharge sensors in need. The $\mathcal{MC}$ is equipped with wireless power transfer technology, and it can recharge a single sensor at a time when in its proximity. The time spent by the $\mathcal{MC}$ to recharge a battery is proportional to the level of residual

energy of the battery to be charged: when recharging a node with k% residual energy in its battery, the $\mathcal{MC}$ will spend

$$(1-k) \times \frac{E_{max}}{\Delta} \times \frac{1}{\eta}$$

seconds, where Δ is the *recharging rate* in Watts, (i.e., the energy radiation rate with which the $\mathcal{MC}$ is capable to recharge a sensor's battery without any losses); η is the *recharging efficiency*: a battery dependent constant describing the percentage of transmitted energy that is actually delivered to the sensor's battery. For simplicity[1], we assumed that a non-full battery can always be recharged (as in [33, 127]).

The mobile charger is equipped with a large battery of capacity $E_{\mathcal{MC}}$ (initially fully charged); this capacity is used for moving and recharging purposes and it is assumed to be sufficient to charge all the nodes at least once. When the battery reaches a given threshold (5% of $E_{\mathcal{MC}}$), the $\mathcal{MC}$ travels to a *Service Station* ($\mathcal{SS}$) to recharge (or replace) its battery. The service station has fast recharging (or battery replacement) equipment to guarantee fast service time; e.g., it might be connected to the electricity grid or might have large energy storage that stores energy from various renewable or nonrenewable energy sources. After its battery is recharged or replaced, the $\mathcal{MC}$ resumes its operations.

The mobile charger moves at a constant velocity v, consuming a constant amount of energy E_{move} for every meter it travels. Moving from location x to location y, the $\mathcal{MC}$ consumes $d(x,y) \times E_{move}$ amount of energy and takes $d(x,y)/v$ time where $d(x,y)$ denotes the distance (in meters) between x and y.

The mobile charger can communicate with the sensors within its communication range, which we assume not to be less than that of the sensors (for our purposes, no stronger capability is required). The $\mathcal{MC}$ has enough local memory to store basic

[1] With the current technology, a battery can be used and recharged 500 times ([125, 126]), a large but still limited number.

information about the nodes (e.g., ID, location, energy level, and distance between nodes); for our purposes, four vectors of size $O(n)$ suffice. The information contained in these structures might not be current; initially, no information is available to the $\mathcal{MC}$. As for computational power, we only require the $\mathcal{MC}$ to be able to perform simple arithmetic operations.

3.3 Recharging Strategies

The *recharging strategy* is the set of procedures that the system entities (i.e., mobile charger, sensors, BS, and SS) follow to determine which node should be recharged next. It is perhaps the most crucial element for successfully maintaining operation of the system at the highest level of coverage. For a given recharging strategy, the order that the mobile charger actually follows in visiting nodes to recharge their batteries is called the *recharging schedule*.

There are many classes of recharging strategies, depending on how the decision is made, the type of information on which the decision is based, and how the information is acquired.

At one end of the spectrum are the *global* strategies; they are characterized by the concept that, at any given time, the decision of the node to be visited next is made taking into account the current status of the entire network and continuously solving (approximately) the corresponding TSP-like optimization problem (e.g., [61]). As discussed in the previous chapters, the knowledge required by these strategies is either assumed to be available a-priori (and typically includes the energy consumption rate of each node), as in the case of offline solutions (and, thus, mainly of mathematical interest), or is to be acquired through immediate communication to the $\mathcal{MC}$ or BS (and, thus, hardly scalable), as in the case of on-line on-demand solutions. Furthermore, substantial computational capabilities are required by the $\mathcal{MC}$ (or BS).

At the opposite end of the spectrum, and of particular interest here, are the *static* or *periodic* strategies. Clearly, the simplest among all strategies, they are characterized by having a fixed circular order $\mathcal{X} =< x_0, x_1, ..., x_{n-1} >$ of the sensors. Starting from x_0, the $\mathcal{MC}$ moves (recharging if needed) from x_i to x_{i+1}, where all operations on the indices are modulo n. In other words, a periodic strategy consists of an infinite sequence of identical rounds, where all nodes are visited in each round in the same order (e.g., [33, 35, 127, 128]). Hence, these strategies are simple, highly scalable, and require very limited (or no) global communication. Furthermore, the $\mathcal{MC}$ needs to have only very simple computational power and memory; hence these strategies can be implemented using very weak (computation and communication wise) robots.

The time spent by the $\mathcal{MC}$ in a round is composed of the time it spends recharging the nodes in need plus the time spent travelling from one node to the next. The latter cost is $v^{-1} \sum_{0 \leq i \leq n-1} d(x_i, x_{i+1})$, where v is the speed of the $\mathcal{MC}$; this cost clearly depends on the chosen order $\mathcal{X}$. This cost is minimized if $\mathcal{X}$ is an optimal Hamiltonian cycle; because of the computational costs, an approximate solution is usually employed (e.g., [128]). We shall denote by **H** a periodic recharging strategy that uses such an order.

In this thesis, we considered a new strategy, which belongs to neither of the classes mentioned above. Described in Chapter 4 and analyzed in the subsequent chapters, this on-line strategy as we will show, has all the practical advantages of the periodic ones: it is simple, highly scalable, has very little communication requirements (and all local). Furthermore, the $\mathcal{MC}$ needs to have only very basic computational power and memory; hence, it can be implemented using a very weak (computation and communication wise) robot. At the same time, it outperforms the periodic strategies (including H) in terms of number of sensing holes and their duration. As will be shown experimentally, in comparison to periodic strategies, it is immortal or near-immortal for even larger networks, it causes fewer sensing holes to exist at any time; and, more importantly, the duration of a sensing hole is significantly lower.

3.4 Performance Metrics

The effectiveness of any strategy reflects the degree to which the strategy is successful in producing a desired results or in achieving pre-planned goals. In our context, the goal is to have most of (possibly all) the network nodes operational at all times and to ensure that whenever a node stops operating, its battery will be recharged within a small amount of time.

The *effectiveness* of a recharging strategy is, thus, evaluated in terms of two measures: operational size and disconnection time.

The *operational size* $\mathcal{S}ize(t)$ at time t is the number of sensors that is operational at that time. Note that the quantity $\mathcal{H}ole(t) = n - \mathcal{S}ize(t)$ measures the number of sensing holes at time t.

The *disconnection time* for a node s is the amount of time from the moment s becomes inactive to the time when the $\mathcal{MC}$ arrives to recharge it. Disconnection time is, of course, zero if the node is charged before it becomes inactive. More precisely, the disconnection time for node s at time t (denoted by $Dis(s,t)$) is the amount of time s has been non-operational since last serviced by the $\mathcal{MC}$ before or at time t. This measure indicates *how long a sensing hole lasts*.

The highest level of effectiveness is achieved in the ideal situation when no sensing holes are created. We say that the recharging strategy allows the sensor network to achieve *immortality* (e.g., [33, 128]) if within finite time (i.e., after a transient), all nodes are always operational from that time on; that is, there exists a time t such that $\mathcal{S}ize(t') = n$ for all $t' \geq t$; in such a case, clearly, $Dis(s,t') = 0$ for all $s \in \mathcal{S}$.

The next highest level of effectiveness is when the recharging strategy allows the sensor network to achieve *near-immortality*, defined below. When a node's battery is depleted and the node becomes inactive, we measure the loss of active time in the

network due to the node's inactivity in terms of (by comparing it with) the node's active lifetime. Clearly, in the absence of recharging, the average node lifetime is $T_{E_{max}}$=E_{max}/P, where P is the average power consumption. Let Dis denote the average duration of a sensing hole, and h the average number of simultaneous sensing holes. We say that the recharging strategy allows the sensor network to achieve *near-immortality* if, within finite time (i.e., after a transient),

$$h/n \leq 0.05 \text{ and } Dis \times T_{E_{max}} \leq 0.05.$$

That is, in a near-immortal system, at least 95% of sensors are operational at any time, *and* the average disconnection time of a sensor does not last more than 5% of the battery's lifetime.

3.5 Network Parameters and Simulation Environment

The sensors and the mobile charger's characteristics depend on a variety of parameters that regulate the sensors' consumption, the charger's recharging rate, etc. Such parameters have clearly a great impact on the performance of a given recharging strategy. In the following part, we indicate the choices made in the thesis when conducting simulations to determine the performance of the system. Some parameters are fixed, while others are varied to test the flexibility of a given algorithm in different settings or when faced with changing environments.

In the thesis, the sensors are always deployed in a square area of 1000m×1000m, with the Base Station at the origin and the Service Station at the center (500m, 500m) [33]. The mobile charger ($\mathcal{MC}$) is equipped with a battery of capacity $E_{\mathcal{MC}} = 770KJ$. The $\mathcal{MC}$ radiated power with efficiency $\eta = 95\%$ [68]. The initial state of charge of each sensor is a random ratio (90% -100%) of E_{max}; a sensor is consider non-operational if the state of charge is below 5% of E_{max}. The list of parameters that are fixed

throughout the thesis is given in Table 3.1.

Table 3.1: Fixed simulation parameters.

Parameter	value
Network Area	1000×1000
$\mathcal{MC}$ battery capacity ($E_{\mathcal{MC}}$)	770KJ
Non-Operational threshold (τ)	5% of E_{max}
Charging efficiency (η)	95%

Several parameters are instead varied throughout the thesis to test their impact on the network performance when executing a given recharging algorithm.

In the thesis, we considered networks composed of n sensors with n varying between 100 and 500 ($n = 100, 200, 300, 400, 500$). We considered two types of sensor batteries: NiMH batteries with maximum capacity $E_{max} = 10.8$KJ [33] and Li-Ion batteries with maximum capacity $E_{max} = 15.98KJ$ [87]. Consequently, the non-operational threshold $\tau = 5\% \times E_{max}$ is $\tau = 540$J or $\tau = 799$J. As commonly done in the literature, the sensors' data rate is randomly generated following a Poisson distribution [88] within the range of [1-5]kbps or [1-10]kbps.

The mobile charger ($\mathcal{MC}$) travels with a speed $v = 2m/s$ (e.g., [45,59]), or $v = 5$m/s (e.g., [33,34]), consuming 5 J/meter (e.g., [87,88]).

In the thesis, we considered the recharging rate $\Delta = 5W$ [24], which is the de facto standard in the literature (e.g., [33,34,52,129]). For comparison purposes, in the thesis we also sometimes consider the less efficient $\Delta = 3.4W$ [130].

Table 3.2: Variable simulation parameters.

Parameters	**value**
Sensors' battery-capacity (E_{max})	10.8KJ, 15.98KJ
$\mathcal{MC}$ Speed (v)	2m/s, 5m/s
Data Rate (λ)	[1-5]kbps, [1-10]kbps
Recharging Rate (Δ)	3.4 W, 5 W
Network Size (n)	100, 200, 300, 400, 500

A summary of the variable parameters is given in Table 3.2.

For our experimental evaluations, we used a discrete event simulator developed in MATLAB. In each experiment, for each combination of the values of the considered parameters, we executed 50 runs and computed the average operational size and disconnection time. All results are computed with confidence level of 95%.

Chapter 4

Continuous Local Learning Strategy

4.1 Introduction

In this chapter, we investigate the energy restoration problem and propose an efficient distributed recharging strategy to be used by the mobile charger ($\mathcal{MC}$) to restore the energy supply to nodes in need.

Our recharging strategy, based on Local Learning, operates under dynamic network conditions without any a-priori knowledge of the network. It is based on simple computations by the $\mathcal{MC}$ with little memory requirements and is highly effective, keeping the network perpetually operating and achieving near-immortality even in large networks.

This chapter is organized as follows. The proposed strategy is described in the next section, and the experimental results and discussions are presented in Section 4.3. In Section 4.4, we summarize the chapter results and findings.

4.2 The Strategy

4.2.1 Overview

Recall that, as described in Chapter 3, the sensors are homogeneous but, depending on their activities, nodes might consume energy at different rates. We assumed that the $\mathcal{MC}$ has no prior information about the sensors' locations, their number, and their state of charge.

The proposed strategy employed by the $\mathcal{MC}$ is composed of two phases: an *Initialization phase*, followed by an endless *Learning and Charging phase*.

The goal of the Initialization phase is to determine information on the sensors' locations (*discovery* round) and to make an initial estimate of the current charging needs of the sensors (*base-estimation* round). Should this information be already available to the $\mathcal{MC}$, the entire phase can be skipped.

Once the initialization is completed, the $\mathcal{MC}$ has sufficient data to determine a base recharging order, and starts the endless execution of the Learning and Charging phase. In this phase, the $\mathcal{MC}$ charges the sensors starting with the base recharging order while continuously collecting local data when servicing nodes, updating its estimate accordingly, and dynamically revising the recharging order.

4.2.2 Initialization Phase

The initialization phase is composed of two rounds: the *discovery* round and the *base-estimation* round.

In the discovery round, the $\mathcal{MC}$ moves around the network in a depth-first search fashion (DF) to collect the information necessary for the base-estimation round; while

doing so, if it encounters a sensor in need of charge, it recharges it. More precisely, the general idea of the discovery round is for the robot to visit the sensors greedily moving for each new visit to the closest among its unvisited neighbours, and backtracking when all the neighbours of the node under visit have been already visited.

When reaching node s (for the first time) during this traversal at time t, the $\mathcal{MC}$ stores the node's location, its state of charge $S_1(s) := S(s,t)$ and the current timestamp $T_1(s) := t$; in case $S_1(s) < E_{max}$, the $\mathcal{MC}$ charges s.

The goal of the base-estimation round is to determine a first estimate of the consumption rate of each sensor and, thus, their future needs. To do so, the $\mathcal{MC}$ performs another DF traversal (possibly using the same route); when reaching node s during the second traversal, at time t', it collects the current state of charge and information, $S_2(s) := S(s,t')$ and $T_2(s) := t'$. Once this information is collected, the $\mathcal{MC}$ estimates the *consumption rate* $\delta(s)$ of node s as follows:

$$\delta(s) = \frac{S_2(s) - S_1(s)}{T_2(s) - T_1(s)} \tag{4.1}$$

Using this information, the $\mathcal{MC}$ estimates the sensors' battery remaining lifetime.

4.2.3 Learning and Charging Phase

After the Initialization phase, the $\mathcal{MC}$ knows the location of the sensors and has an estimate of their consumption rate. It then starts the endless process of the Learning and Charging phase (shown in `Algorithm` 2). In each step of the process, the $\mathcal{MC}$ moves to recharge the sensor deemed to be most in need, according to the selection process described below.

Let t be the current time and $d(s,t)$ the distance from the $\mathcal{MC}$ to node s at time t. Then, the time that it would be required for the $\mathcal{MC}$ to reach s starting to move at

time t is $T(s,t) = d(s,t)/v$, where v m/s is the speed of the $\mathcal{MC}$.

The *expected energy* $S_{Exp}(s,t')$ of sensor s at time $t' = t + T(s,t)$ is calculated as follows:

$$S_{Exp}(s,t') = S_2(s) - \delta(s) \times (t - T_2(s) + T(s,t)) \tag{4.2}$$

Let us point out that this measure of expected energy encompasses simultaneously all three metrics considered separately in [131]: the distance to the sensor, its state of charge, and its remaining lifetime.

At any point in time t, the next sensor to be charged is chosen to be the one with the lowest expected energy, $\min_s\{S_{Exp}(s,t)\}$, with ties broken arbitrarily.

Once the selection has been made, the $\mathcal{MC}$ moves to charge the selected node and, after completing the recharge, it updates the records of time stamps and consumption rate for this node before determining the next node to charge and moving there.

During each subsequent recharging step, the $\mathcal{MC}$ keeps recording the current state of charge values, updating the expected energy values of each sensor it charges, so that the charging schedule is always based on the most up-to-date information.

4.2.4 Algorithm Details

The details of the Initialization phase of **CLL** are shown in `Algorithm` 1. The details of the Learning and Charging phase are shown in `Algorithm` 2. Observe that for both the Initialization and the endless Learning and Charging phases, the storage space needed by the $\mathcal{MC}$ consists only of four vectors of size n.

Algorithm 1 Initialization

Input: $\mathcal{S} = \{s_1 \ldots, s_n\}, BS, SS, \mathcal{MC}, v,$
Output: $FL, T_{old}, S_{old}, \delta.$
/* t denotes the current time; $\mathcal{MC}_{loc}$ denotes the current position of the $\mathcal{MC}$ */
First Round (Discovery):
$L := neighbours(BS);$
$Visited := \emptyset;$
$D := \{distance(\mathcal{MC}_{loc}, \ell) | \ell \in L\};$
while $L \neq \emptyset$ **do**
  $target := \ell \in L : D(\ell) = Min_{s \in L}\{D(s)\};$ ▷ /* Closest node in the list */
  move to $target$
  if $S(target) < E_{max}$ **then**
    charge $target \leftarrow E_{max}$ ▷ /* Charge the sensor until full*/
  end if
  $S_1(target) := S(target);$ ▷ /* Save current charge S*/
  $T_1(target) := t;$ ▷ /* Save current time t*/
  $Visited := Visited \cup \{target\};$
  $L := L \cup (neighbours(target) \setminus Visited);$
  $D := \{distance(\mathcal{MC}_{loc}, \ell) | \ell \in L\};$
end while
Second Round (Base-Estimation):
$L := Visited;$
$D := \{distance(\mathcal{MC}_{loc}, \ell) | \ell \in L\};$
while $L \neq \emptyset$ **do**
  $target := \ell \in L : D(\ell) = Min_{s \in L}\{D(s)\};$
  move to $target$
/* **estimate power consumption rate** */
  $\delta(target) := (S_1(target) - S(target))/(t - T_1(target))$
  if $S(target) < E_{max}$ **then**
    charge $target \leftarrow E_{max}$ ▷ /* Charge the sensor until full*/
  end if
  $S_2(target) := S(target);$ ▷ /* Save current charge S*/
  $T_2(target) := t;$ ▷ /* Save current time t*/
  $L := L \setminus \{target\};$
end while
$T_{old} := T_2;\ S_{old} := S_2;\ FL := Visited;$

Algorithm 2 Learning and charging

Input $\mathcal{S}, \delta, FL, T_{old}, S_{old}, v$

/* t denotes the current time; $\mathcal{MC}_{Loc}$ denotes the current position of the $\mathcal{MC}$ */

repeat

$D := \{distance(\mathcal{MC}_{loc}, \ell) | \ell \in L\}$;

$S_{Exp} := S_{old} - \delta \times (t - T_{old} + D/v)$;

$target := \ell \in FL : S_{Exp}(\ell) = Min_{s \in FL}\{S_{Exp}(s)\}$;

move to $target$;

$\delta(target) := (S(target) - S_{old}(target))/(t - T_{old}(target))$;

$S_{old}(target) := S(target)$;

$T_{old}(target) := t$;

if $S(target) < E_{max}$ **then**

charge $target \leftarrow E_{max}$;

$S_{old}(target) := E_{max}$;

end if

until Forever

4.3 Experimental Analysis

In this section, we describe the experimental evaluation of the effectiveness of the proposed algorithm. Recall that effectiveness is evaluated in terms of *operational size* and *disconnection time* (see Section 3.4), where the operational size is the number of sensors the strategy is able to maintain operational at any given time, and the disconnection time of a sensor is the time from the moment the sensor becomes inoperative to the time when the $\mathcal{MC}$ arrives to recharge it. In particular, we present and discuss the results of the experiments focusing on the settings where *immortality* has been described in the literature (e.g., [33]). In the rest of the thesis we will sometime refer to the settings indicated in Table 4.1 as the *default* settings.

Parameter	values
Network Size (n)	100, 200, 300, 400, 500
Sensors' battery-capacity (E_{max})	10.8KJ
$\mathcal{MC}$ Speed (v)	5m/s
Data Rate (λ)	[1-5]kbps
Recharging Rate (Δ)	3.4 W, 5 W

Table 4.1: Simulation parameters.

4.3.1 Operational Size

We first consider the standard recharging rate for non-radioactive wireless energy transfer technology, $\Delta = 5W$ [24].

The results show that our strategy enables the network to be *immortal* (i.e., all sensors are always operational at all times) for all considered network sizes, even for $n = 500$ (see Figure 4.1). In the literature, immortality for such value of Δ were reported only for $n \leq 100$.

Summarizing, under the considered parameters *no other recharging strategy can do better, regardless of the amount of communication and complex computations it employs.*

Since with $\Delta = 5W$ our strategy achieves optimal performance, to further analyze the effectiveness of our algorithm we studied its performance under the significantly lower recharging rate of $\Delta = 3.4W$ [130].

Also in these conditions, our **CLL** strategy maintains a high operational size. In particular, it achieves *immortality* with up to $n = 300$ sensors, and near immortality with $n = 400$.

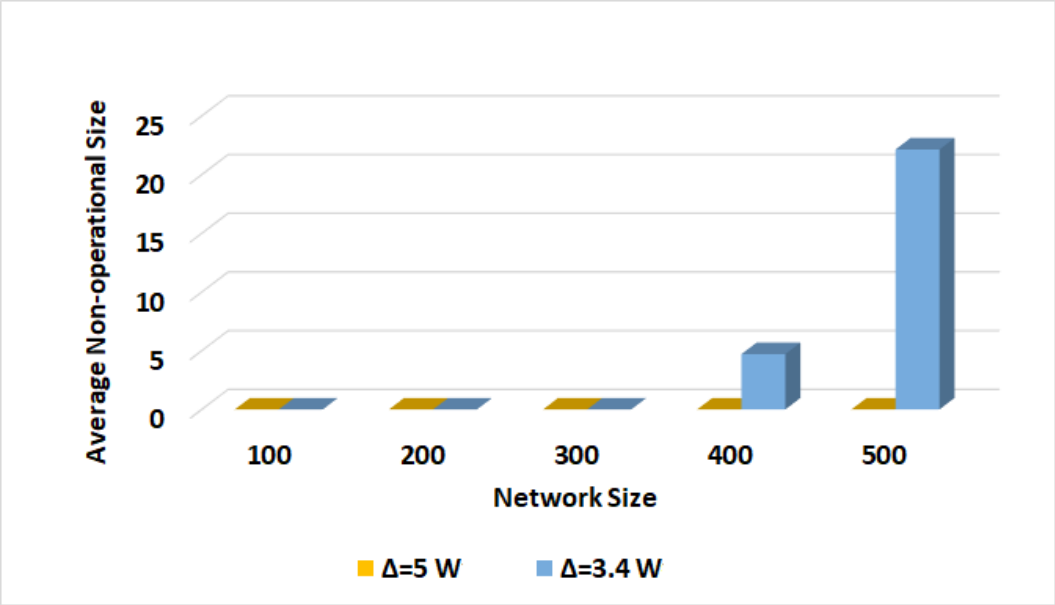

Figure 4.1: Average non-operational size with various Δ.

By increasing the number of sensors, the number of non-operational nodes clearly increases (and the operational size decreases); however, only about 5 sensors become non-operational in average for $n = 400$, and about 22 sensors for $n = 500$. In other words, with $n = 400$, at least 98.8% of the sensors are operational at any point in time and more than 95% of the sensors are always operational for $n = 500$.

4.3.2 Disconnection time

We now turn to disconnection time to evaluate the duration of a sensing hole (see Figure 4.2).

As discussed in the previous section, under **CLL** the network is immortal regardless of the network size when $\Delta = 5W$, and for $n \leq 300$ when $\Delta = 3.4W$. Thus, in all these cases, no sensor is ever disconnected.

In the case of $\Delta = 3.4W$, for $n = 400$, the average disconnection time is about 7.46 hours, which is 4.35% of $T_{E_{max}}$. For $n = 500$, the average disconnection time is less

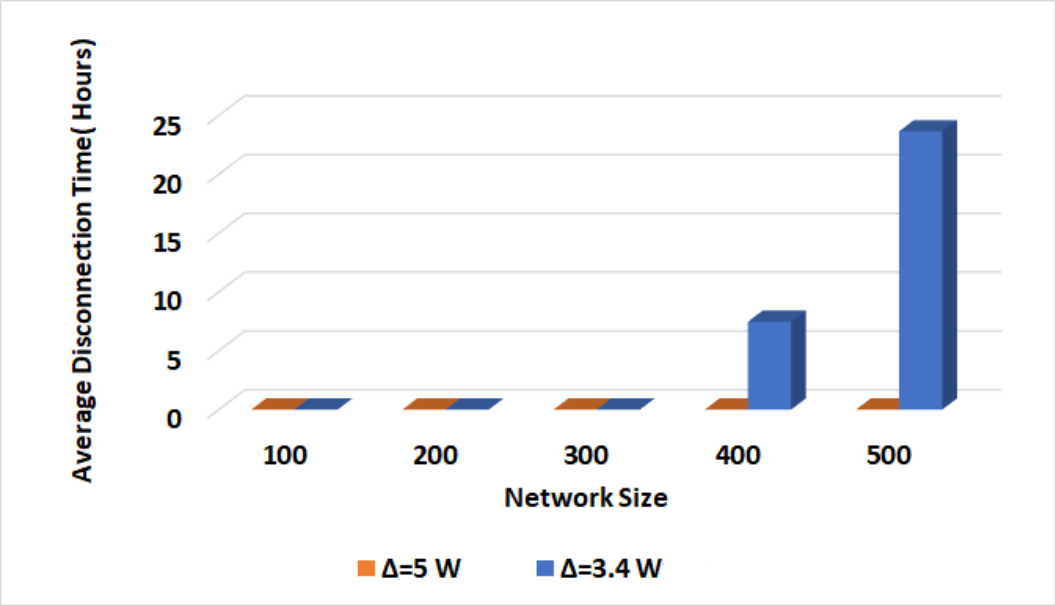

Figure 4.2: Average disconnection time with various Δ.

than 24 hours, that is, 13.8% $T_{E_{max}}$.

4.3.3 On Partial Recharging

In our strategy and in all our experiments, the $\mathcal{MC}$ always fully recharges a battery. In some studies, however, it has been suggested that a predefined bound on the amount of energy be imposed, expressed as a percentage, θ, of the sensors' battery-capacity, E_{max}; that is, when recharging, the $\mathcal{MC}$ does not provide more than $\theta \times E_{max}$ energy to the node [54, 112, 113].

In this section, we considered this idea of using partial recharging for our strategy, and investigated the effectiveness of the system for a large range of values of the recharging percentage θ $(20\%, 40\%, 60\%, 80\%, 100\%)$ of E_{max}.

The results clearly indicate that partial recharging is not convenient; indeed, both the average number of non-operational sensors and the disconnection time are inversely proportional to θ.

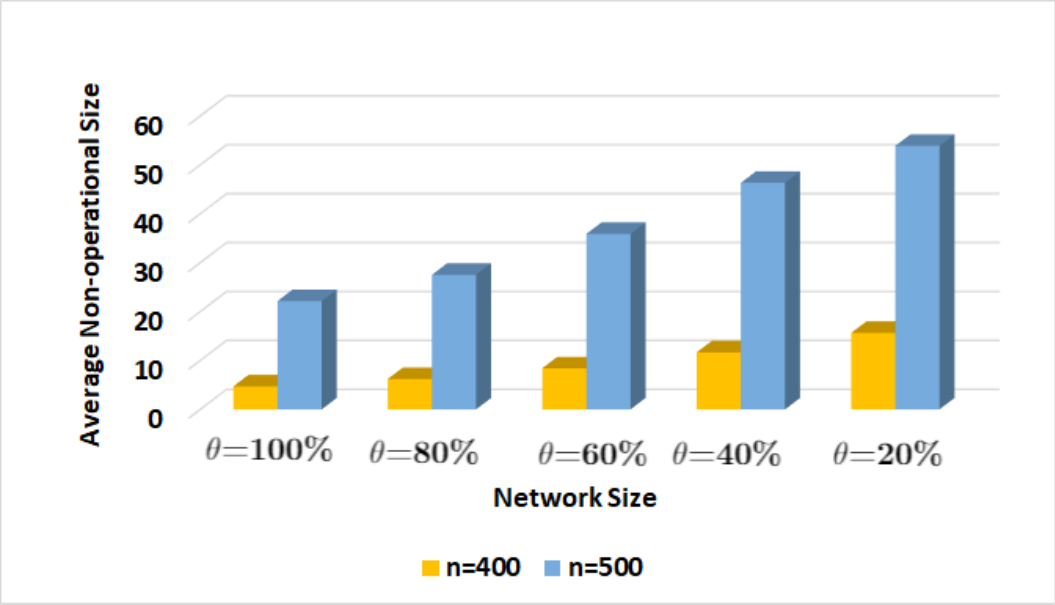

Figure 4.3: Average non-operational size for $n = \{400, 500\}$ with $\Delta = 3.4W$.

In Figure 4.3 (resp. 4.5), we show the average number of non-operational sensors for $n = \{400, 500\}$ with recharging rate $\Delta = 3.4W$ (resp. $\Delta = 5W$), and in Figure 4.4 (resp. 4.6), we show the average disconnection time for $n = \{400, 500\}$ with recharging rate $\Delta = 3.4W$ (resp. $\Delta = 5W$).

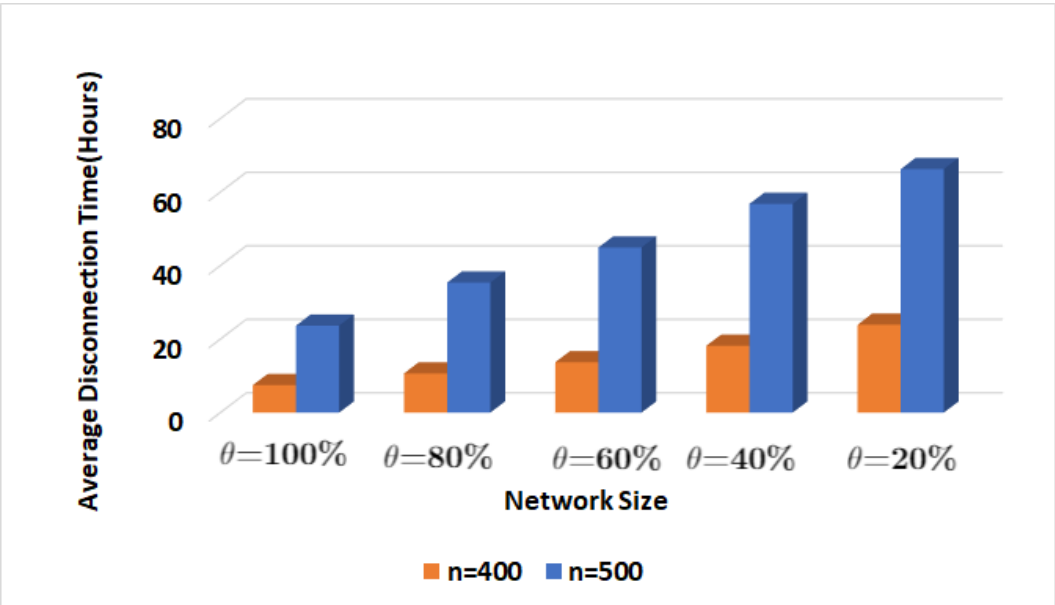

Figure 4.4: Average disconnection time for $n = \{400, 500\}$ with $\Delta = 3.4W$.

For instance, as shown in Figure 4.3, the number of non-operational sensors for a network of size $n = 500$ with $\Delta = 3.4W$, which is around 22 sensors in case of full recharging (i.e., $\theta = 100\%$), gradually increases when decreasing the recharging percentage, until reaching about 54 non-operational sensors when $\theta = 20\%$. As shown in Figure 4.4, the average disconnection time follows the same behaviour and increases from 23.65 hours when $\theta = 100\%$ to 62.24 hours when $\theta = 20\%$

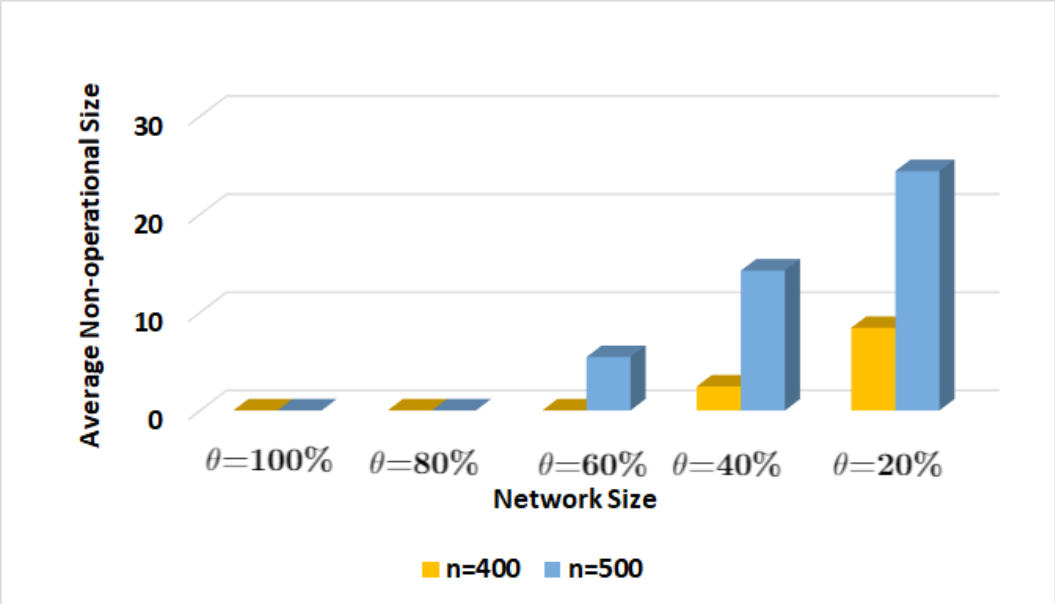

Figure 4.5: Average non-operational size for $n = \{400, 500\}$ with $\Delta = 5W$.

Analogous observations can be made for the case of $\Delta = 5W$, when the decrease of the recharging percentage gradually increases both non-operational size and disconnection time.

These results reveal that partial recharging is not the best option for our strategy. This is likely due to the fact that, with partial recharging, the mobile charger needs to travel more, and during this extra time more sensors get depleted and wait for longer time for the mobile charger to reach them.

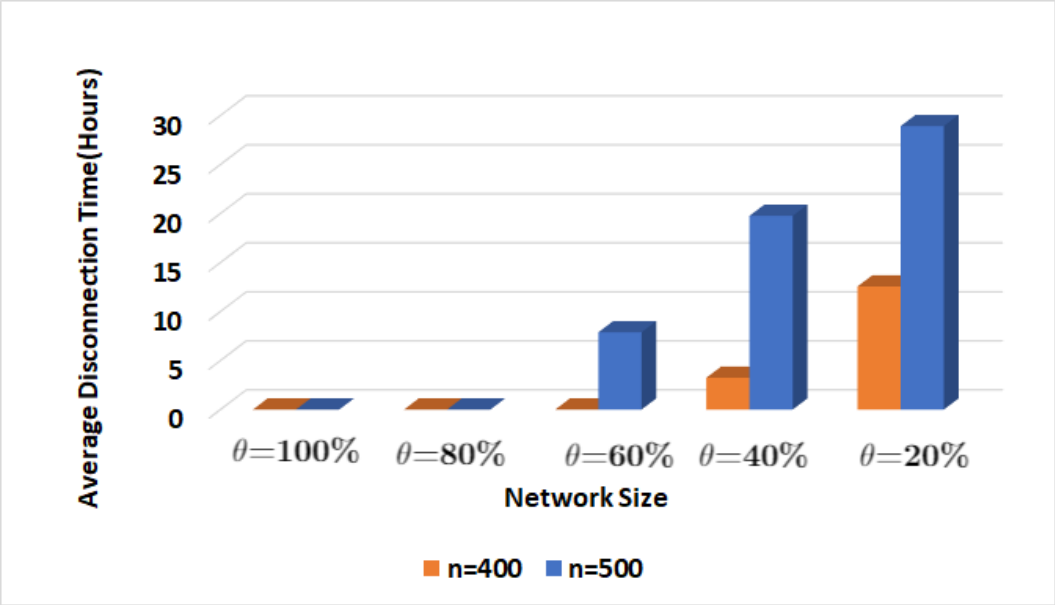

Figure 4.6: Average disconnection time for $n = \{400, 500\}$ with $\Delta = 5W$.

4.4 Conclusion

In this chapter, we introduced a new on-line recharging strategy for sensor networks (**CLL**), and we analyzed its performance in terms of the number of non-operational sensors and the disconnection time under both the commonly used recharging rate and a lower one.

We observed that **CLL** achieves immortality (all sensors are always operational at all times) with $\Delta = 5W$ for all networks. This includes the settings where immortality had been reported in the literature (but only for $n \leq 100$).

With the significantly smaller $\Delta = 3.4W$, **CLL** achieves immortality with up to $n = 300$ sensors, and near immortality with $n = 400$ (at any time at most 4.71 sensors are non-operational, for less than 4.4% of $T_{E_{max}}$); for even larger networks ($n = 500$) the number of non-operational sensors never exceeds 4.4 % of their total number.

Unlike previous studies, our technique is distributed and uses only local communication between the $\mathcal{MC}$ and its neighbouring nodes without any a-priori knowledge of

the network. Moreover, in the proposed solution, the sensors do not need to request recharging when they are in need. Using only local communication between the mobile charger and nearby sensors highly reduces the consumed energy and obviously helps to prolong the sensor's lifetime. Additionally, this approach has the advantage of reducing the possibility of transmission errors.

In the next chapter, we study the performance of **CLL** under changes in various network parameters to assess its flexibility.

Chapter 5

Flexibility of Continuous Local Learning Strategy

5.1 Introduction

WSNs are used in a wide range of applications. Each application has its own characteristics and requirements, including the number of sensors, sensors' battery-capacity, the size of the sensing area, and the power of the $\mathcal{MC}$ (e.g., speed, recharging distance, recharging rate).

Those parameters may have an impact on both coverage and disconnection time, which means that the effectiveness of a recharging strategies may vary greatly in different application settings. Hence, another important measure of a restoration strategy is its *flexibility*: its capacity to be effective over a wide range of values of different parameters, i.e., in several different applications.

We have already seen how the Continuous Local Learning Strategy, introduced in Chapter 4, is highly effective in settings where immortality has been studied in the

literature. This leads us to the question of whether this simple and efficient energy restoration strategy would still be effective under quite different settings.

In this chapter, we study the flexibility of the Continuous Local Learning strategy in two ways. First we study the impact of each single system parameter with respect to the performance of the system under the default settings of Chapter 4, and then with respect to the worst case combination of the other parameters. More precisely, in Section 5.2.1, we start from the default parameters studied in Chapter 4 of battery-capacity $E_{max} = 10.8KJ$, speed of the mobile charger $v = 5m/s$, data rate $\lambda = [1-5]kbps$ and, to study the impact of E_{max}, v, and λ, we vary each of these parameters, maintaining the others to their default values. This study is done for the two recharging rates considered in Chapter 4 ($\Delta = 3.4W$ and $\Delta = 5W$), always varying the network size from 100 to 500, shown in table 5.1. In Section 5.2.2, we analyze the impact of E_{max}, v, and λ varying each of these parameters, maintaining all the others to their worst possible values.

5.2 Experimental Analysis

Parameter	**value**
Network Size (n)	100, 200, 300, 400, 500
Sensors' battery-capacity (E_{max})	10.8KJ, 15.98KJ
$\mathcal{MC}$ Speed (v)	2 m/s, 5m/s
Data Rate (λ)	[1-5]kbps, [1-10]kbps
Recharging Rate (Δ)	3.4W, 5W

Table 5.1: Variable simulation parameters.

5.2.1 Impact on Default Setting

5.2.1.1 Impact of E_{max}

The first parameter that we studied to assess the flexibility of the **CLL** strategy was the sensors' battery-capacity (E_{max}). To test the influence of E_{max}, we conducted experiments for two sensor battery-capacities $E_{max} = \{10.8, 15.98\}$KJ, maintaining the default parameters of $v = 5m/s$, and data rate $\lambda = [1 - 5]kbps$. We discuss separately the case of $\Delta = 5W$ and the one of $\Delta = 3.4W$.

Recharging rate $\Delta = 5W$.

With $\Delta = 5W$, for all choices of the other parameters *the network always maintains immortality for all network sizes.*

Recharging rate $\Delta = 3.4W$.

We then turn our attention to the case of $\Delta = 3.4W$. Figure 5.1 shows the influence of E_{max} on the number of non-operational sensors.

Regardless of E_{max}, all networks with $n \leq 300$ are immortal, and those of size $n = 400$ are near-immortal also for all E_{max} values.

For larger networks of size $n = 500$, we observed that with the larger E_{max}, the number of non-operational sensors slightly increased from 22.14 to 23.05.

Turning to the average disconnection time, we observed that by increasing E_{max}, the average disconnection time increased from about 7.46 hours to about 8 hours in a network of $n = 400$, and from about 24 hours to about 25 hours in a network of size $n = 500$ (see Figure 5.2).

In conclusion, the experiments show that the increases of non-operational size and disconnection time, due to the fact that larger batteries require longer recharging time,

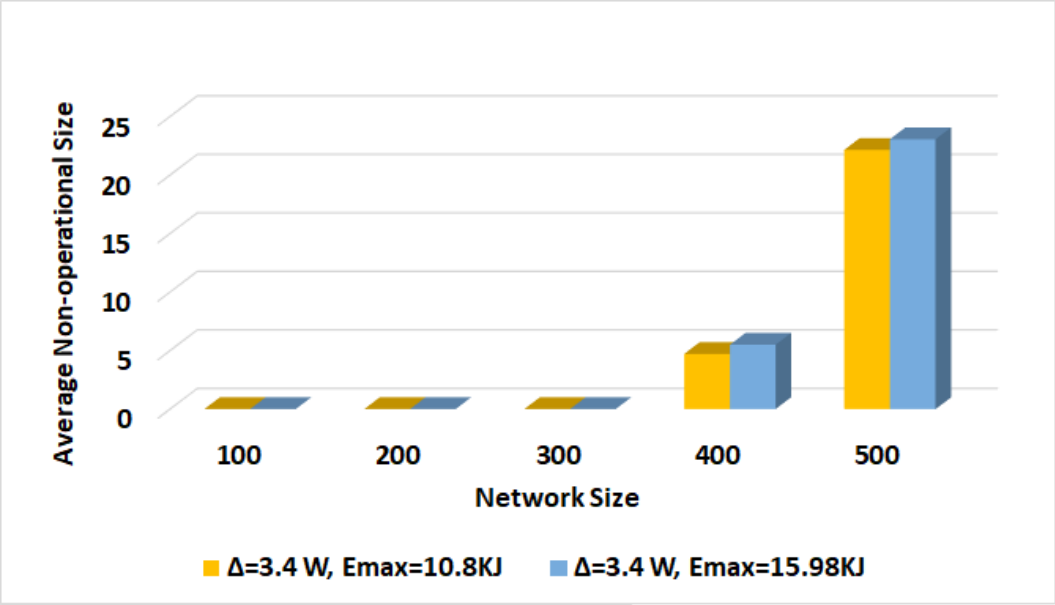

Figure 5.1: Average non-operational size with various E_{max}, and ($v = 5m/s$, $\lambda = [1 - 5]kbps$).

are rather small.

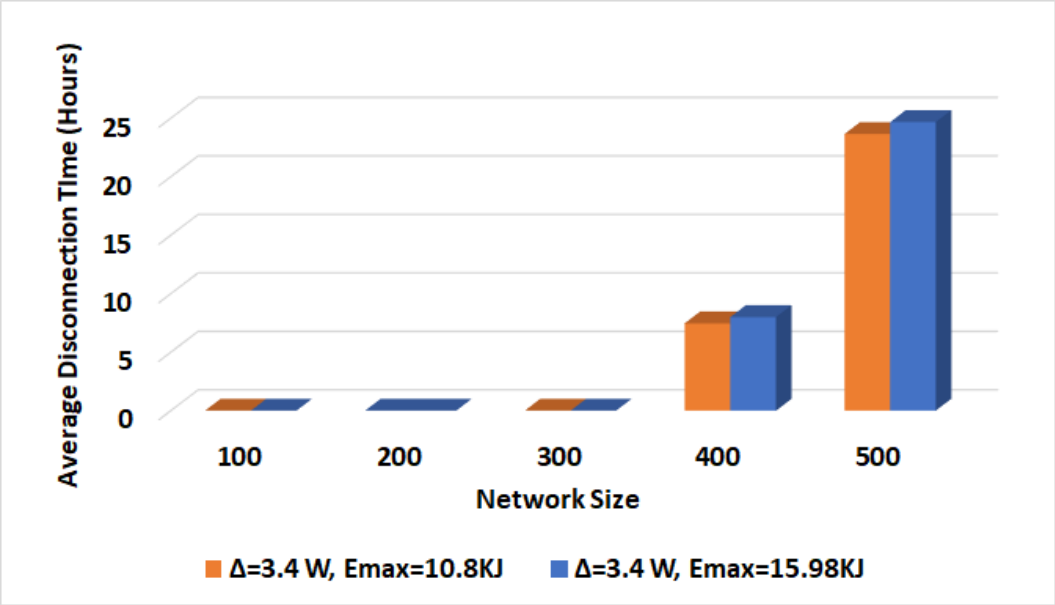

Figure 5.2: Average disconnection time with various E_{max}, and ($v = 5m/s$, $\lambda = [1 - 5]kbps$).

5.2.1.2 Impact of v

We turn to study the impact of speed of the $\mathcal{MC}$ on operational size and disconnection time. If the $\mathcal{MC}$ has a higher speed, the performance of the system would obviously improve. To test the impact of this parameter, we fixed the default values of $E_{max} = 10.8KJ$ and $\lambda = [1-5]kbps$, and varied the speed and the network size ($v = 2m/s$ and $v = 5m/s$). We discuss separately the case of $\Delta = 5W$ and the one of $\Delta = 3.4W$

Recharging rate $\Delta = 5W$.

With $\Delta = 5W$, for all choices of the other parameters *the network always maintains immortality.*

Recharging rate $\Delta = 3.4W$.

We now turn to the case of $\Delta = 3.4W$.

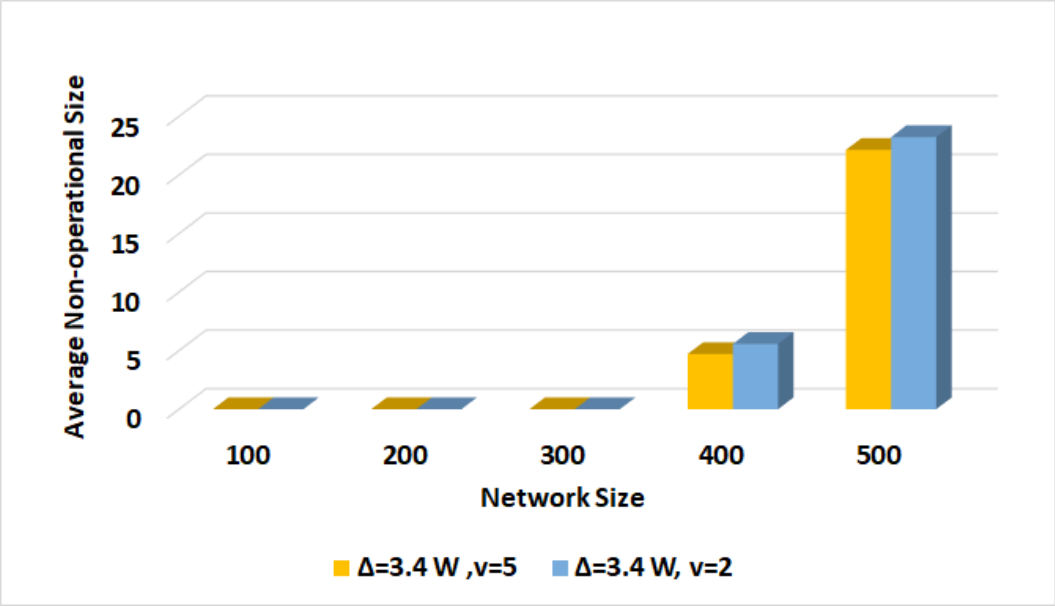

Figure 5.3: Average non-operational size with various $\mathcal{MC}$ speeds(v)

.

We noticed that higher $\mathcal{MC}$ speed slightly decreased the non-operational size (see Figure 5.3). Considering a network of size $n = 400$, we noticed that increasing the speed

from $v = 2m/s$ to $v = 5m/s$ the number of non-operational sensors decreased from about 5.57 sensors (1.4% of network size)to about 4.71 (1.18% of network size)sensors, while for a network size of $n = 500$, the change was from 23.23 (4.65% of network size)to 22.14 sensors (4.4% of network size).

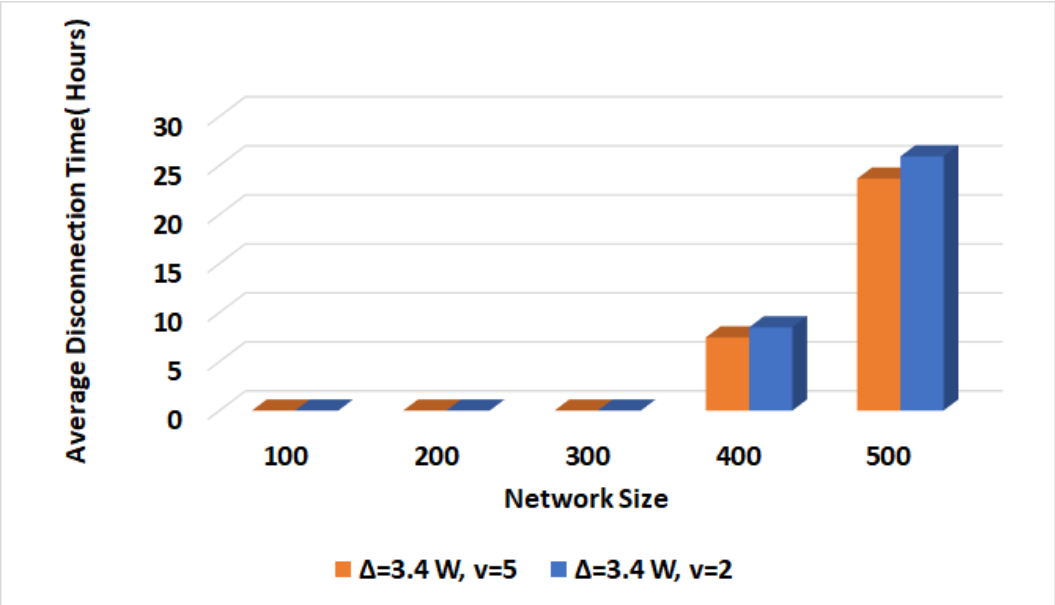

Figure 5.4: Average disconnection time with various $\mathcal{MC}$ speeds(v).

Looking at the average disconnection time, shown in Figure 5.4, we observed that the $\mathcal{MC}$ speed had a higher influence on this metric. In fact, the average disconnection time slightly decreased from 8.49 hours to 7.46 hours in the case of $n = 400$, and from 25.92 to 23.65 hours in the case of $n = 500$.

5.2.1.3 Impact of λ

We also studied the influence of changing the sensors' data rate (λ). In this subsection, we investigated the performance of the **CLL** strategy by increasing the sensors' data rate from the default $\lambda = [1 - 5]kbps$ to $\lambda = [1 - 10]kbps$, maintaining the default parameters of $v = 5m/s$, and $E_{max} = 10.8KJ$. We discuss separately the case of $\Delta = 5W$ and the one of $\Delta = 3.4W$

Recharging rate $\Delta = 5W$.

As already seen in Chapter 4, with $\Delta = 5W$ and $\lambda = [1-5]kbps$ *the network always maintains immortality* regardless of its size.

On the other hand, with the larger data rate ($\lambda = [1-10]$kbps), **CLL** achieved immortality for all settings only when $n \leq 300$. For $n = 400$, the number of non-operational sensors became 8.22 (2% of network size), and the disconnection time became 21.34 hours. Finally, for $n = 500$, the number of non-operational sensors became to 14.66 (2.9% of network size), while the disconnection time became 29.3 hours . See Figures 5.5 and 5.6.

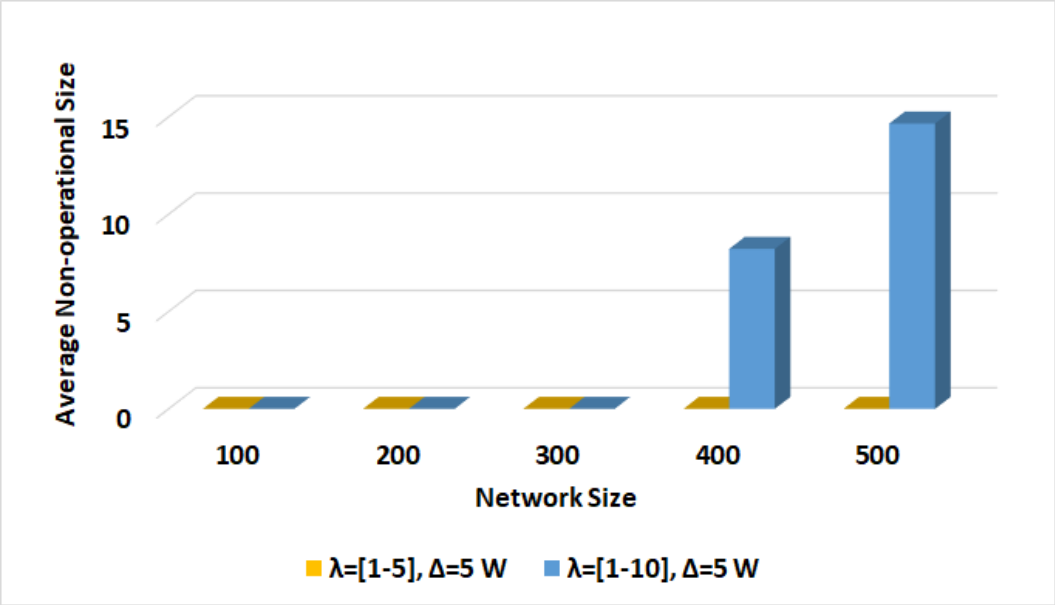

Figure 5.5: Average non-operational size for various λ with $\Delta = 5W$.

Recharging rate $\Delta = 3.4W$.

In Figure 5.7, we present the impact of λ on the number of non-operational sensors. From the experiments, we noticed that the number of non-operational sensors increased with the increase of the network size. In the case of $n = 300$, the number of non-operational sensors increased from null to 2.74 sensors (an increase of 0.9% of the network size). For $n = 400$, the number of non-operational sensors noticeably increased

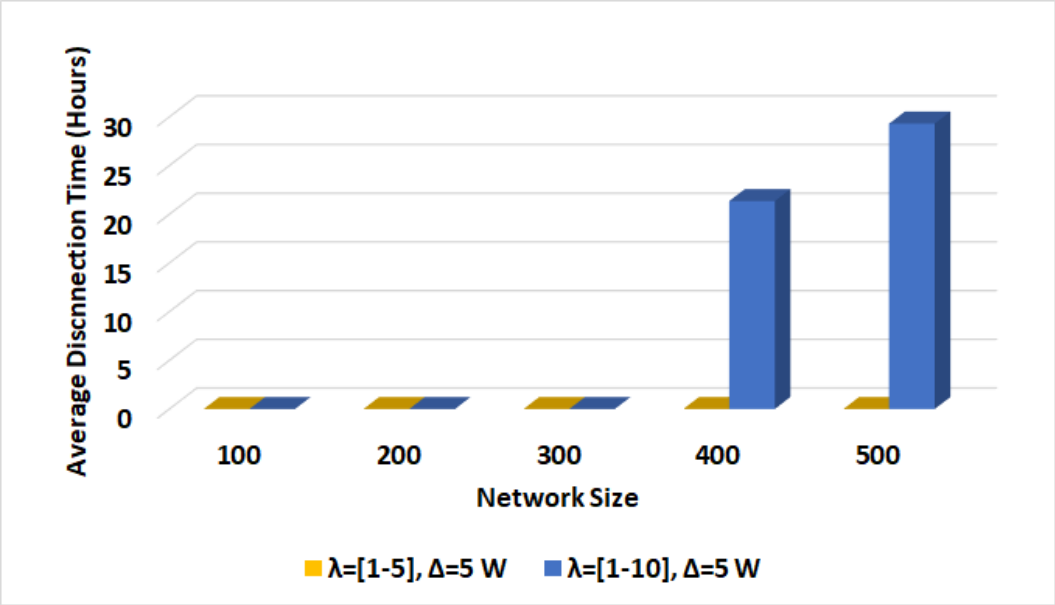

Figure 5.6: Average disconnection time for various λ with $\Delta = 5W$.

from 4.71 to 22.28 (an increase of 4.4% of the network size). For $n = 500$, the non-operational size increased from 22.14 sensors to 46.37 sensors (an increase of 4.8% of the network size).

Considering the average disconnection time, we noticed that for $n = 300$, the average disconnection time increased from null to about 9.24 hours. In the case of $n = 400$, the average disconnection time increased from 7.46 hours to reach 52.88 hours. Finally, for network of size $n = 500$, the disconnection time increased from 23.65 hours to 82.12 hours.

The results show that $\lambda = [1 - 10]$kbps has the highest impact on operational size and disconnection time, and becomes critical in combination with the slower recharging rate ($3.4W$).

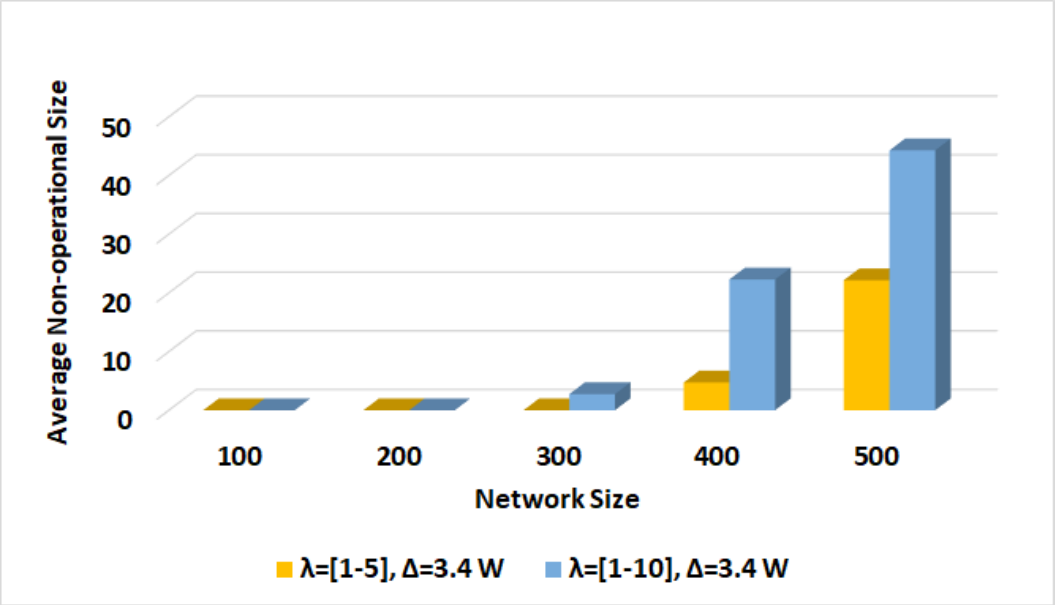

Figure 5.7: Average non-operational size varying λ with $\Delta = 3.4W$.

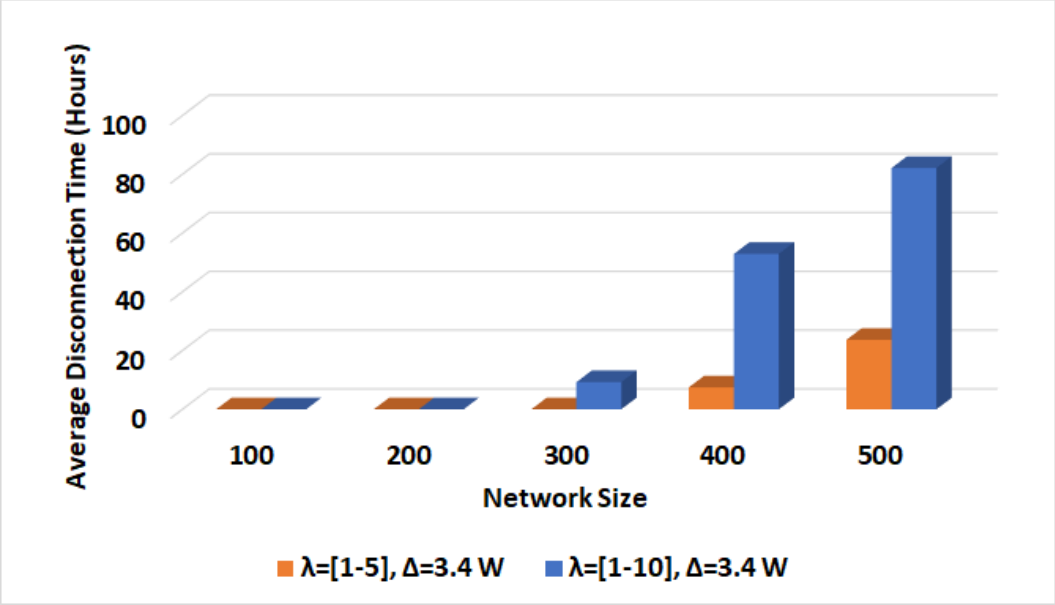

Figure 5.8: Average disconnection time varying λ with $\Delta = 3.4W$.

5.2.2 Impact on Worst Case Settings

To further examine the impact of the various parameters and their relative importance, we also observed the changes in non-operational size and disconnection time, when

varying one parameter fixing the others to the worst possible values.

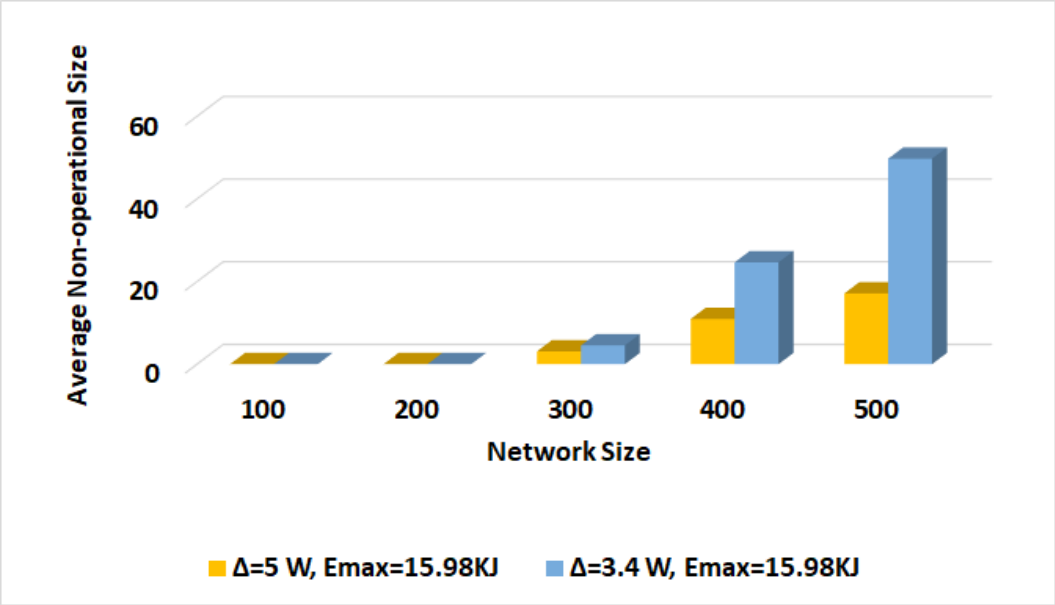

Figure 5.9: Average non-operational size varying Δ with the worst setting.

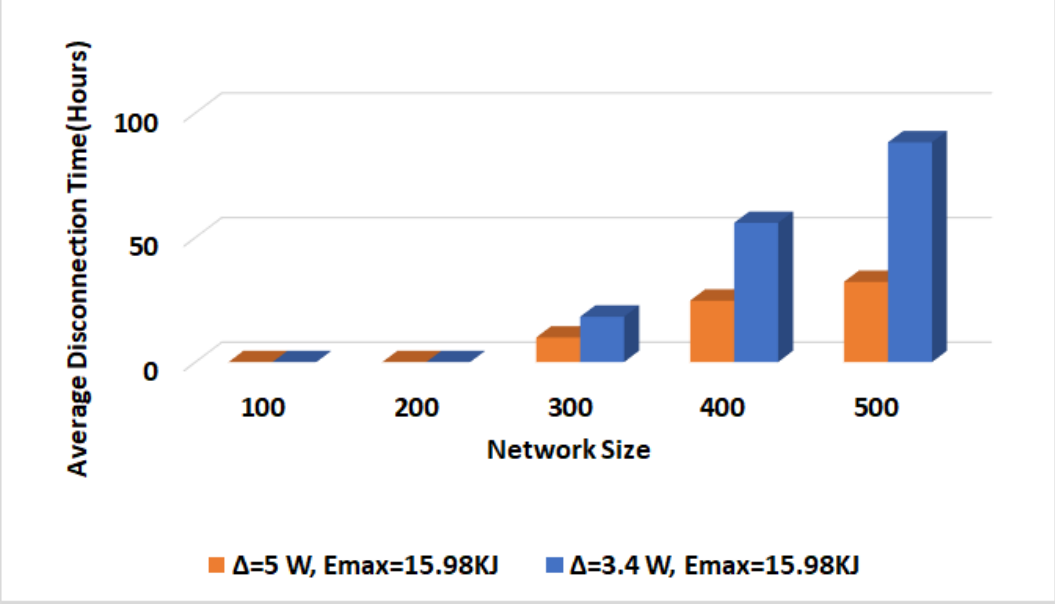

Figure 5.10: Average disconnection time varying Δ with the worst setting.

- Varying Δ: $n = 500$, $v = 2m/s$, $\lambda = [1 - 10]kbps$, $E_{max} = 15.98KJ$.

  The highest effect on the operational size and disconnection time comes from the recharging rate Δ. As shown in Figure 5.9, when Δ decreased from $5W$ to $3.4W$,

the operational size increased from 17.11 sensors to 49.72 sensors (an increase of 6.5% of the network size), and the disconnection time increased from 32.2 hours to 88.16 hours.

- Varying λ: $n = 500$, $v = 2m/s$, $E_{max} = 15.98KJ$, $\Delta = 3.4W$.

  The second most influential factor on both metrics is the data rate of the sensors λ. By varying λ in the setting considered above with the worst choice of Δ ($\Delta = 3.4W$), the number of non-operational sensors went from 49.72 (9.94% of network size) to 24.90 sensor (4.98% of network size) (see Figure 5.11), while the disconnection time changed from 88.16 to 27.35 hours (see Figure 5.12).

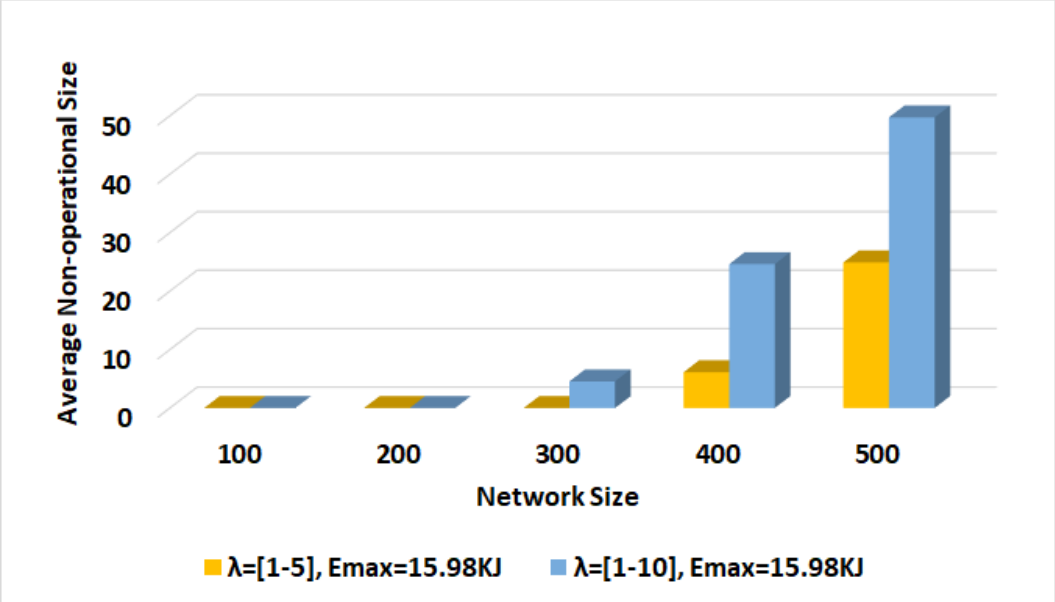

Figure 5.11: Average non-operational size for various λ with $v = 2m/s$.

- Varying v: $n = 500$, $\Delta = 3.4W$, $\lambda = [1 - 10]kbps$, $E_{max} = 15.98KJ$.

  By varying v and maintaining the setting considered above with the worst values for Δ, λ, and E_{max}, we observed that the number of non-operational sensors increased slightly from 46.54 (9.31% of network size) to 49.72 sensors (9.94% of network size) and the disconnection time varied from 84.2 hours to 88.16 hours (see Figure 5.13 and Figure 5.14).

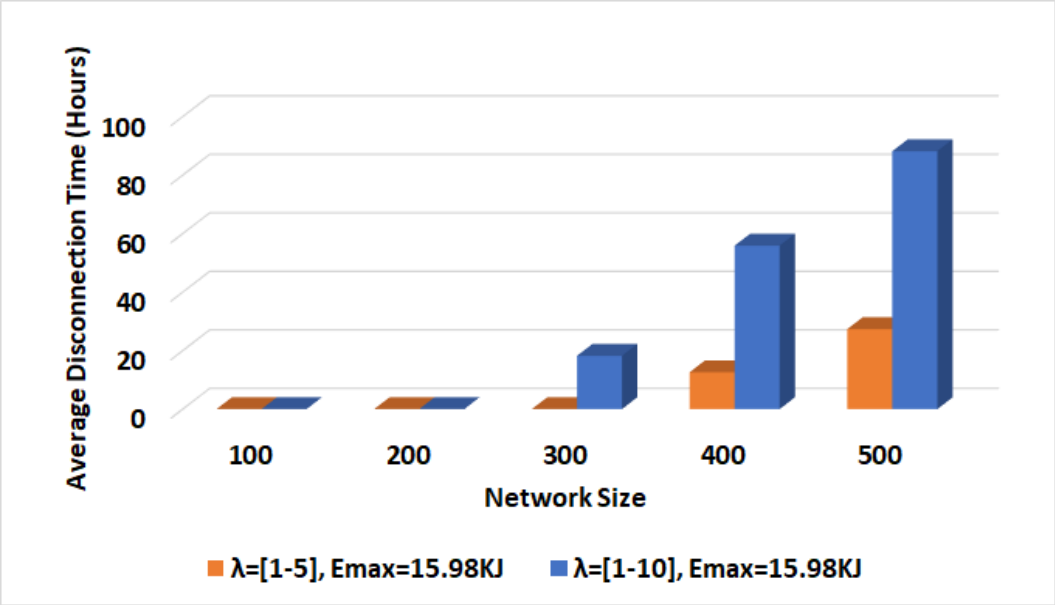

Figure 5.12: Average disconnection time for various λ with $v = 2m/s$.

- Varying E_{max}: $n = 500$, $v = 2m/s$, $\Delta = 3.4W$, $\lambda = [1 - 10]kbps$.

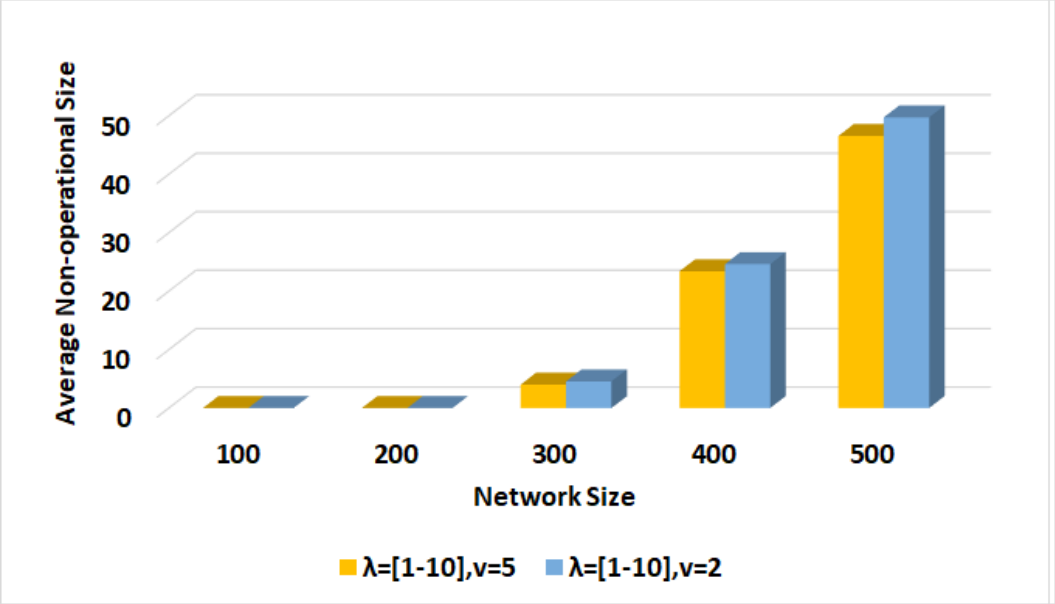

Figure 5.13: Average non-operational size for various v and $\lambda = [1 - 10]kbps$ with $\Delta = 3.4W$.

Finally, the sensor's battery-capacity (E_{max}) seem to have the lowest impact. In fact, by varying E_{max} and maintaining the setting considered above with the worst values for Δ and λ, we observed that the number of non-operational sensors

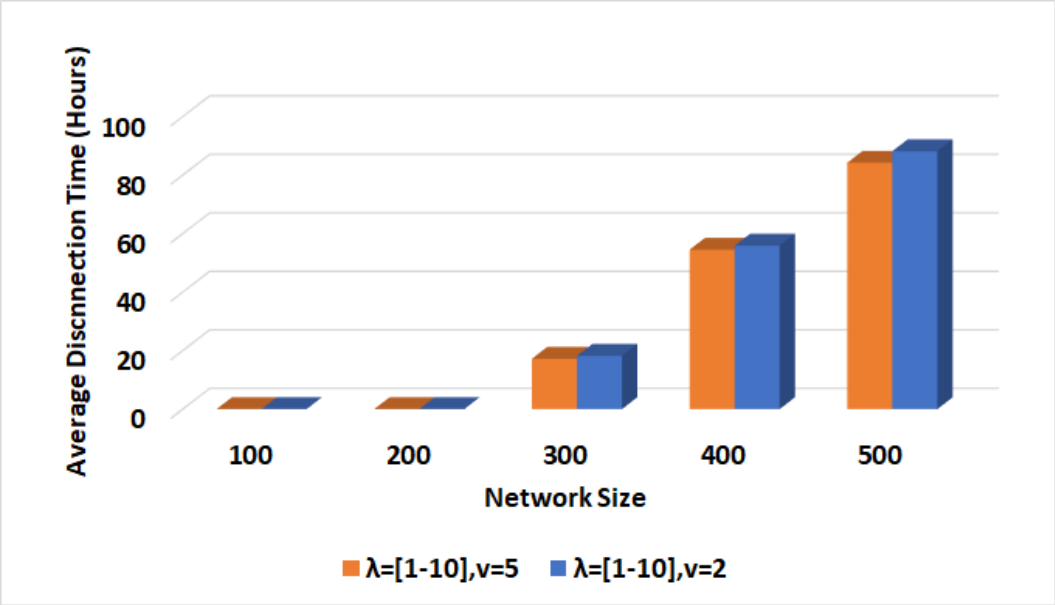

Figure 5.14: Average disconnection time for various v and $\lambda = [1 - 10]$kbps with $\Delta = 3.4W$.

varied from 49.72 to 46.37, while the disconnection time varied slightly from 88.16 to 85.26 hours (see Figure 5.15 and Figure 5.16).

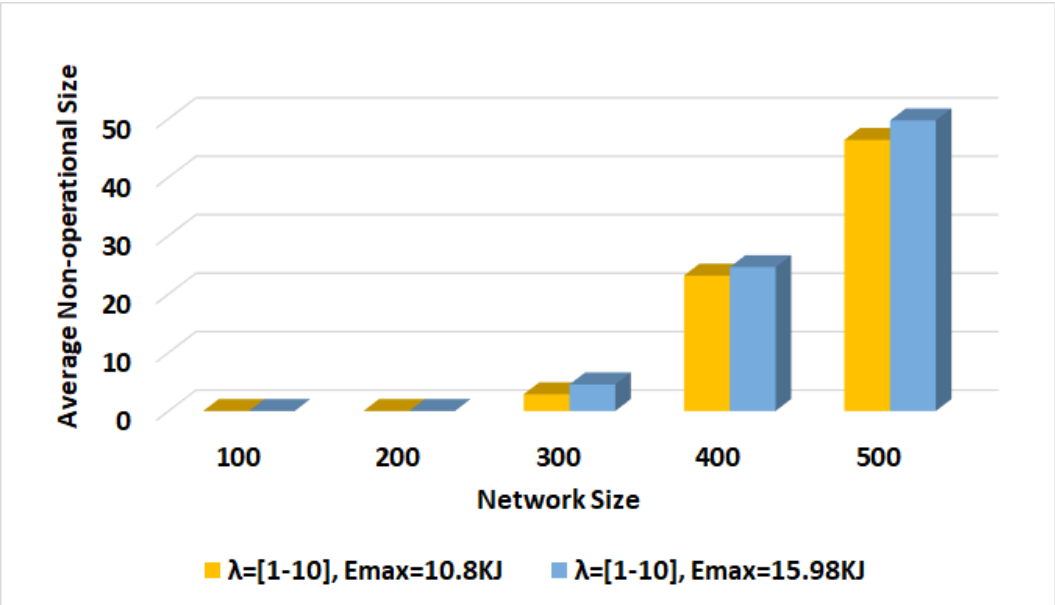

Figure 5.15: Average non-operational size for various E_{max}, $\lambda = [1 - 10]$Kbps with $\Delta = 3.4W$.

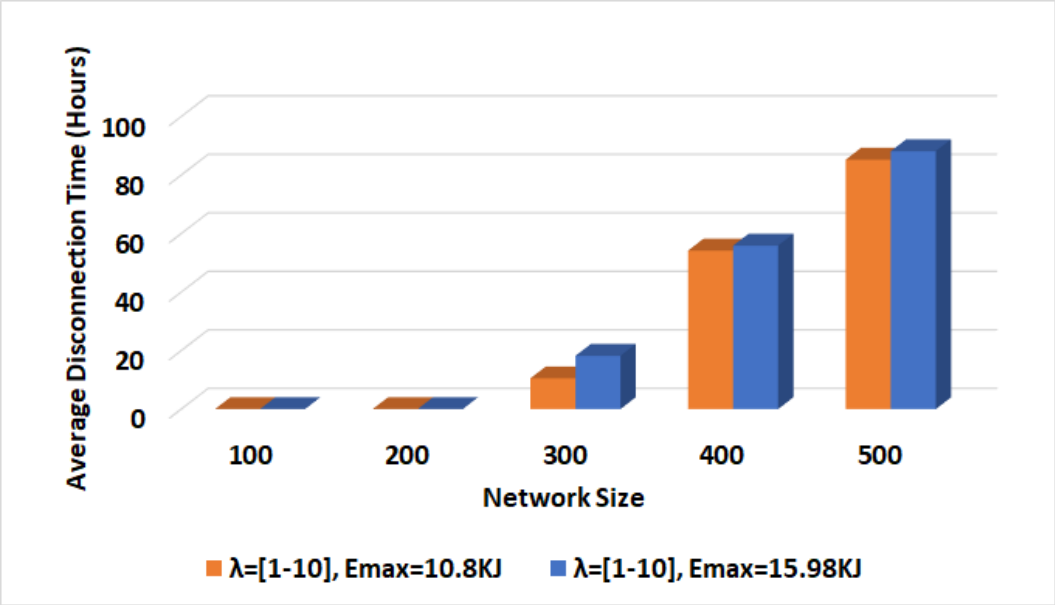

Figure 5.16: Average disconnection time for various E_{max}, $\lambda = [1 - 10]$kbps with $\Delta = 3.4W$.

The same type of impact can be observed for the four parameters for $n = 300, 400$ (for smaller values of n, the system is always immortal), confirming the importance of the choice of Δ and λ over those of E_{max} and v.

5.3 Conclusions

In this chapter, we considered the flexibility of the Continuous Local Learning Strategy proposed in the previous chapter to solve the problem of recharging WSN using a mobile charger. In particular, we studied its flexibility and applicability under a wide range of values of different parameters: number of sensors, $\mathcal{MC}$ speed, sensor's battery-capacity, sensor's data rate, and recharging rate.

We found that with $\lambda = [1 - 5]$ under all choices of the other parameters, the strategy achieved immortality for small network sizes of $n \leq 300$ sensors, that is, no sensor became non-operational even for a small time. Moreover, networks of size $n = 400$ achieved immortality or near-immortality. With $n = 500$, **CLL** achieved

immortality only with $\Delta = 5W$, while with $\Delta = 3.4W$ 95.2% of the sensors were always operational (see Table 5.2).

Furthermore, with $\lambda = [1 - 10]$, networks of size $n \leq 200$ continued to achieve immortality in all settings. Networks of size $n = 300$ achieved immortality with small E_{max} and large Δ, while they were not immortal in other settings but still reaching excellent performances: in fact, at least 98.5% of sensors were always operational in the most undesirable scenario, and their average disconnection time was at most 18.2 hours.

Large networks of size $n = 400$ and $n = 500$ reached immortality only with the combination of ($\Delta = 5W$ and $\lambda = [1 - 5]$), and networks of size $n = 400$ reached near-immortality with the combination ($\Delta = 3.4W$ and $\lambda = [1 - 5]$) while those of size $n = 500$ remained 95.2% operational under the most unfavorable conditions of the other parameters. With $\lambda = [1 - 10]$, large networks of size $n = 400$ and $n = 500$ did not reach immortality nor near-immortality, but their performance was still very good. In fact, at least 93.8% (resp. 90%) of the sensors were always operational in the most undesirable scenario in networks of size $n = 400$ (resp. $n = 500$).

Setting	$\lambda = [1 - 5]$kbps		$\lambda = [1 - 10]$kbps	
	$\Delta = 5W$	$\Delta = 3.4W$	$\Delta = 5W$	$\Delta = 3.4W$
$n \leq 200$	100%	100%	100%	100%
$n = 300$	100%	100%	98.96%	98.5%
$n = 400$	100%	98.47%	97.26%	93.8%
$n = 500$	100%	95.2%	96.6%	90%

Table 5.2: Chapter Summary: operational size under the worst combination of the parameters not shown.

Moreover, we found that the highest impact on the operational size and the disconnection time comes from the recharging rate, followed by the data rate, the $\mathcal{MC}$

velocity and the sensor's battery-capacity.

The results showed the flexibility of this strategy as it adapts well to changes in the system parameters. The success of the method is due to the ability of the mobile charger to "learn" the global distribution of battery discharges.

Chapter 6

Continuous Local Learning vs Periodic Strategies

6.1 Introduction

In the previous chapters, we introduced the new Continuous Local Learning recharging strategy and experimentally analyzed its effectiveness in a variety of contexts. The results have shown that the strategy is highly effective, with the system achieving immortality or near-immortality even for rather large network sizes.

The important attractive feature of **CLL** is that it achieves these results while being simple, highly scalable, and requiring very limited communication and computational capabilities.

As mentioned in Section 3.3, these qualities of simplicity and limited communication are shared also by the class of *periodic* (or *static*) recharging strategies. Recall that, in these strategies, the $\mathcal{MC}$ always visits the nodes (recharging the battery if needed) periodically according to a predetermined order $\mathcal{X}$ (e.g., [30, 33, 35]); except for the

initial pre-computation of $\mathcal{X}$, no other global computation is performed. Hence, the visits by the $\mathcal{MC}$ proceed in an endless sequence of identical rounds; the time spent by the $\mathcal{MC}$ in a round is composed of the time it spends recharging the nodes in need plus the time spent travelling from one node to the next. The latter quantity clearly depends on the chosen order, and it is minimized if $\mathcal{X}$ is an optimal Hamiltonian cycle. We shall denote by **H** a periodic recharging strategy that uses[1] such an order.

While sharing the same features of simplicity, scalability, and minimal communication and computation costs, the class of periodic strategies and **CLL** have a fundamental structural difference: periodic strategies are, by definition, *static* (the recharging order remains unchanged regardless of the current conditions of the network); on the other hand, **CLL** is inherently *adaptive* (the recharging order changes based on the discovered conditions of the network).

The goal of this chapter is to examine the advantages that this difference brings to the effectiveness of **CLL** with respect to the periodic strategies, focusing on the one, **H**, with the minimum amount of travel time.

This chapter is composed of two distinct, but interrelated parts. In the first part (Section 6.2), we show that **CLL** outperforms **H** in terms of number of sensing holes and their duration. We show experimentally that it causes fewer sensing holes to exist at any time; and, more importantly, the duration of a sensing hole is significantly (up to 11 times) lower.

In the second part of the chapter (Sections 6.3-6.3.2), we continue the comparative analysis of **CLL** and the periodic strategies focusing on two settings where the sensors are heterogeneous in the sense that, for a group of nodes located around BS, the energy consumption rate is much higher than the rest. We show that **CLL** outperforms **H** in all cases.

[1]In reality, because of the high computational costs involved, only an approximate solution is employed (e.g., [128]).

Conclusions and discussion on all the results of both parts are in Section 6.4.

6.2 Homogeneous Consumption: Experimental Results

In the experimental analysis, we used the parameters indicated in Table 6.1.

Parameter	**value**
Network Size (n)	100, 200, 300, 400, 500
Sensors' battery-capacity (E_{max})	10.8KJ, 15.98KJ
$\mathcal{MC}$ Speed (v)	2m/s, 5m/s
Data Rate (λ)	[1-5]kbps
Recharging Rate (Δ)	3.4W, 5W

Table 6.1: Simulation parameters.

We now consider separately the operational size and the disconnection time using the two strategies.

6.2.1 Operational Size

First, we consider the case of $\Delta = 5W$. We observed that **CLL** achieves immortality for all network sizes, while **H** achieves immortality for $n \leq 400$ only and for $n = 500$ has about 4 non-operational sensors in all settings (see Figure 6.1).

We consider next the case of $\Delta = 3.4W$.

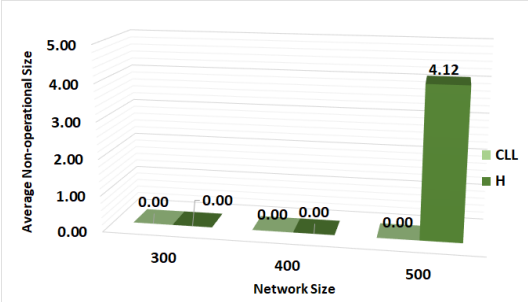

(a) $E_{max} = 10.8KJ, v = 2m/s$.

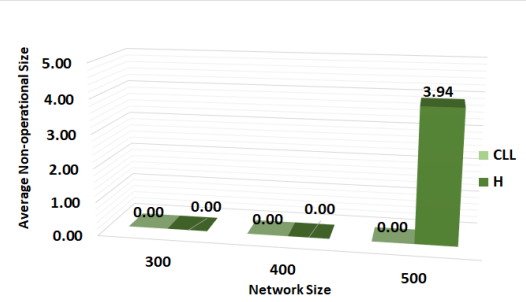

(b) $E_{max} = 10.8KJ, v = 5m/s$.

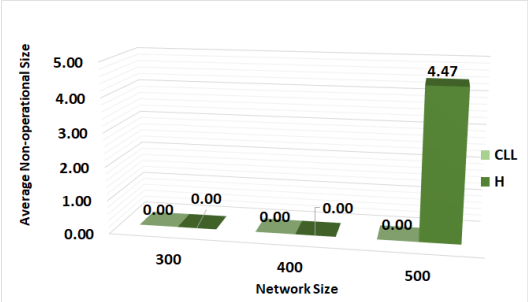

(c) $E_{max} = 15.98KJ, v = 2m/s$.

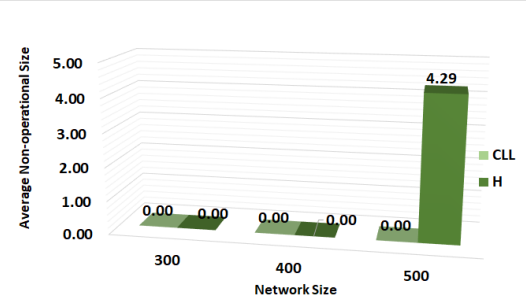

(d) $E_{max} = 15.98KJ, v = 5m/s$.

Figure 6.1: Average non-operational size for $n = 500$ and $\Delta = 5W$.

		Settings$(E_{max}\|v)((KJ\|m/s))$			
Strategy	n	**10.8|2**	**10.8|5**	**15.98|2**	**15.98|5**
CLL	500	23.23	22.14	24.90	23.05
H	500	28.32	27.16	30.17	28.34
CLL	400	5.57	4.71	6.42	5.56
H	400	7.09	6.67	8.28	7.79
CLL	300	0.0	0.0	0.0	0.0
H	300	1.29	0.88	1.5	1.03

Table 6.2: Average non-operational size for $\Delta = 3.4W$.

Both strategies reach immortality under $\Delta = 3.4W$ for $n \leq 200$. We then concentrate on larger networks ($n \geq 300$).

Figure 6.2 and Table 6.2 show the operational size under the four combinations of

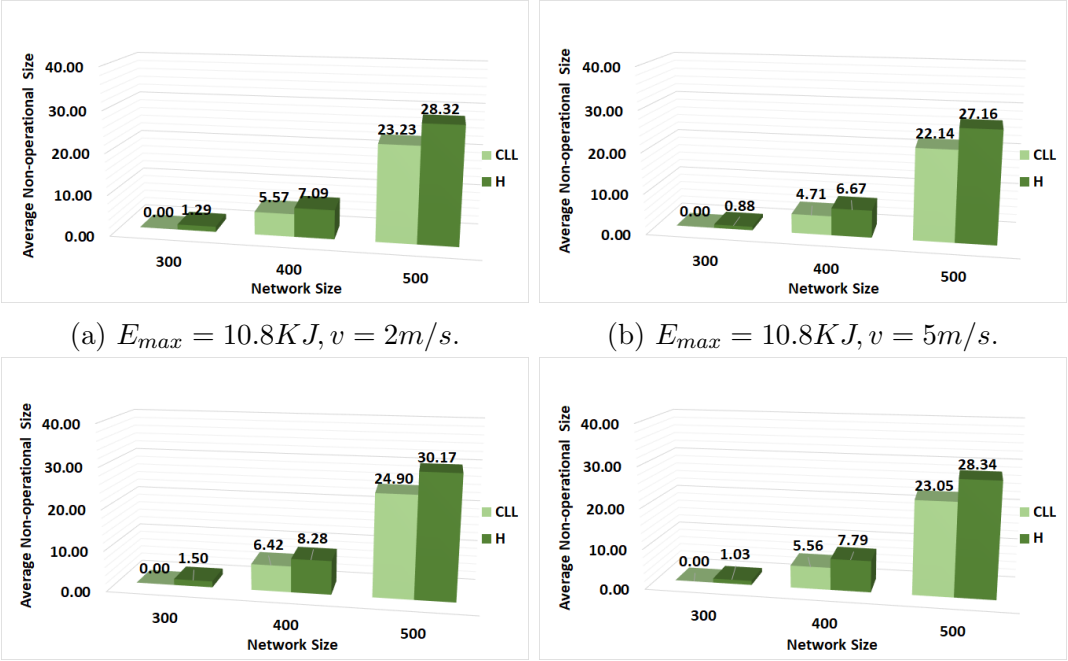

(a) $E_{max} = 10.8KJ, v = 2m/s$. (b) $E_{max} = 10.8KJ, v = 5m/s$.

(c) $E_{max} = 15.98KJ, v = 2m/s$. (d) $E_{max} = 15.98KJ, v = 5m/s$.

Figure 6.2: Average non-operational size for $\Delta = 3.4W$.

E_{max} and v for $n \geq 300$. Let us first observe the impact of the sensors' battery-capacity E_{max} on the performance of both strategies, when the mobile charger speed is fixed.

Figure 6.2 (b) and (d) illustrate the impact of E_{max} when $v = 5m/s$. For $n = 300$, with both battery-capacities $E_{max} = \{10.8KJ, 15.98KJ\}$, **CLL** achieves immortality, while **H** has a small but not null number of non-operational sensors (around 1 sensor). For network size of $n = 400$ and $n = 500$, the difference between the performance of **CLL** and that of **H** becomes more noticeable. In the case of $E_{max} = 15.98KJ$, **CLL** is 1.40 times better than **H** with $n = 400$ and 1.23 times better than **H** with $n = 500$.

A similar behaviour is observable in Figure 6.2 (a) and (c), when $v = 2m/s$. **CLL** reaches immortality for $n = 300$, while **H** has about 1.5 non-operational sensors. For larger networks, considering large $E_{max} = 15.98KJ$ **CLL** outperforms **H** by 1.29 times for $n = 400$ and by 1.21 times for $n = 500$. Looking at the small $E_{max} = 10.8KJ$, we can see that **CLL** is better than **H** by 1.27, and 1.22 times for networks sizes of $n = 400$, and $n = 500$ respectively.

The influence of the $\mathcal{MC}$ speed ($v = 2m/s$ versus $v = 5m/s$) on the performance of **CLL** and **H** can be observed in Figure 6.2 (a) and (b) for ($E_{max} = 10.8KJ$) and (c) and (d) (for $E_{max} = 15.98KJ$). Not surprisingly, a higher $\mathcal{MC}$ speed increases the operational size for both strategies, and they both perform well. Indeed, when $v = 5m/s$, the operational size increases by at least 4.3%.

In conclusion, as expected, the coverage of both **CLL** and **H** deteriorates with the increase of the network size for higher capacity and lower speed; both strategies, however, maintain a good operational size, with **CLL** always outperforming **H**.

6.2.2 Disconnection time

With respect to the average disconnection time, the difference between the two strategies becomes more evident.

For $\Delta = 5W$, as mentioned, **CLL** is immortal for all n. As for **H**, we observe that the disconnection time increased from 9.67 hours for $E_{max} = 10.8KJ$ and $v = 5m/s$ reaching 11.91 hours in case of $E_{max} = 15.98KJ$ and $v = 2m/s$ (see Figure 6.3).

We now consider the influence of the lower recharging rate of $\Delta = 3.4W$ on disconnection time. As mentioned, for $n \leq 200$ both strategies reach immortality. We then concentrate on $n \geq 300$.

		Settings($E_{max}|v$)(($KJ|m/s$))			
Strategy	n	**10.8|2**	**10.8|5**	**15.98|2**	**15.98|5**
CLL	500	25.92	23.65	27.35	24.67
H	500	40.19	38.66	43.79	40.94
CLL	400	8.49	7.46	11.76	8.2
H	400	22.87	22.16	24.9	23.83
CLL	300	0.0	0.0	0.0	0.0
H	300	2.48	1.25	2.82	1.65

Table 6.3: Average disconnection time for $\Delta = 3.4W$.

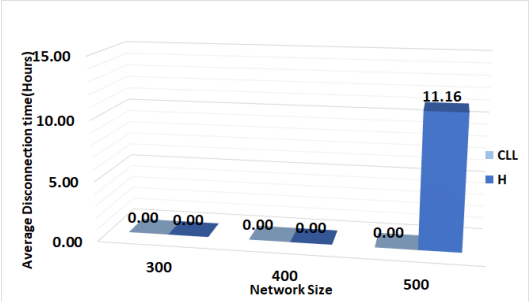

(a) $E_{max} = 10.8KJ, v = 2m/s$.

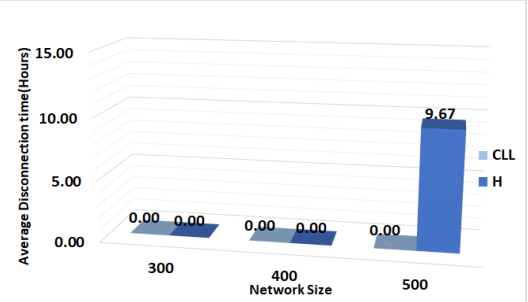

(b) $E_{max} = 10.8KJ, v = 5m/s$.

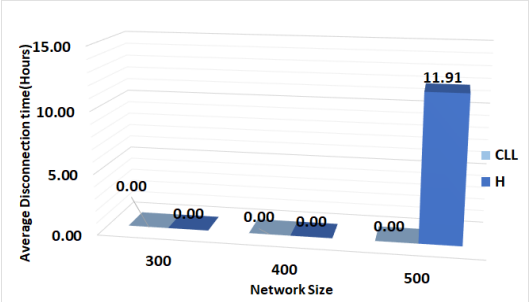

(c) $E_{max} = 15.98KJ, v = 2m/s$.

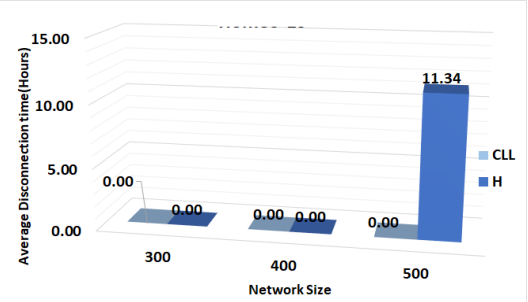

(d) $E_{max} = 15.98KJ, v = 5m/s$.

Figure 6.3: Average disconnection time for $\Delta = 5W$.

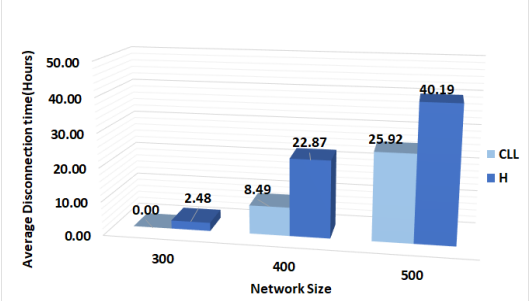

(a) $E_{max} = 10.8KJ, v = 2m/s$.

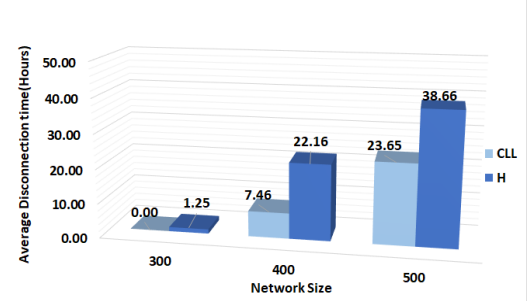

(b) $E_{max} = 10.8KJ, v = 5m/s$.

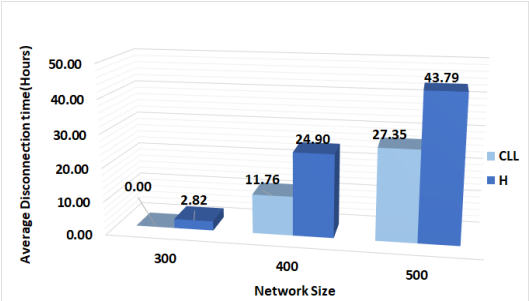

(c) $E_{max} = 15.98KJ, v = 2m/s$.

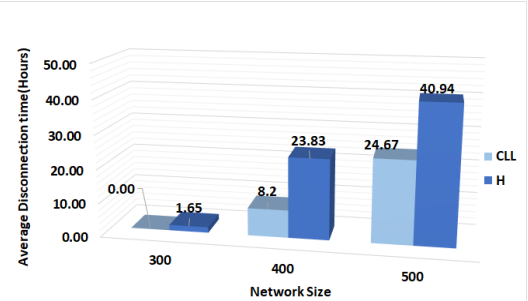

(d) $E_{max} = 15.98KJ, v = 5m/s$.

Figure 6.4: Average disconnection time for $\Delta = 3.4W$.

Figure 6.4 and Table 6.3 show the disconnection time under the four combinations

of E_{max} and v for $n \geq 300$, and we can clearly notice a significant difference between the two strategies.

The influence of the sensors' battery-capacity for both **CLL** and **H** is shown in Figure 6.4 (a) and (c) (when $v = 2m/s$) and in Figure 6.4 (b) and (d) (when $v = 5m/s$). Consider first the case of $E_{max} = 15.98KJ$ and $v = 5m/s$. For a network of size $n = 300$, **CLL** achieves immortality and zero disconnection time, while with **H**, sensors disconnects on average for 1.65 hours. For $n = 400$, **CLL** has an average disconnection time of 8.2 hours (or 4.8% of $T_{E_{max}}$), while **H** has an average disconnection time of around 23.83 hours, which makes **CLL** 2.9 times more efficient than **H**. This disconnection time ratio decreases for $n = 500$ sensors, where **CLL** is 1.66 times better than **H** (24.67 hours versus 40.94 hours). Considering the disconnection time for the smaller $E_{max} = 10.8KJ$ and $v = 5m/s$, naturally, the performance increases compared with the $E_{max} = 15.98KJ$ case. For instance, for $n = 500$, **CLL** leads to 23.65 hours of disconnection time, while **H** reaches 38.66 hours, which means that **CLL** is still 1.65 times more efficient than **H**. The gap between **CLL** and **H** increases for $n = 400$, where in the case of the small E_{max} and high v, the performance of **CLL** is about 2.97 times better than that of **H** (**CLL** has an average disconnection time of about 7.46 hours, while **H** has about 22.16 hours average disconnection time).

The influence of the speed of the $\mathcal{MC}$ for both **CLL** and **H** is shown in Figure 6.4 (a) and (b) (for $E_{max} = 10.8KJ$) and Figure 6.4 (c) and (d) (for $E_{max} = 15.98KJ$). In particular, when $E_{max} = 10.8KJ$, we noticed that **CLL** achieves at least 1.55 times better results than **H** for all settings. For instance, in a network size of $n = 500$ with $E_{max} = 10.8KJ$ and $v = 2m/s$, **CLL** has an average disconnection time of 25.92 hours in comparison to 40.19 hours in the case of **H** for the same setting. In a network size of $n = 400$ with $E_{max} = 10.8KJ$ and $v = 2m/s$, the difference is even more noticeable because **CLL** has almost three times the average disconnection time of **H** for the same setting (8.49 hours versus 22.49 hours).

6.2.3 Summary

With the standard $\Delta = 5W$, **CLL** achieves immortality for all values of the other parameters; on the other hand, **H** achieves immortality only for the networks of size $n \leq 400$, and it is near-immortal for $n = 500$.

The difference between the performance of the two strategies appears more clearly when using the smaller recharging rate of $\Delta = 3.4W$. In fact, smaller networks ($n = 100$ and $n = 200$) remain immortal with both strategies, and **CLL** continues to achieve immortality even for $n = 300$; moreover, for larger networks ($n \geq 400$) **CLL** outperforms **H** under all the different scenarios.

6.3 Heterogeneous Energy Consumption

In all preceding chapters and sections, we considered sensor nodes with homogeneous consumption behaviour; that is, as usually done in the literature, we considered that the energy consumption rates of all nodes follow the same Poisson distribution.

In the rest of this chapter, we explore the case when there might be more than one consumption behaviour among the nodes. More precisely, we study sensor networks where there are two different energy consumption rates, with some of the nodes following one range while the rest follows the other range.

We analyze how this heterogeneous consumption behaviour impacts the efficiency of our strategy, **CLL**, in comparison with the periodic strategy **H**.

We first consider the situation (Scenario **A**), where for one group of nodes, the energy consumption rate is as studied in the previous sections while, for the second group, located[2] around the BS, the consumption rate is double. We then investigate

[2]It is realistic to assume that nodes around the BS consume energy at a higher rate than the other

the situation (Scenario **B**) where the consumption rate of the second group is even higher: five times that of the first group.

6.3.1 Heterogeneous Consumption: Scenario A

In this section, the data rate of the sensors, within 300 meters from the BS is doubled; all the other parameters are as shown in Table 6.1. We study both **CLL** and **H** under this new setting.

6.3.1.1 Operational Size

The experimental results show that, with the standard $\Delta = 5W$, **CLL** continues to achieve immortality for networks of size $n \leq 400$, and near-immortality for those of size $n = 500$ (with 4.36 non-operational sensors in the most undesirable setting). On the other hand, **H** achieves immortality for networks of size $n \leq 300$, it has a very small non-operational size for networks of size $n = 400$. For networks of size $n = 500$, it has a double non-operational size in comparison to **CLL** (See Table 6.4 and Figure 6.5).

		Settings$(E_{max}\|v)((KJ\|m/s))$			
Strategy	n	**10.8|2**	**10.8|5**	**15.98|2**	**15.98|5**
CLL	500	4.17	4.02	4.36	4.21
H	500	8.62	8.49	8.92	8.78
CLL	400	0.0	0.0	0.0	0.0
H	400	0.25	0.19	0.45	0.38

Table 6.4: Average non-operational size in scenario A, $\Delta = 5W$.

In the rest of this section we focus on the case of $\Delta = 3.4W$. For $n = 100$ and

sensors in the network because they relay more packets toward the BS [96, 132].

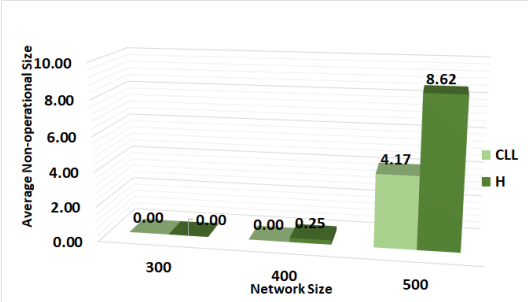

(a) Scenario A - $E_{max} = 10.8KJ, v = 2m/s$.

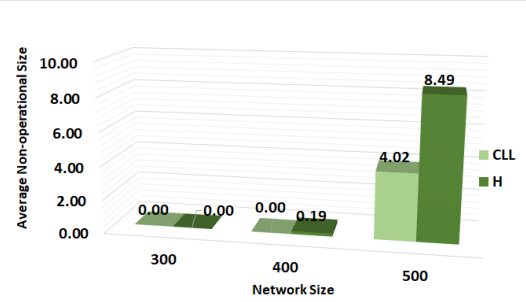

(b) Scenario A - $E_{max} = 10.8KJ, v = 5m/s$.

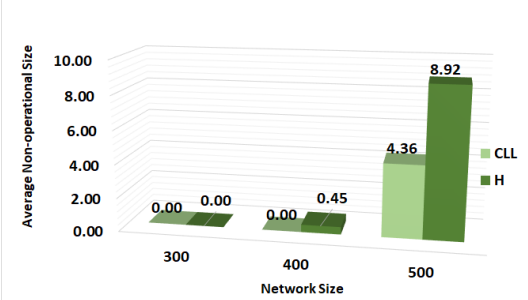

(c) Scenario A - $E_{max} = 15.98KJ, v = 2m/s$.

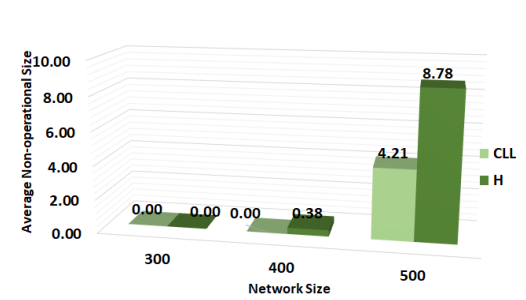

(d) Scenario A - $E_{max} = 15.98KJ, v = 5m/s$.

Figure 6.5: Average non-operational size for scenario A with $\Delta = 5W$.

$n = 200$, both strategies reach immortality. We then concentrate on larger networks ($n \geq 300$).

		Settings($E_{max}|v$)(($KJ|m/s$))			
Strategy	n	**10.8|2**	**10.8|5**	**15.98|2**	**15.98|5**
CLL	500	24.46	23.06	25.20	23.25
H	500	30.24	28.78	30.97	29.14
CLL	400	6.32	5.66	7.13	5.72
H	400	8.54	8.12	9.53	8.58
CLL	300	0.0	0.0	0.0	0.0
H	300	2.14	1.82	2.58	2.12

Table 6.5: Average non-operational size in scenario A with $\Delta = 3.4W$.

Figure 6.6 shows the non-operational size under the four combinations of E_{max} and v for $n \geq 300$. By using a fixed $v = 5m/s$ and varying E_{max}, we noticed that for

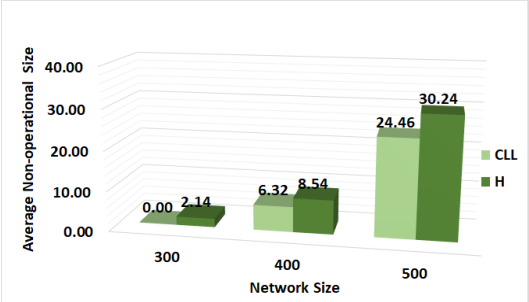

(a) Scenario A - $E_{max} = 10.8KJ, v = 2m/s$.

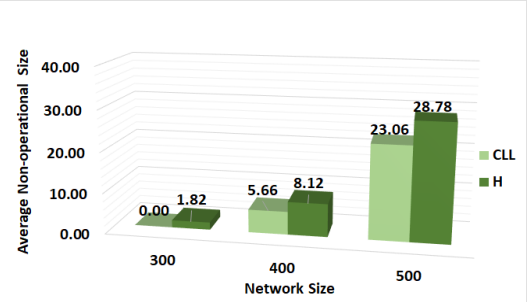

(b) Scenario A - $E_{max} = 10.8KJ, v = 5m/s$.

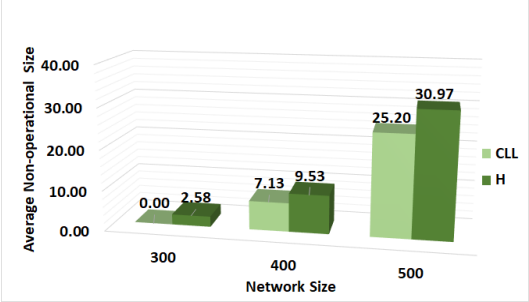

(c) Scenario A - $E_{max} = 15.98KJ, v = 2m/s$.

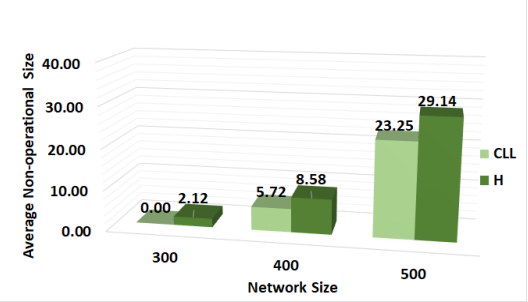

(d) Scenario A - $E_{max} = 15.98KJ, v = 5m/s$.

Figure 6.6: Average non-operational size for scenario A with $\Delta = 3.4W$.

$n = 500$ and the large $E_{max} = 15.98KJ$, **CLL** performs 1.25 times better than **H**. For a network size of $n = 400$ and with large $E_{max} = 15.98KJ$, the number of non-operational sensors increases using both strategies: with **CLL**, 5.72 sensors become non-operational, in average, while with **H**, the number of non-operational sensors reaches 8.58. Also, as expected, the coverage of both **CLL** and **H** decreases with the increase of the network size; both strategies maintain a good operational size, but **CLL** always outperforms **H**.

By using a fixed $E_{max} = 10.8KJ$ and varying the $\mathcal{MC}$ speed, we noticed that higher speed achieves better results for both strategies, and **CLL** continues to outperform **H**.

6.3.1.2 Disconnection Time

Like in the homogeneous case, in this setting, we also observed that the disconnection time reveals a more significant difference between the two strategies, with **CLL** always maintaining a significantly lower disconnection time.

		Settings$(E_{max}\|v)((KJ\|m/s))$			
Strategy	n	**10.8|2**	**10.8|5**	**15.98|2**	**15.98|5**
CLL	500	6.86	6.32	7.46	7.10
H	500	16.84	16.23	17.52	17.26
CLL	400	0.0	0.0	0.0	0.0
H	400	1.45	1.12	2.23	1.86

Table 6.6: Average disconnection time in scenario A with $\Delta = 5W$.

In case of $\Delta = 5W$, we observe that **CLL** has null disconnection time for networks of size $n \leq 400$ while **H** has small disconnection time (i.e., less than 2 hours). Moreover **CLL** achieves around 2.5 times better than **H** in terms of disconnection time for networks of size $n = 500$ (see Table 6.6 and Figure 6.7).

Consider now the case of $\Delta = 3.4W$ (see Table 6.7 and Figure 6.8).

The influence of E_{max} on the disconnection time for both strategies is shown in Figures 6.8 (a) and (c) as well as in (b) and (d), while the impact of the $\mathcal{MC}$ speed on the performance of both strategies is shown in Figures 6.8 (a) and (b), as well as in (c) and (d).

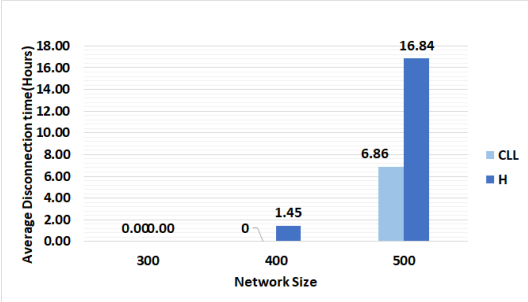

(a) Scenario A - $E_{max} = 10.8KJ, v = 2m/s$.

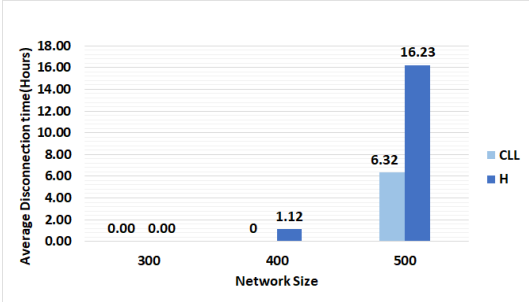

(b) Scenario A - $E_{max} = 10.8KJ, v = 5m/s$.

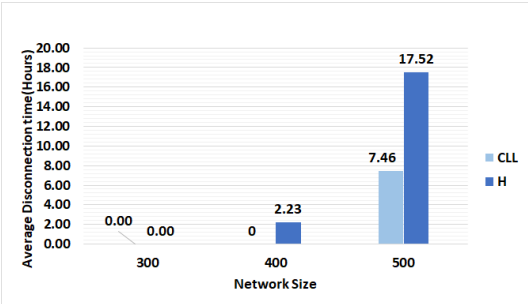

(c) Scenario A - $E_{max} = 15.98KJ, v = 2m/s$.

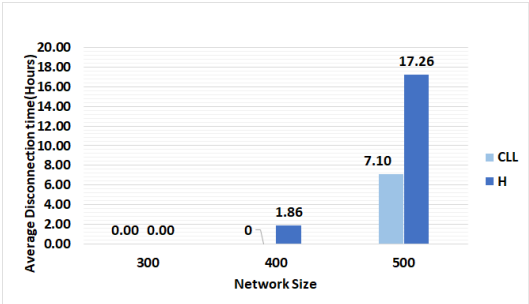

(d) Scenario A - $E_{max} = 15.98KJ, v = 5m/s$.

Figure 6.7: Average disconnection time in scenario A with $\Delta = 5W$.

		Settings$(E_{max}\|v)(KJ\|m/s)$			
Strategy	n	**10.8|2**	**10.8|5**	**15.98|2**	**15.98|5**
CLL	500	27.28	24.12	28.35	24.73
H	500	42.88	39.89	44.39	41.64
CLL	400	11.22	8.64	13.12	8.98
H	400	26.24	25.06	28.24	27.05
CLL	300	0.0	0.0	0.0	0.0
H	300	3.86	3.54	4.22	3.88

Table 6.7: Average disconnection time in scenario A with $\Delta = 3.4W$.

We noticed that in a network size of $n = 500$ sensors, for $v = 5m/s$ and $E_{max} = 15.98KJ$, **CLL** induces a disconnection time that is 1.68 times lower than that induced by **H** (24.73 hours versus 41.64 hours), while for $E_{max} = 10.8KJ$ with the same speed, the disconnection time created by **CLL** is 1.65 lower than that induced by **H**. More

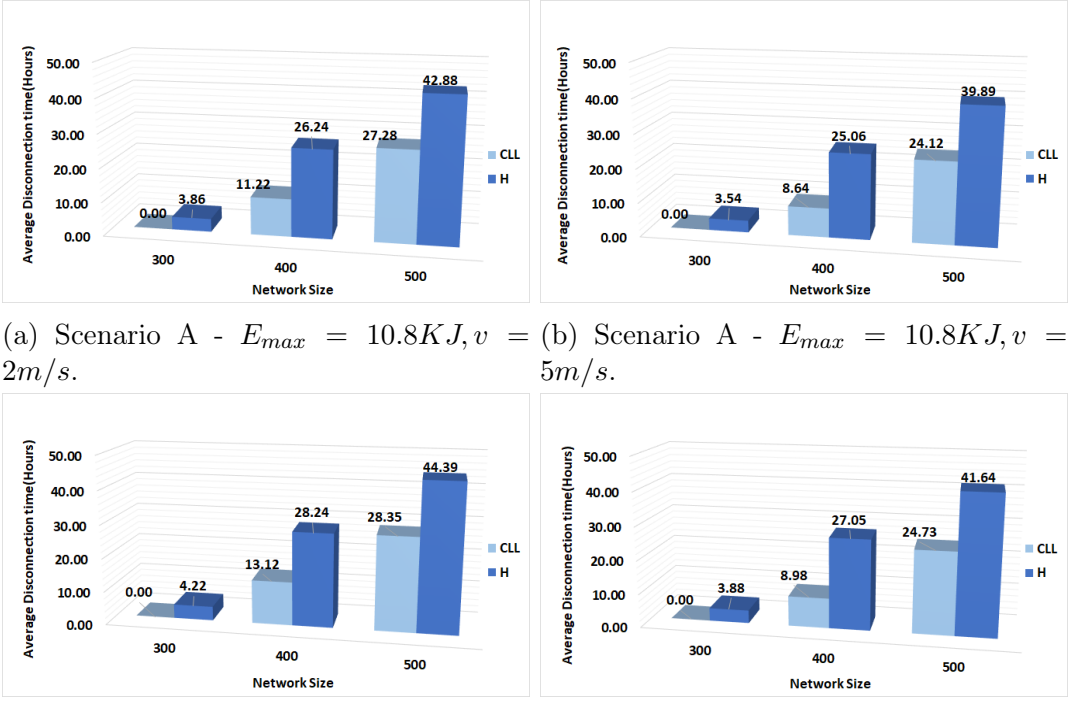

(a) Scenario A - $E_{max} = 10.8KJ, v = 2m/s$.

(b) Scenario A - $E_{max} = 10.8KJ, v = 5m/s$.

(c) Scenario A - $E_{max} = 15.98KJ, v = 2m/s$.

(d) Scenario A - $E_{max} = 15.98KJ, v = 5m/s$.

Figure 6.8: Average disconnection time in scenario A with $\Delta = 3.4W$.

significant difference between the performance of the two strategies was observed in the case of $n = 400$, with $v = 5m/s$ and $E_{max} = 15.98KJ$: in this case, the disconnection time induced by **H** (27.05 hours) is more than 3 times higher than that of **CLL** (8.98 hours). Similarly, still with $v = 5m/s$ but with the lower $E_{max} = 10.8KJ$, **CLL** performs 2.9 times better than **H** (8.64 hours versus 25.06 hours).

6.3.2 Heterogeneous Consumption: Scenario B

In this section, the data rate of the sensors, within 300 meters from the BS is 5 times that of the others; all the other parameters are as in Table 6.1. We studied both **CLL** and **H** under this new setting.

6.3.2.1 Operational Size

Let us first study the non-operational size in case of $\Delta = 5W$ under scenario B. As expected, the new setting increases the non-operational size for both strategies. We observed that both strategies continue to achieve immortality for networks of size $n \leq 300$. For those of size $n = 400$, **CLL** is at least 7 times better than **H** (0.46 sensors versus 3.39 sensors). **CLL** is around 1.68 better than **H** for networks of size $n = 500$ (see Table 6.8 and Figure 6.9).

		Settings$(E_{max}\|v)(KJ\|m/s)$			
Strategy	n	**10.8|2**	**10.8|5**	**15.98|2**	**15.98|5**
CLL	500	8.56	8.36	8.72	8.57
H	500	14.36	14.08	14.79	14.43
CLL	400	0.32	0.28	0.46	0.41
H	400	3.13	2.98	3.39	3.29

Table 6.8: Average disconnection time in scenario B with $\Delta = 5W$.

We now focus on the impact of $\Delta = 3.4W$ in Scenario B (see Table 6.9 and Figure 6.10 where the results of the experimental study for both strategies are shown for the four combinations of E_{max} and v). In particular, we concentrated on the results for $n \geq 300$ since smaller networks continue to achieve immortality with both strategies.

		Settings$(E_{max}\|v)(KJ\|m/s)$			
Strategy	n	**10.8|2**	**10.8|5**	**15.98|2**	**15.98|5**
CLL	500	28.68	25.78	29.53	26.12
H	500	36.46	35.14	39.12	35.90
CLL	400	8.62	6.98	9.17	7.32
H	400	13.27	12.46	14.44	13.40
CLL	300	0.55	0.48	0.66	0.59
H	300	3.08	2.92	3.57	3.39

Table 6.9: Average non-operational size in scenario B with $\Delta = 3.4W$.

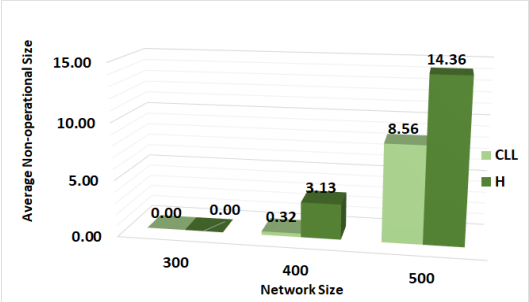

(a) Scenario B - $E_{max} = 10.8KJ, v = 2m/s$.

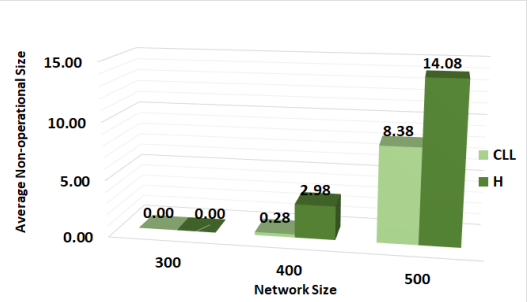

(b) Scenario B - $E_{max} = 10.8KJ, v = 5m/s$.

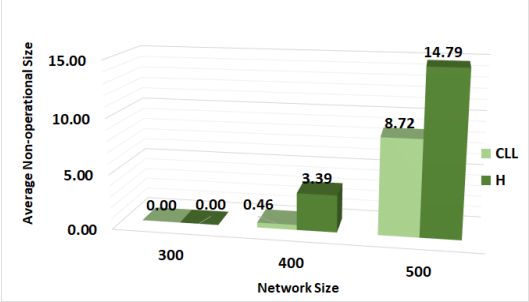

(c) Scenario B - $E_{max} = 15.98KJ, v = 2m/s$.

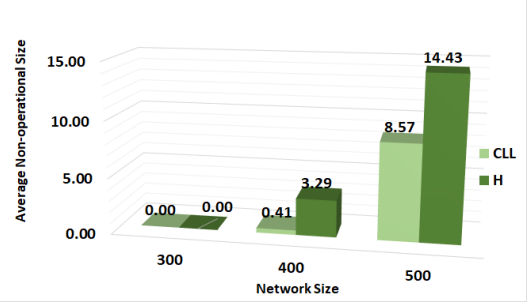

(d) Scenario B -$E_{max} = 15.98KJ, v = 5m/s$.

Figure 6.9: Average non-operational size in scenario B with $\Delta = 5W$.

For $n = 500$, $E_{max} = 15.98KJ$ and $v = 5m/s$, **CLL** performs 1.37 times better than **H** (26.12 non-operational sensors versus 35.9). Similar rates of improvements are observed with the other combinations of E_{max} and v. For networks of size $n = 400$, with $E_{max} = 15.98KJ$ and $v = 5m/s$, the number of non-operational sensors is 1.83 times larger with **H**; also, using the smaller $E_{max} = 10.8KJ$ maintaining the same v, **CLL** is 1.79 times better than **H**. Similar ratios were observed for the other combinations of parameters. In the case of $n = 300$, the difference between **CLL** and **H** in terms of operational size is more noticeable; in all settings, **CLL** is between 5 and 6 times better than **H**.

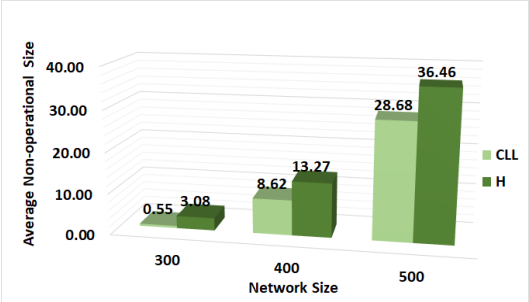

(a) Scenario B - $E_{max} = 10.8KJ, v = 2m/s$.

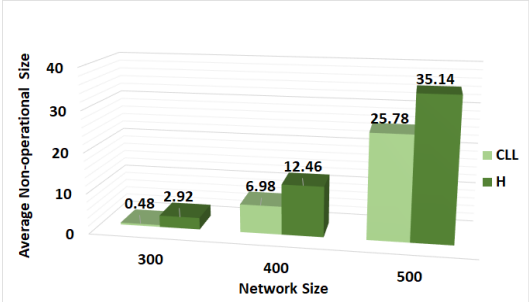

(b) Scenario B - $E_{max} = 10.8KJ, v = 5m/s$.

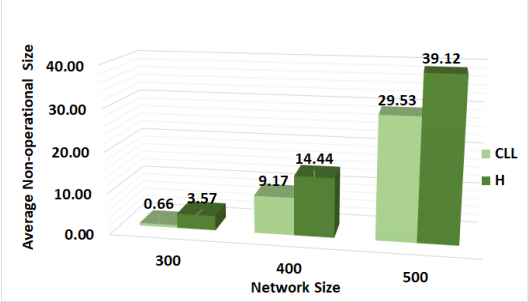

(c) Scenario B - $E_{max} = 15.98KJ, v = 2m/s$.

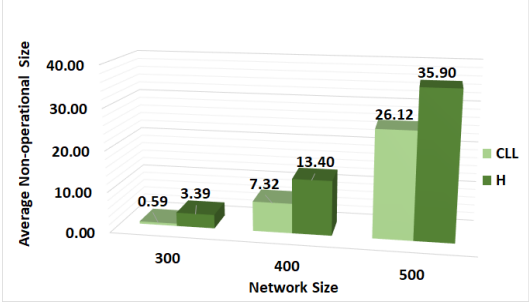

(d) Scenario B -$E_{max} = 15.98KJ, v = 5m/s$.

Figure 6.10: Average non-operational size in scenario B with $\Delta = 3.4W$.

6.3.2.2 Disconnection time

Similarly to what happened in Scenario A, we observed that the disconnection time shows a more significant difference between the two strategies.

Observing the impact of Scenario B on the disconnection time with $\Delta = 5W$ (see Table 6.10 and Figure 6.11), we notice that disconnection time is clearly null for immortal networks of size $n \leq 300$ for both strategies. With networks of size $n = 400$, **CLL** is 10 times better than **H** in the most undesirable setting ($E_{max} = 15.98KJ$ and $v = 2m/s$) where the disconnection time is equal to 0.87 hours for **CLL** while it is equal to 9.19 hours in the case of **H**. For networks of size $n = 500$, **CLL** is better than **H** by 2 to 2.8 times.

		Settings($E_{max}\|v$)($KJ\|m/s$)			
Strategy	n	**10.8|2**	**10.8|5**	**15.98|2**	**15.98|5**
CLL	500	14.39	13.96	14.88	14.42
H	500	30.15	29.22	31.02	30.58
CLL	400	0.74	0.68	0.87	0.78
H	400	8.16	7.76	9.19	8.84

Table 6.10: Average disconnection time in scenario B with $\Delta = 5W$.

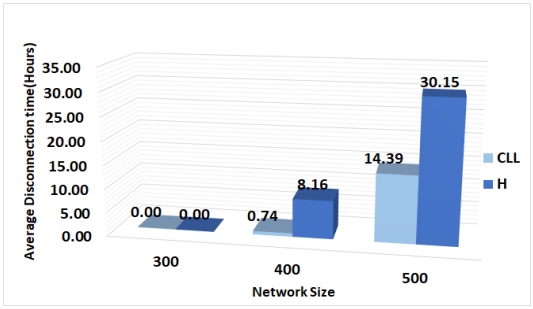

(a) Scenario B - $E_{max} = 10.8KJ, v = 2m/s$.

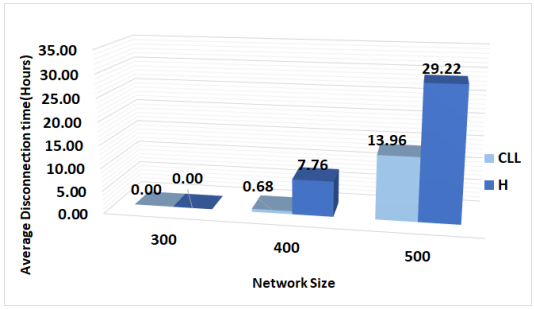

(b) Scenario B - $E_{max} = 10.8KJ, v = 5m/s$.

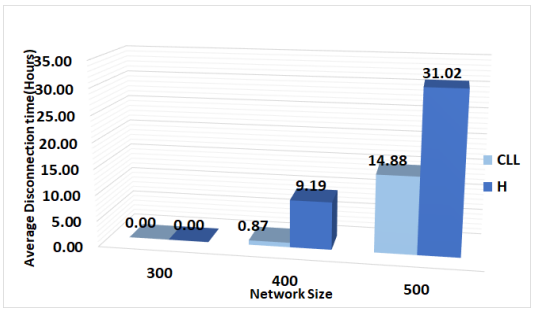

(c) Scenario B - $E_{max} = 15.98KJ, v = 2m/s$.

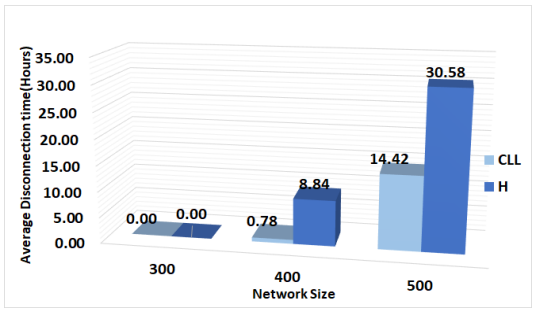

(d) Scenario B - $E_{max} = 15.98KJ, v = 5m/s$.

Figure 6.11: Average disconnection time in scenario B with $\Delta = 5W$.

Table 6.11 shows the disconnection time numerical results for large networks $n \geq 300$ with $\Delta = 3.4W$.

Strategy	n	Settings(E_{max}|v)(KJ|m/s) 10.8|2	10.8|5	15.98|2	15.98|5
CLL	500	32.56	28.98	36.18	33.49
H	500	56.88	55.24	59.64	57.62
CLL	400	14.76	10.56	15.96	11.19
H	400	35.34	34.52	36.98	34.47
CLL	300	1.06	0.92	1.23	1.08
H	300	7.58	6.33	7.98	6.88

Table 6.11: Average disconnection time in scenario B with $\Delta = 3.4W$.

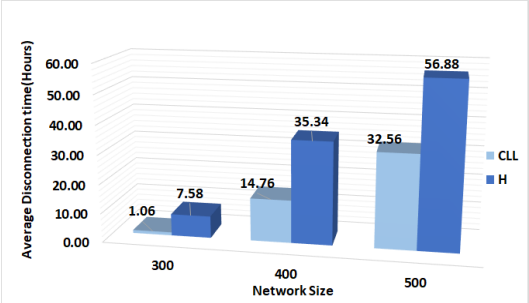

(a) Scenario B - $E_{max} = 10.8KJ, v = 2m/s$.

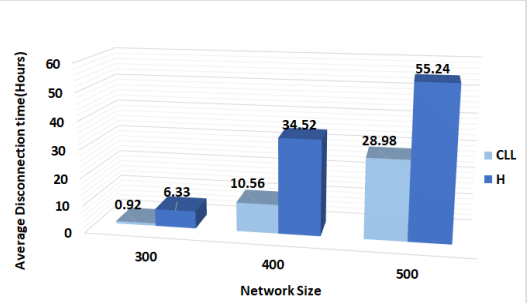

(b) Scenario B - $E_{max} = 10.8KJ, v = 5m/s$.

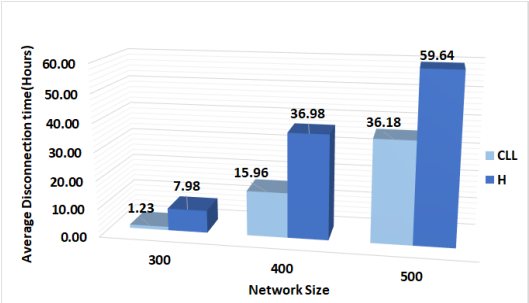

(c) Scenario B - $E_{max} = 15.98KJ, v = 2m/s$.

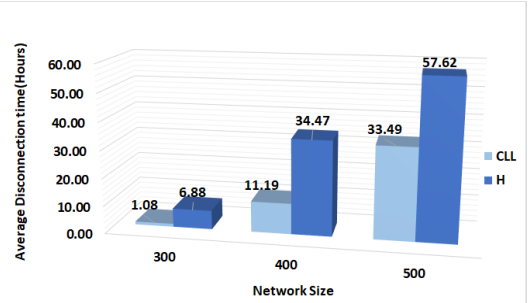

(d) Scenario B - $E_{max} = 15.98KJ, v = 5m/s$.

Figure 6.12: Average disconnection time in scenario B with $\Delta = 3.4W$.

Figure 6.12 shows the results under the four combinations of parameters for $n \geq 300$. Like in the homogeneous case and in Scenario A, the network size of $n = 300$ reveals the highest difference between the performance of **CLL** and that of **H**. For $E_{max} = 15.98KJ$, **CLL** performs 6.5 and 6.4 times better than **H** with $v = 5m/s$ and $v = 2m/s$ respectively. Considering $E_{max} = 10.8KJ$, the disconnection time

with **H** is about 7 times larger than the one of **CLL**. Also in the case of $n = 400$, $E_{max} = 15.98KJ$ and $v = 5m/s$, the discrepancy between the two strategies is very noticeable. The disconnection time induced by **CLL** is 11.19 hours, which is 3 times better than that of **H** (34.47 hours), while it performs 3.27 times better than **H** with the same speed but lower $E_{max} = 10.8KJ$ (10.56 hours versus 34.52 hours). Finally, looking at the results of the low $\mathcal{MC}$ speed, $v = 2m/s$, and $E_{max} = 10.8KJ$, we observed that the disconnection time for a network size of $n = 500$ is 32.56 hours for **CLL**, while it is 55.24 hours for **H**, which means that **CLL** is 1.75 times better than **H**. In networks of size $n = 400$, the ratio between the two strategies increases to 2.39 (14.76 hours in the case of **CLL** and 35.34 hours in the case of **H**).

6.4 Discussion and Conclusions

In all considered scenarios, **CLL** outperforms **H** under all settings.

Tables (6.12 and 6.13) show the comparison between the two strategies under $\Delta = 5W$ in the worst case setting for each scenario. In the Homogeneous scenario, **CLL** always achieves immortality, for any network size, while in networks of size $n = 500$ **H** has at any time about 4 non-operational sensors, each disconnected for about 11 hours. In scenario A, **CLL** achieves immortality for networks of size $n \leq 400$ where **H** is near-immortal; with $n = 500$, **CLL** is almost 2 times better than **H** in non-operational size and disconnection time. In scenario B, for $n = 400$ both strategies become near-immortal but **CLL** is at least 7 times better in terms of operational size (0.46 non-operational sensor versus 3.39); for $n = 500$ **CLL** is almost twice as good as **H**.

		Scenarios		
Strategy	n	**Homogeneous**	**ScenarioA**	**ScenarioB**
CLL	500	0.0	4.36	8.72
H	500	4.47	8.92	14.79
CLL	400	0.0	0.0	0.46
H	400	0.0	0.45	3.39

Table 6.12: Average non-operational size of worst case settings with $\Delta = 5W$.

		Scenarios		
Strategy	n	**Homogeneous**	**ScenarioA**	**ScenarioB**
CLL	500	0.0	9.46	14.88
H	500	11.91	17.52	31.02
CLL	400	0.0	0.0	0.87
H	400	0.0	2.23	9.19

Table 6.13: Average disconnection time of worst case settings with $\Delta = 5W$.

In the case of $\Delta = 3.4W$, the impact of the variable settings on the efficiency of the strategies as well as the difference between the performance of **CLL** and that of **H** are particularly evident when observing the disconnection time. In particular, we observe the following:

- In all settings, **CLL** always outperforms **H**. See Figures 6.13, 6.14, 6.15, which show the disconnection time of the three settings (Homogeneous, Scenario A and Scenario B) under the four combinations of E_{max} and v for both **CLL** and **H** for $n = 300$, $n = 400$ and $n = 500$ respectively.

- From all the experiments, it is evident that both the sensors' battery-capacity E_{max} and the $\mathcal{MC}$ speed v influence the performance of both strategies. Clearly, the combination of $E_{max} = 10.8KJ$ and $v = 5m/s$ is the most advantageous, while the combination of $E_{max} = 15.98KJ$ and $v = 2m/s$ is the worst. On

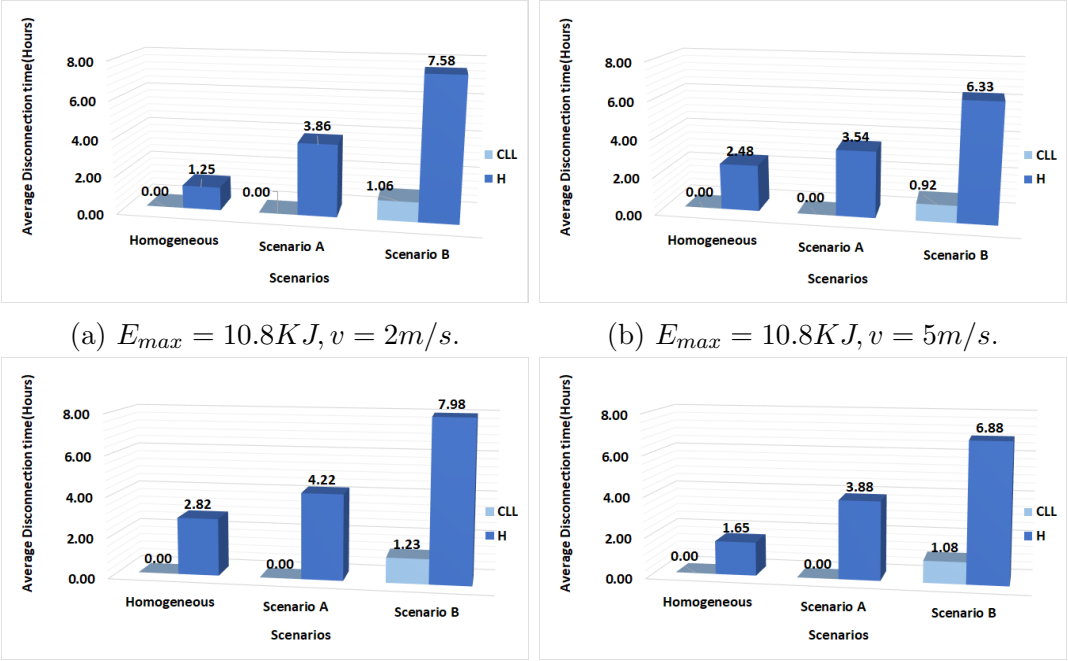

(a) $E_{max} = 10.8KJ, v = 2m/s$. (b) $E_{max} = 10.8KJ, v = 5m/s$.

(c) $E_{max} = 15.98KJ, v = 2m/s$. (d) $E_{max} = 15.98KJ, v = 5m/s$.

Figure 6.13: Average disconnection time for various settings and scenarios for n=300 with $\Delta = 3.4W$.

the other hand, all the results for all network sizes show that the combination of $E_{max} = 15.98KJ$ and $v = 5m/s$ leads to better performance than the combination of $E_{max} = 10.8KJ$ and $v = 2m/s$ (see Figures 6.13, 6.14, and 6.15). This indicates that, with the considered values of the various parameters, the $\mathcal{MC}$ speed has a stronger impact on both operational size and disconnection time than the sensors' battery-capacity; this is particularly evident when observing the disconnection time.

- As we already observed, **CLL** always outperforms **H**. Interestingly, the difference in the disconnection time between **CLL** and **H** grows when moving from the Homogeneous setting to Scenario A to Scenario B, indicating a higher adaptability of **CLL** to changes in the sensors' consumption rate (see Figure 6.16). This occurs in all four combinations of E_{max} and v.

The last observation hints at the adaptiveness of **CLL** to changes in the sensors'

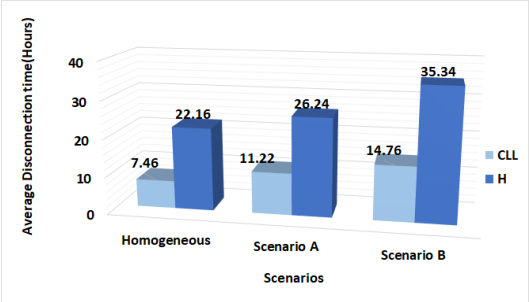

(a) $E_{max} = 10.8KJ, v = 2m/s$.

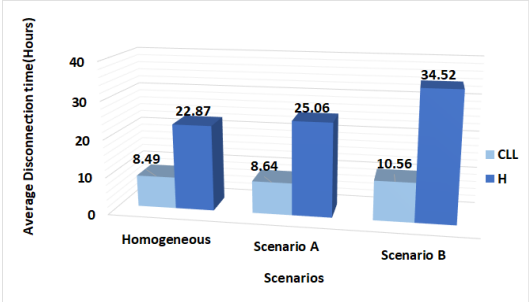

(b) $E_{max} = 10.8KJ, v = 5m/s$.

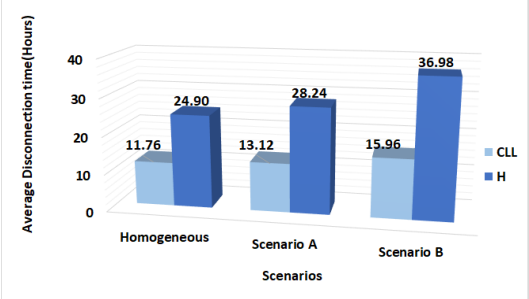

(c) $E_{max} = 15.98KJ, v = 2m/s$.

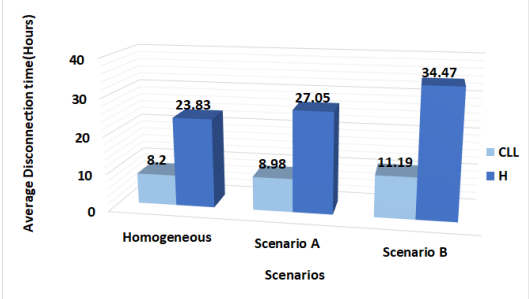

(d) $E_{max} = 15.98KJ, v = 5m/s$.

Figure 6.14: Average disconnection time for various settings and scenarios for n=400 with $\Delta = 3.4W$.

consumption, further considered in the next chapter.

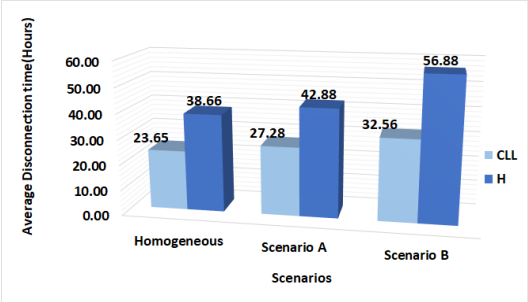

(a) $E_{max} = 10.8KJ, v = 2m/s$.

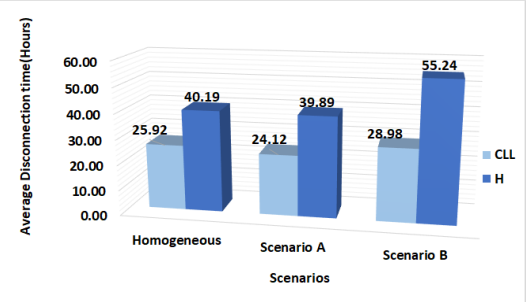

(b) $E_{max} = 10.8KJ, v = 5m/s$.

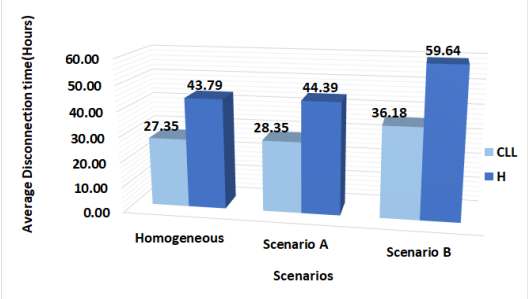

(c) $E_{max} = 15.98KJ, v = 2m/s$.

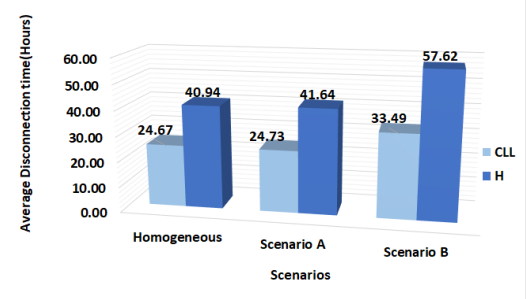

(d) $E_{max} = 15.98KJ, v = 5m/s$.

Figure 6.15: Average disconnection time for various settings and scenarios for n=500 with $\Delta = 3.4W$.

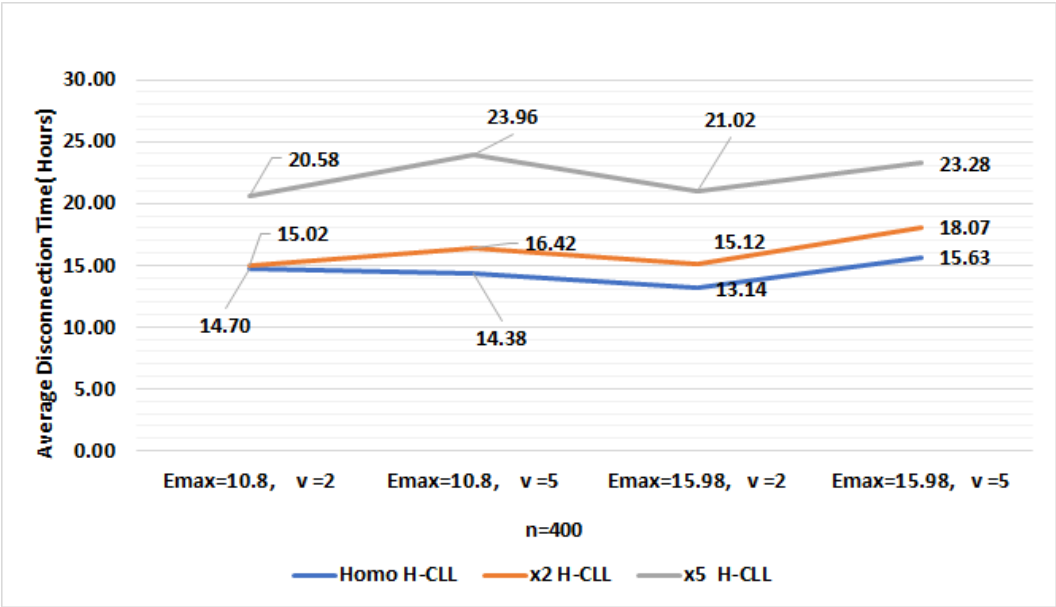

Figure 6.16: Numerical difference between disconnection time of **H** and **CLL** in the 3 scenarios, with $\Delta = 3.4W$, and $n = 400$.

Chapter 7

Adaptiveness of Continuous Local Learning Strategy

7.1 Introduction

Although the WRSN that we considered is composed of static nodes (i.e., they do not move), a network is typically dynamic in other ways with many changes expected to occur during its operations. Indeed, the amount of transmission and reception operations performed by a node (and thus its battery consumption) may change in time (possibly in dramatic ways), depending on the changes in the monitored environment. In particular, sudden changes in data rate (spikes) may severely impact the nodes, in terms of energy consumption, and thus network performance. Thus, it is important for the recharging strategy to adapt to these changes, modifying its behaviour in an automatic and seamless way; ideally, its overall effectiveness should persist, except possibly for a very limited amount of time.

In this chapter, we study the effectiveness of the Continuous Local Learning Strategy, under the system settings of Chapter 4, in presence of sudden changes in data

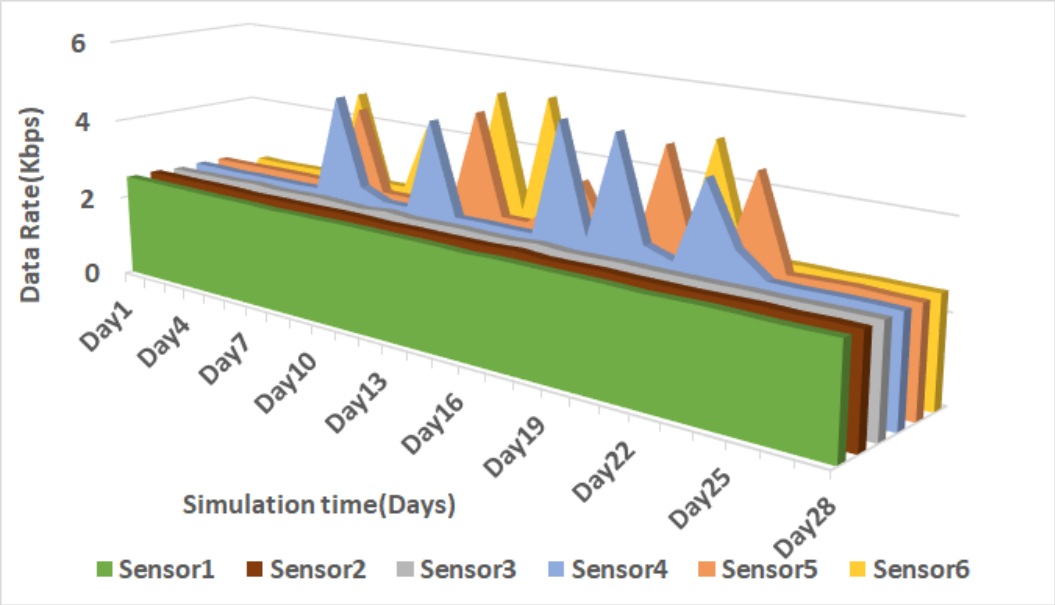

Figure 7.1: Illustration of spikes characteristics.

rate, called *spikes*.

Spikes have four characteristics: *Spread*, *Intensity*, *Duration*, and *Occurrence*. We define below each one of these terms.

- **Spike Spread (S):** refers to the percentage of the number of sensors (out of n) that are affected by the spikes. For example, in Figure 7.1, the spikes spread is 50% (3 out of 6 sensors are affected by spikes).
- **Spike Occurrence (O) :** refers to the number of spikes experienced by the affected sensor. For example, in Figure 7.1, $O = 5$ (each affected sensor is affected by five spikes).
- **Spike Duration (D) :** refers to the duration of each spike. In the illustration figure and in the rest of the chapter, each spike lasts for one day.
- **Spike Intensity (I) :** In previous chapters, we used data rates generated using a Poisson distribution range of $[1-5]$kbps. In this chapter, we will use the same rate $\lambda \in [1-5]$ kbps for normal sensors and a multiple of λ for the spikes.

The spike intensity refers to the multiplicative factor of the spike data rate in comparison with the normal data rate.

The effectiveness and adaptiveness of **CLL** in presence of spikes under the above spike parameters is examined in the next section; the experimental results indicate that **CLL** is capable of adapting and coping with the sudden presence of spikes with little impact on operational size and disconnection time.

We also examine, in Section 7.3, the different impact the presence of spikes has on **CLL** with respect to that it has on the static recharging strategy **H**, examined in the previous Chapter. The experimental results indicate that **CLL** outperforms **H** also in presence of spikes.

7.2 Experimental Analysis

In this section we discuss the effectiveness and adaptiveness of **CLL** to the presence of spikes under various spike parameters.

We first study the effectiveness of **CLL** when varying Spread and Occurrence while fixing the Intensity of the spikes to the worst case. We then observe the performances when considering the worst case condition for the Occurrence parameter while varying Spread and Intensity.

7.2.1 Simulation Environment

In the experimental analysis, we used the system parameters employed in Chapter 4, and summarized in Table 7.1.

To study the performance of the spikes, and in particular the impact of each parameter of the spikes, we consider a range of spike parameters. Specifically, we consider

Parameter	Default setting
n	100, 200, 300,400, 500
E_{max}	10.8 KJ
v	5m/s
Δ	3.4 W, 5 W
λ	[1-5]kbps

Table 7.1: Simulation parameters.

Parameter	Values
Duration	1 Day
Occurrence O	3, 5
Intensity I	1.5, 2, 3
Spread S	10%, 20%, 30%, 50%

Table 7.2: Spikes settings

that an intensity I of the spikes 1.5, 2, and 3 times the default data rate. Another important variable is the occurrence of the spike O, and we consider the cases of 3 and 5 occurrences. The sensors affected by spikes are randomly chosen with a spread S being a ratio of the network size that varies from 10% to 50%. Finally, every time a spike occurs, we assume it lasts for 24 hours, which is the spike duration D. All the considered values of the spike parameters are shown in Table 7.2.

In the following, when we refer to the *default* setting, we mean the setting where no spikes are present (i.e., $I = 1$ $O = 0$, $S = 0\%$).

7.2.2 Varying O and S

In this subsection, we present and discuss the results on the impact of the spike occurrence, O, under various spikes spreads, fixing the intensity to $I = 3$.

7.2.2.1 Recharging rate $\Delta = 5W$

Investigating the influence of the spikes occurrence in the case of $\Delta = 5W$, we observe that networks of size $n \leq 400$ maintain their immortal status regardless of the choice of the other parameters. In networks of size $n = 500$, **CLL** achieves immortality in most of settings, and near-immortality in the others. In particular, **CLL** is near-immortal with 4.49 non-operational sensors when $O = 3$, and with 4.87 non-operational sensors when $O = 5$ (see Figure 7.2). In this case, the disconnection time increases from 7.23 hours with $O = 3$ to 7.88 hours with $O = 5$ (see Figure 7.3).

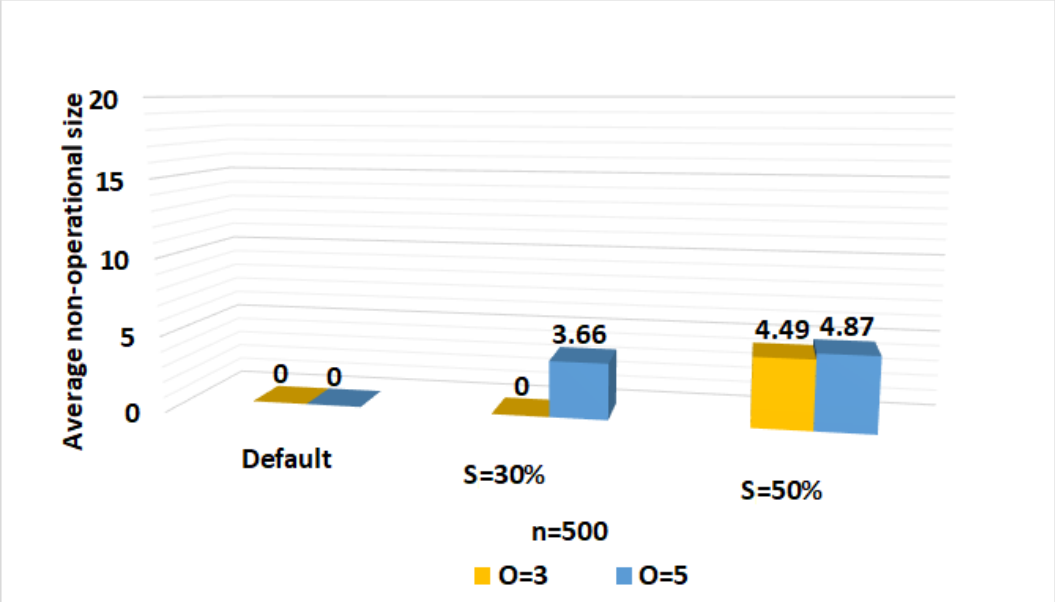

Figure 7.2: Average non-operational size with $\Delta = 5W$.

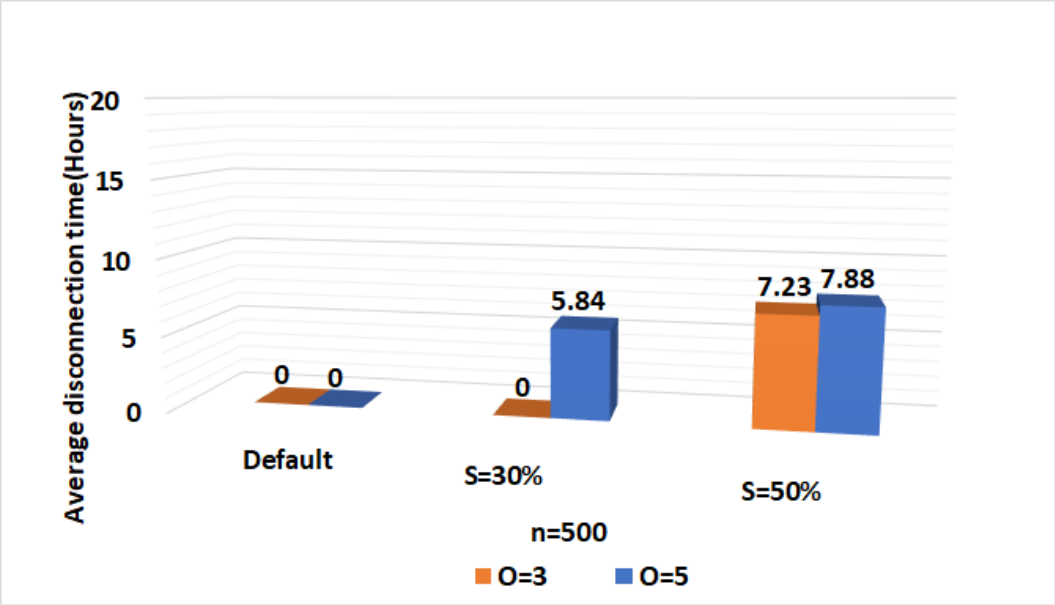

Figure 7.3: Average disconnection time with $\Delta = 5W$ and $I = 3$.

7.2.2.2 Recharging rate $\Delta = 3.4W$: Operational Size

The experimental results, shown in Figure 7.4(a-d), indicate that small networks of size $n \leq 200$ continue to achieve immortality in all settings. For $n = 300$, the network achieves immortality in most of the settings, and is near-immortal in the others, where the impact of O and S is negligible. For $n = 400$, the number of additional sensors that become non-operational in presence of spikes is very small and never reaches 0.5% of the network size. For $n = 500$, it grows slightly, but the difference remains very small reaching 0.76% of the network size in the most unfavorable condition of 50% spread.

Observe that the difference between the results of the default setting and $O = 3$, as well as those between $O = 3$ and $O = 5$ increases when the spread ratio increases, which is expected due to the larger portion of the network impacted by the spikes. The increase is however always slight. For example, if we focus on the worst scenario of $S = 50\%$ (Figure 7.4(d)), we observe that the number of non-operational sensors increases from 22.14 sensors in the case of the default setting to 25.62 sensors for $O = 3$ and reaches 25.93 sensors for $O = 5$, with only 3.79 extra sensors becoming non-

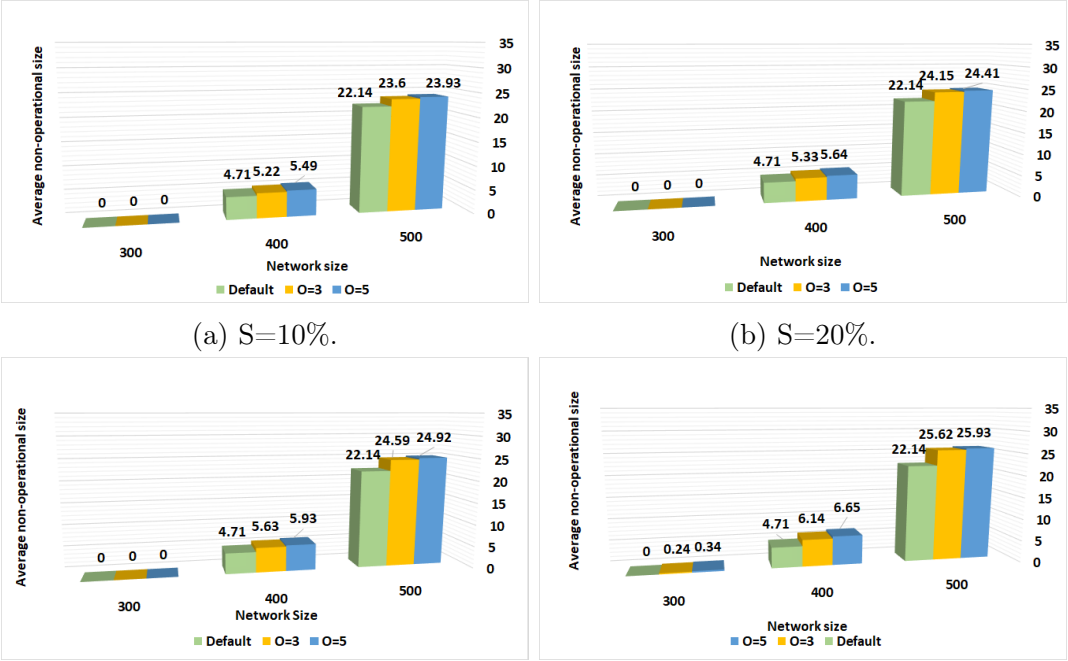

(a) S=10%. (b) S=20%.

(c) S=30%. (d) S=50%.

Figure 7.4: Impact of spike occurrence (O) on operational size

operational when the default setting is compared to the worst setting, which constitutes about 0.76% of the network size.

Also focusing on the increase of non-operational size with the increase of spread (under the most unfavorable conditions for O and I), we observe a very small growth for all network sizes (see Figure 7.5).

We can conclude that **CLL** continues to keep the number of non-operational sensors below 5.2% of the network size even in the most undesirable setting ($O = 5, S = 50\%, I = 3, n = 500$), which constitutes only a (0.76 % of network size) increase from the results observed in the absence of spikes.

7.2.2.3 Recharging rate $\Delta = 3.4W$: Disconnection Time

We now discuss the impact of O on the *disconnection time* of the network under various spike spreads and network sizes (see Figure 7.6(a-d)).

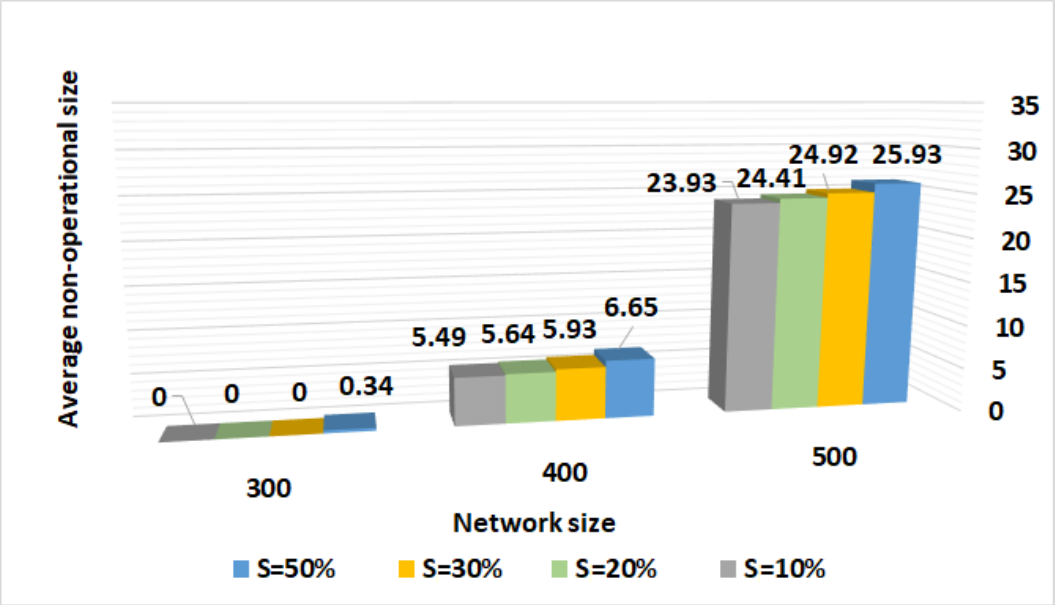

Figure 7.5: Impact of Spike spreads on the operational size with $I = 3$, $O = 5$.

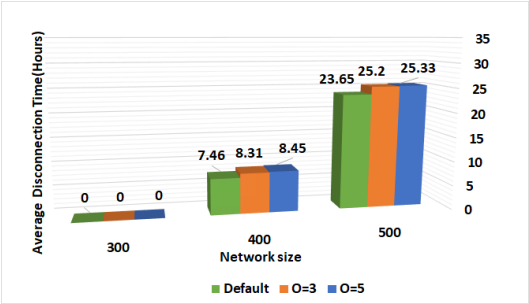

(a) S=10%.

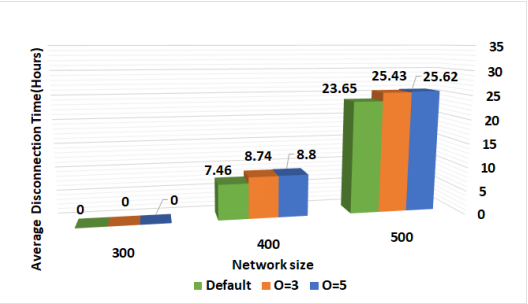

(b) S=20%.

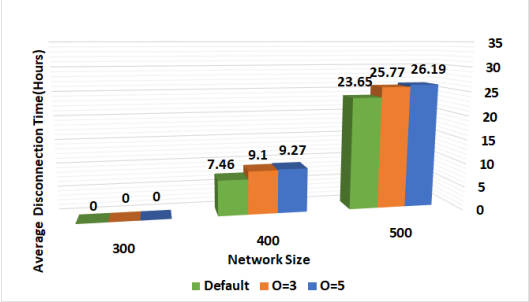

(c) S=30%.

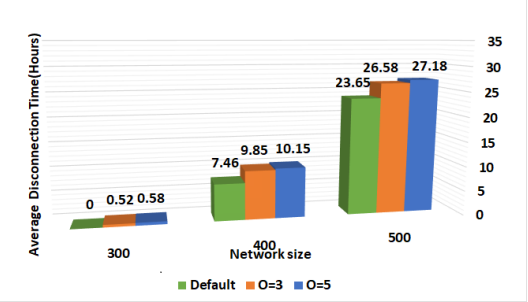

(d) S=50%.

Figure 7.6: Impact of spike occurrence (O) on disconnection time.

As already mentioned, network sizes of $n \leq 200$ remain immortal and those of size $n = 300$ stay immortal or near-immortal also under the least favorable circumstances.

Not surprisingly, the impact of O grows with the increase in spread. For example, consider the largest network size of $n = 500$ and the worst case of $O = 5$; in this case, the disconnection time with the default setting is 23.65 hours, and it grows by roughly 0.5 hour for each 10% increase in spread, finally reaching an increase of 3.23 hours in the least favorable circumstance ($n = 500, S = 50\%, I = 3$).

The disconnection time clearly grows also with the network size, the largest difference being the one between the default setting and $O = 3$. With the maximum spread of 50%, for example, the disconnection time for $n = 500$ goes from 23.65 hours in the default case, to 26.58 hours for $O = 3$ and to 27.18 for $O = 5$. A smaller increase is observed in the case of $n = 400$, when the disconnection time goes from 7.46 hours to 9.85 hours and then to 10.15 hours. A much smaller increase can be observed for the network size of $n = 300$ (only 4 *min* between $O = 3$ and $O = 5$).

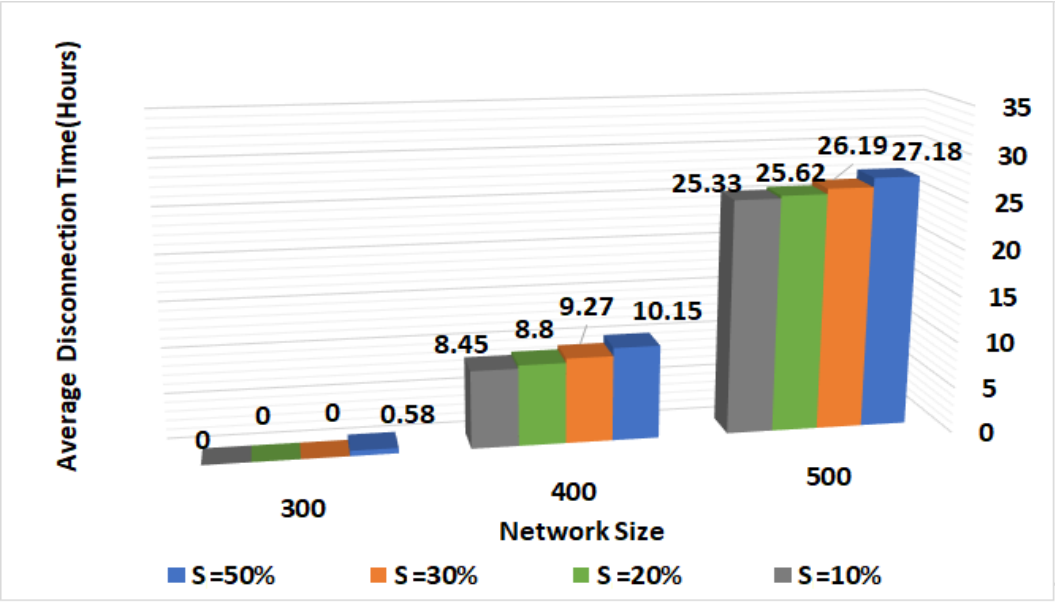

Figure 7.7: Impact of spike spreads on the disconnection time with $I = 3$ and $O = 5$.

The disconnection time increases only slightly also with the increase of the spread, under the most unfavorable conditions for O and I (see Figure 7.5).

Summarizing, we observe that the spike occurrence and their spread cause only slight increases also on disconnection time, showing that **CLL** adapts well to their

presence.

7.2.3 Varying I and S

In this subsection, we present and discuss the results on the impact of the spike intensity, I, under various spikes spreads, fixing the occurrence to $O = 5$.

7.2.3.1 Recharging rate $\Delta = 5W$

We observe that **CLL** achieves near-immortality even under the most unfavourable setting ($S = 50\%$, $O = 5$, $n = 500$). In this setting, **CLL** increased from null in the default setting to 3.81 non-operational sensors with $I = 1.5$, the difference between $I = 1.5$ and $I = 2$, as well as the one between $I = 2$ and $I = 3$ are very small (0.43, and 0.63 sensors, respectively) (see Figure 7.8).

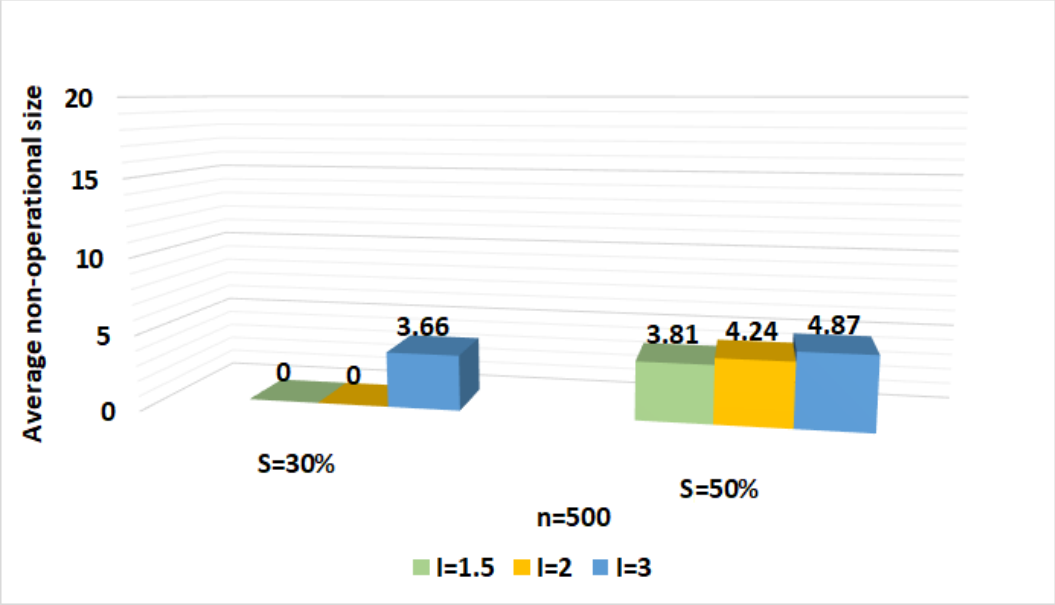

Figure 7.8: Average non-operational size with $\Delta = 5W$.

Also the *disconnection time* is affected very slightly; in fact, under the most unfavourable setting ($S = 50\%$, $O = 5$, $n = 500$), it increased from null in the default

setting to 6.19 hours with $I = 1.5$, the difference in disconnection time between $I = 1.5$ and $I = 2$ is about 0.57 hour and about 1.12 hours between $I = 2$ and $I = 3$ (see Figure 7.9).

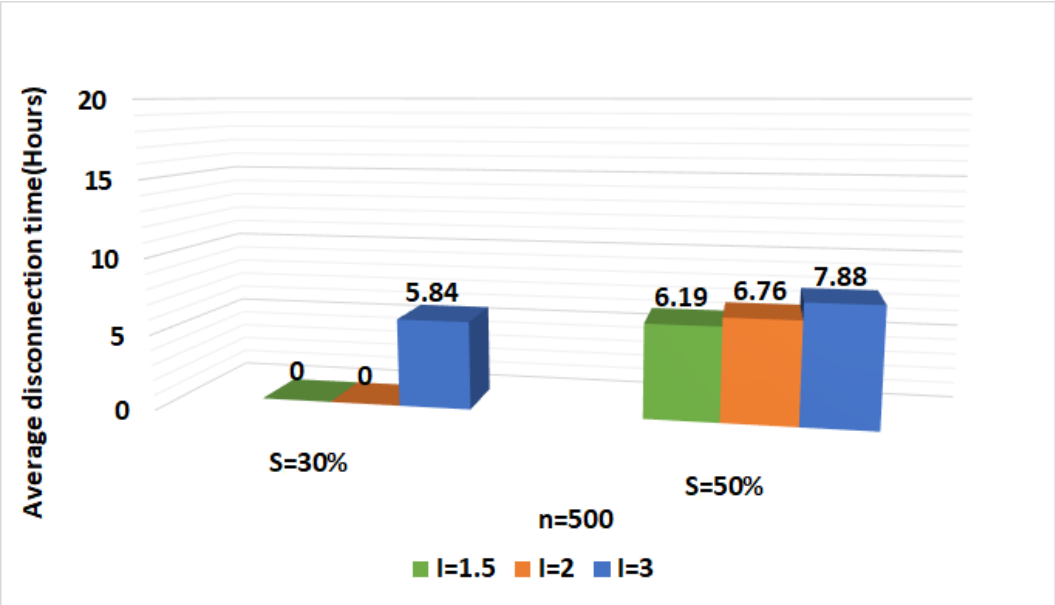

Figure 7.9: Average disconnection time with $\Delta = 5W$.

7.2.3.2 Recharging rate $\Delta = 3.4W$: Operational Size

Networks of size $n \leq 200$ continue to achieve immortality (see Figure 7.10), and those of size $n = 300$ are immortal or near-immortal. For larger networks, we observed slight changes in the operational size, which are larger than what we observed when varying O, but the changes are still very small, indicating the good adaptability of the strategy to spike intensity.

Investigating the results (shown in Figures 7.10(a-d)), we observed that for the worst possible setting ($S = 50\%$, $O = 5$, $n = 500$), the number of non-operational sensors increased from 22.14 in the absence of spikes to 24.46 with $I = 1.5$, 24.95 with $I = 2$, reaching about 25.93 sensors with $I = 3$. Each increase in intensity corresponds to a slight increase in non-operational size: An increase from $I = 1.5$ to $I = 2$ affects

0.1% of the network size (0.49 sensors), and from $I = 2$ to $I = 3$ affects 0.2% of the network size (0.98 sensors).

The impact of larger intensities is even smaller with $n = 400$, where the number of non-operational sensors in the default setting is 4.71, grows to 5.31 with $I = 1.5$, to 5.82 with $I = 2$ and to 6.65 with $I = 3$; overall, an increase of 1.94 sensors from the default to the worst intensity is observed here, which corresponds to 0.49 % of the network size. When considering a smaller network size of $n = 300$, the impact of the growing intensity becomes negligible (the network stays immortal or near-immortal).

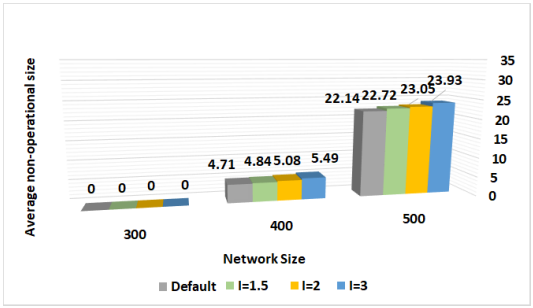

(a) S=10%.

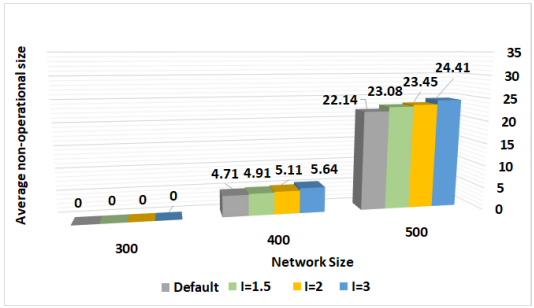

(b) S=20%.

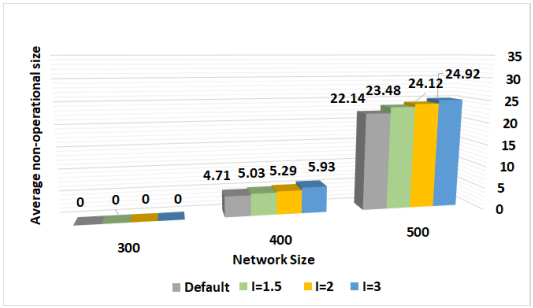

(c) S=30%.

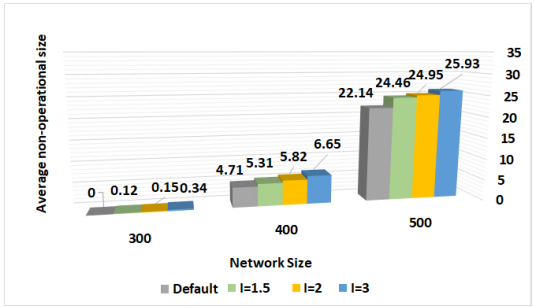

(d) S=50%.

Figure 7.10: Impact of spike intensity I on operational size.

Summarizing, we observe that the spike intensity and their spread cause only slight increases on the operational size, showing that **CLL** adapts well to their presence for all I and S.

7.2.3.3 Recharging rate $\Delta = 3.4W$: Disconnection Time

We now focus on the impact of the spike intensity on disconnection time (see Figure 7.11). We discuss these results in particular under the worst settings ($S = 50\%$, $O = 5$).

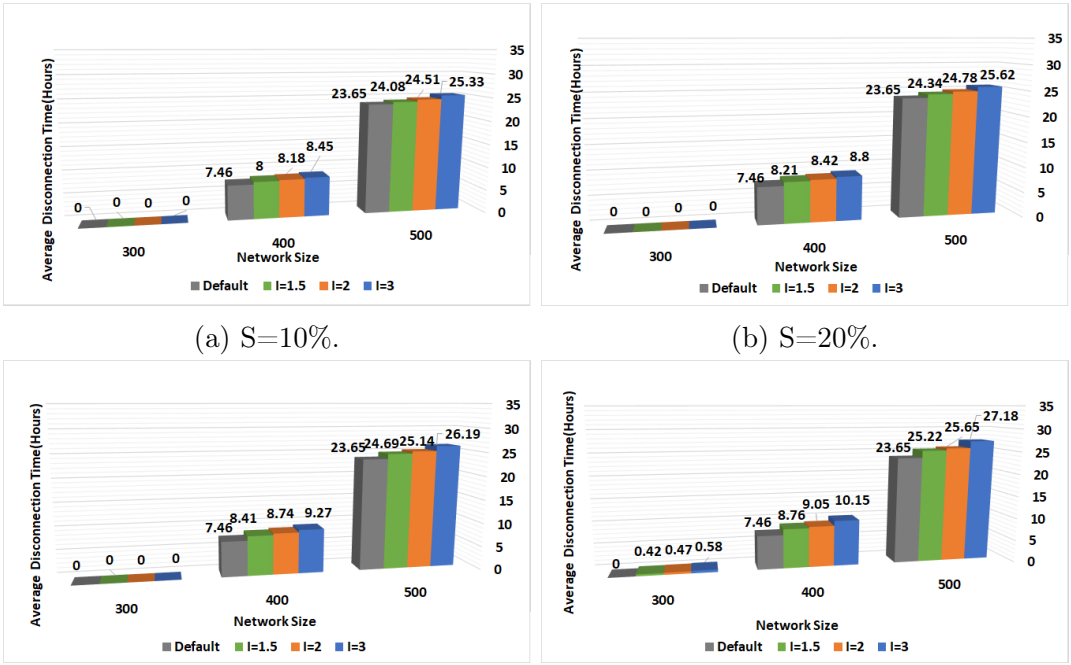

(a) S=10%. (b) S=20%.

(c) S=30%. (d) S=50%.

Figure 7.11: Impact of spike intensity I on disconnection time.

Observing the results shown in Figure 7.11 with $n = 500$, we noticed that the disconnection time for $I = 2$ increases by 0.43 hour from $I = 1.5$ (i.e., 25.22 hours versus 25.65 hours); also, it increases by about 1.5 hour from $I = 2$ to $I = 3$ (i.e., 25.65 hours versus 27.18 hours). With $n = 400$, the disconnection time for $I = 3$ increases by 1.39 hours, from $I = 1.5$, and for the same network, it increases by 1.1 hours from $I = 2$ to $I = 3$ (9.05 hours versus 10.15 hours). Finally, with $n = 300$, the disconnection time increases almost negligibly, and for all choices of I, the network remains near-immortal.

Summarizing, the spike intensity and their spread cause only slight increases also

on disconnection time, showing that **CLL** adapts well to their presence for all I and S.

7.2.4 Concluding Remarks

In this section, we studied the impact of various spikes parameters on operational size and disconnection time; summarizing our results, we reach the following conclusions:

- All spike parameters increase the non-operational size and the disconnection time of the system, by varying ratios. The difference between the result in the absence of spikes (default setting) and those in the worst setting ($I = 3$, $O = 5$, $S = 50\%$, and $n = 500$) is 3.79 sensors, which represent only 0.76% of the network size. Moreover, the difference in disconnection time between the default setting and the worst setting is about 3.53 hours (i.e., less than 2.06% of $T_{E_{max}}$).

- In general, **CLL** continues to achieve immortality for small networks ($n \leq 200$); no sensor ever becomes non-operational. Moreover, **CLL** achieves immortality or near-immortality for $n = 300$ in all cases (the number of non-operational sensors is at most 0.11% of the network size and the average disconnection time is always less than 0.34% of $T_{E_{max}}$).

- For all networks, the operational size decreases by at most 0.76% of the network size in comparison to the setting without spikes, while disconnection time increases by at most 2.06% of $T_{E_{max}}$.

Summarizing, the experimental results indicate that the **CLL** strategy is capable of adapting and coping with the sudden presence of spikes with little impact on operational size and disconnection time.

7.3 Impact of Spikes: CLL vs H

In this section, we compare the impact of the spikes on **CLL** and **H**. Experimental results show that, while both strategies continue to achieve immortality for small networks ($n \leq 200$), **CLL** outperforms **H** under all spikes settings for large networks ($n \geq 300$).

The analysis has been done using the default setting of the previous section (and of Chapter 4), under the worst condition of recharging rate $\Delta = 3.4W$.

7.3.1 Impact of Intensity

We first analyze the performance of both strategies fixing the intensity of the spikes under the worst conditions of the other parameters ($O = 5$, $S = 50\%$). See Figures 7.12 and 7.13.

We observe that the operational size decreases and the disconnection time increases with both strategies by increasing the network size and the spike intensity. Moreover, for all values of I and n, **CLL** outperforms **H** and, for each network size, the higher I the more significant is the advantage of **CLL** over **H**.

More precisely, for $n = 300$ **CLL** is up to 8 times better in terms of non-operational size (0.34 sensors vs. 2.68 when $I = 3$) and about 9 times in terms of disconnection time (35 min vs. 5.58 hours when $I = 3$). Looking at $n = 400$ **CLL** is up to 1.54 times better in terms of non-operational size (6.65 sensors vs. 10.26 when $I = 3$) and up to 2.8 times better than **H** in terms of disconnection time (10.15 hours versus 28.86 when $I = 3$). Finally, for $n = 500$, **CLL** is up to 1.25 times better than **H** in terms of non-operational size and 1.7 times in terms of disconnection time (25.93 versus 32.38 sensors are non operational, and they stay disconnected for an average of 27.18 hours versus 46.52 when $I = 3$).

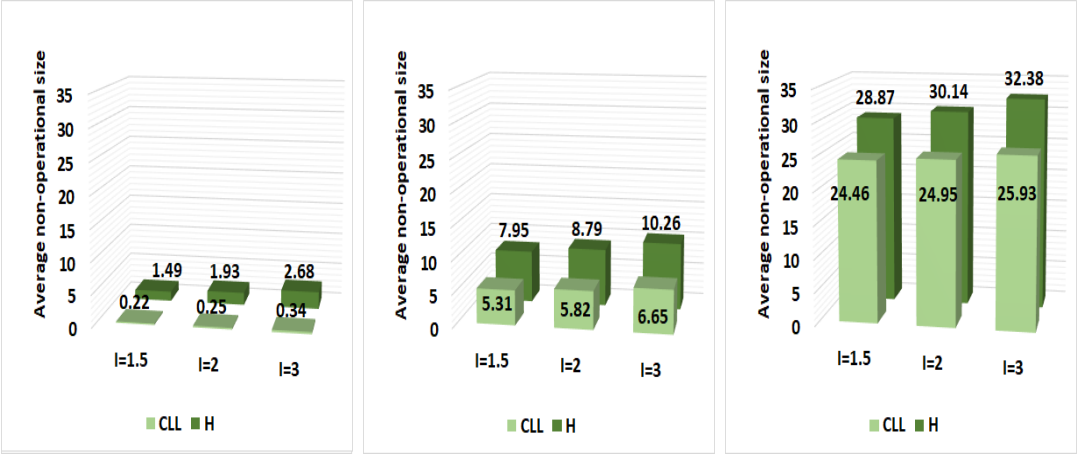

(a) n=300. (b) n=400. (c) n=500.

Figure 7.12: Impact of spike intensity (I) on operational size with $O = 5$, $S = 50\%$ and $\Delta = 3.4W$

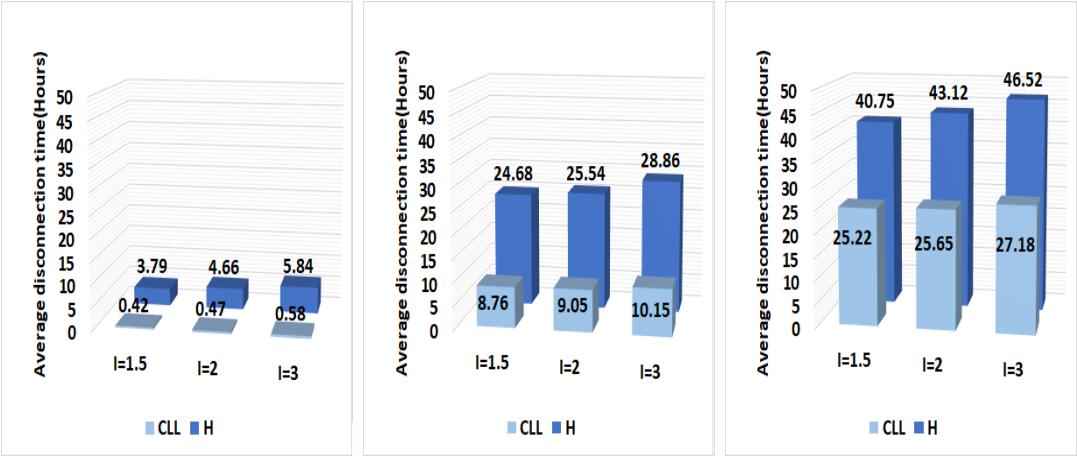

(a) n=300. (b) n=400. (c) n=500.

Figure 7.13: Impact of spike intensity (I) disconnection time with $O = 5$, $S = 50\%$ and $\Delta = 3.4W$

With lower intensities the impact is a bit lower; for instance, **CLL** in a network of $n = 500$ sensors with $I = 2$ outperforms **H** by 1.21 times in contrast to 1.25 times with $I = 3$, and for $I = 1.5$ **CLL** is better than **H** by 1.18 times. For $n = 400$ **CLL** is better than **H** by 1.51 times with $I = 2$ and 1.54 times with $I = 3$. In other words, increasing the intensity of the spikes, the discrepancy between the two strategies grows.

7.3.2 Impact of Occurrence

We now turn to study the impact of spike occurrence on both strategies, varying I and fixing $S = 50\%$ and $O = 5$. Again, **CLL** continues to outperform **H** under various spike occurrences.

Looking at the non-operational size of both strategies with $n = 300$, we observe that **CLL** outperforms **H** by about 8 times with $O = 3$ (0.24 versus 1.98 sensor), and by 7.9 times with $O = 5$. For $n = 400$ with $O = 3$, **CLL** is better than **H** by 1.47 times, while with $O = 5$ **CLL** outperforms **H** by 1.54 times (6.65 versus 10.26 sensors).

For networks of size $n = 500$ with $O = 3$, the non-operational size with **CLL** is 25.62 sensors and with **H** is about 31.45 sensors (i.e., **CLL** is 1.23 better), with $O = 5$ **CLL** has about 25.93 non-operational sensors, which is 1.25 better than **H** (32.38 sensors).

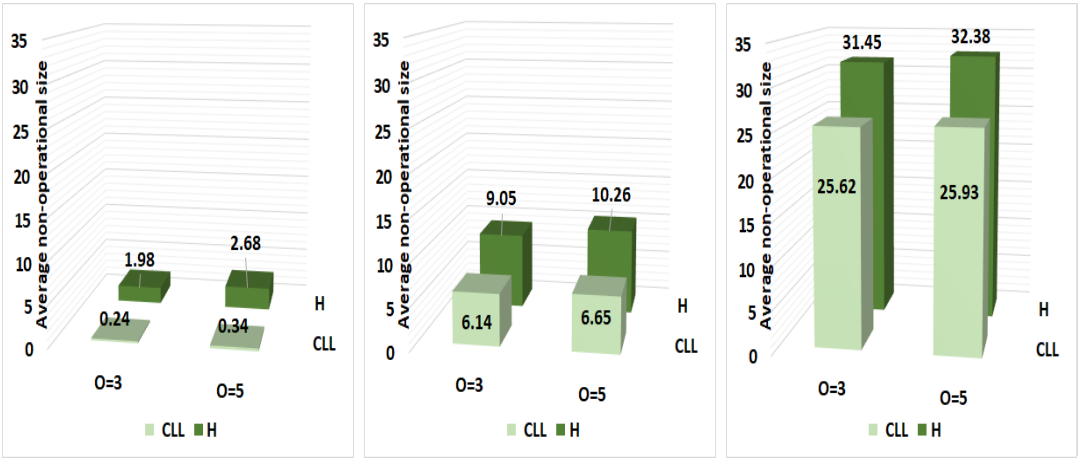

(a) n=300. (b) n=400. (c) n=500.

Figure 7.14: Impact of spike Occurrence (O) on operational size with $I = 3$, $S = 50\%$ and $\Delta = 3.4W$.

Also in this case, disconnection time makes more evident the advantage of **CLL** over **H** (see Figure 7.15). With $O = 3$, for example, **CLL** is 10 times (resp., 2.76, and 1.66 times) better than **H** with $n = 300$ (resp., $n = 400$, and $n = 500$). In particular,

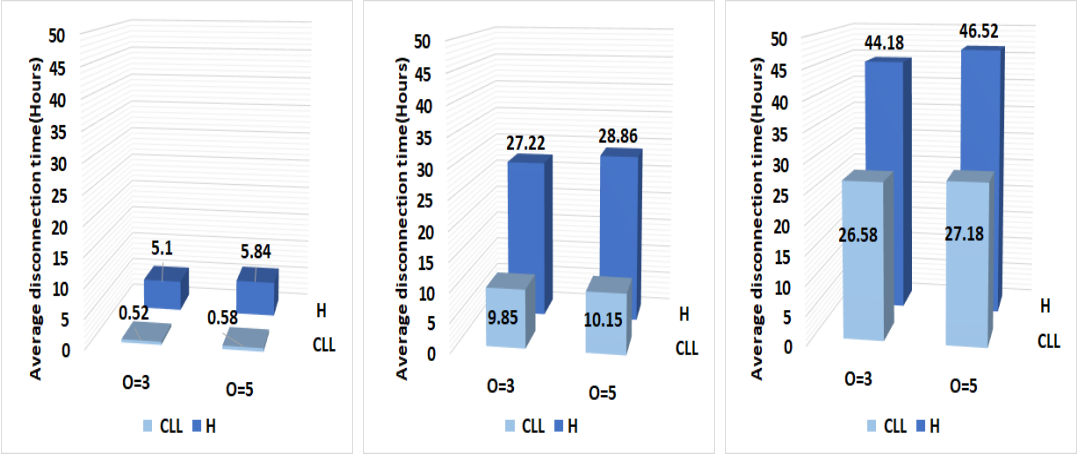

(a) n=300. (b) n=400. (c) n=500.

Figure 7.15: Impact of spike Occurrence (O) on disconnection time with $I = 3$, $S = 50\%$ and $\Delta = 3.4W$.

for the highest $O = 5$, **CLL** outperforms **H** by 10 times, (resp., 2.84, and 1.71 times) with $n = 300$ (resp., $n = 400$ and $n = 500$).

7.3.3 Impact of Spread

In this section, we studied the impact of the spikes' spread S on the operational size and disconnection time for **CLL** and **H**. We studied this parameter while we fixing the $I = 3$ and $O = 5$.

Smaller networks of size $n \leq 200$ continue to achieve immortality for both strategies. For networks of all sizes **CLL** outperforms **H** in all settings (see Figures 7.16-7.17).

For $n = 300$, **CLL** is immortal up to spread $S = 30\%$. For $S = 50\%$ **CLL** has only 0.34 non-operational sensors while **H** has 2.6 non-operational sensors, and its disconnection time is 10 times better than the one of **H**. For $n = 400$, **CLL** is up to 1.5 better than **H** (when the spread is maximum) in terms of operational size, and it is almost 3 times better than **H** under all values of S in terms of disconnection time. Finally, for $n = 500$, **CLL** is up to 1.25 times better than **H** (in correspondence of

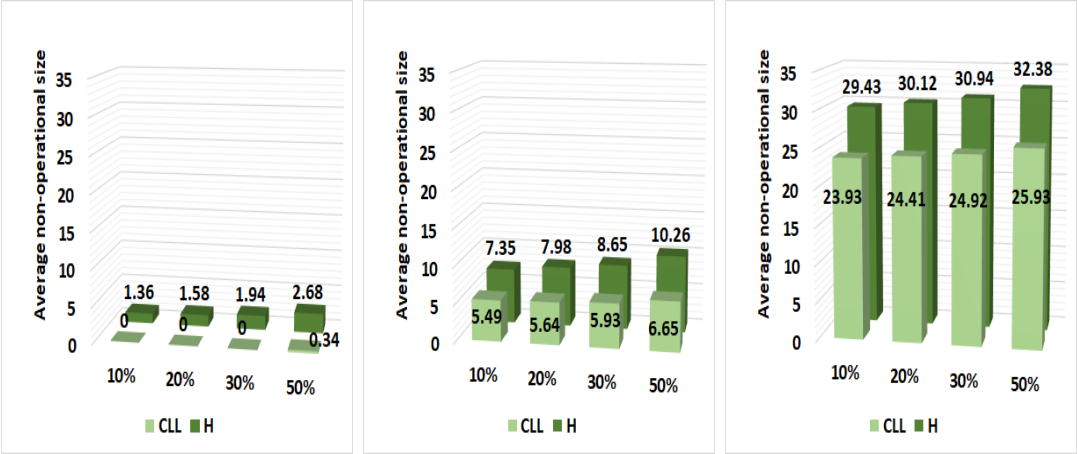

(a) n=300. (b) n=400. (c) n=500.

Figure 7.16: Impact of spike spread on operational size with $I = 3$, $O = 5$ and $\Delta = 3.4W$.

$S = 50\%$) when its average disconnection time is about half the one of **H**.

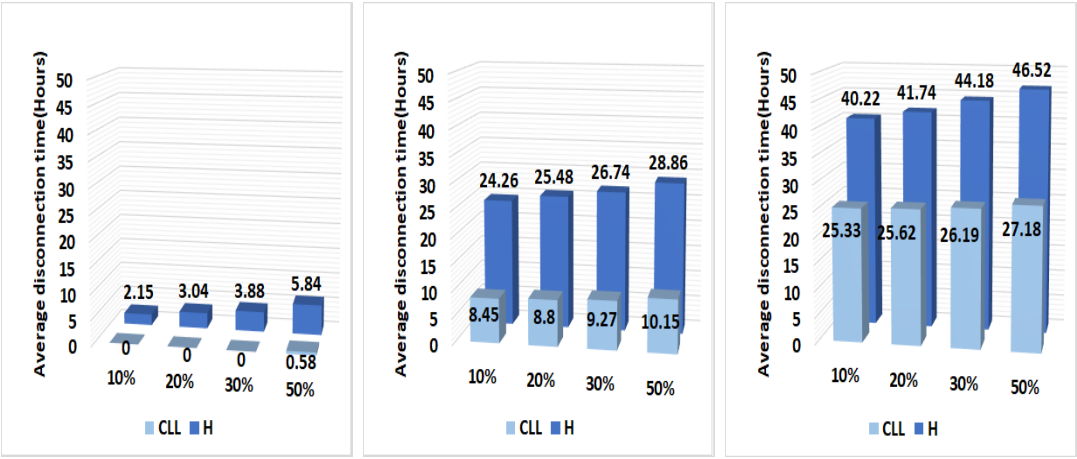

(a) n=300. (b) n=400. (c) n=500.

Figure 7.17: Impact of spike Spread on disconnection time with $I = 3$, $O = 5$ and $\Delta = 3.4W$

7.3.4 Concluding Remarks

We observed that **CLL** continue to outperform **H** under all spike settings which reflects its adaptiveness. Increasing the values of the spike parameters both non-operational

size and disconnection time increase; however, the increase with **CLL** is always significantly less than that with **H**.

Both strategies achieve immortality for small networks of size $n \leq 200$. With networks of size $n = 300$, **CLL** achieves immortality for spreads up to 30% and near-immortality for $S = 50\%$ with 0.34 non-operational sensors that disconnected for about 34 min, while **H** achieves near-immortality for all spread values. For n=400, **CLL** achieves near-immortality for spread up to 20%, while for larger spreads the operational size is 98.3% and the non-operational sensors disconnected for less than 6% of $T_{E_{max}}$. While **H** is outperformed in operational size by at least 1.34 times and disconnected for 16.8% of $T_{E_{max}}$. For $n = 500$, **CLL** outperforms **H** by at least 1.23 times in operational size and 1.59 times in disconnection time.

Moreover, increasing the intensity, the occurrence and the spread of the spikes, the difference between **CLL** and **H** in terms of non-operational size and disconnection time increases.

Furthermore, the operational size with **CLL** under the worse setting never goes below 94.8% of network size and the disconnection time never exceeds 16% of $T_{E_{max}}$. On the other hand, the operational size with **H** is about 93.4% and more importantly, the disconnection time is about 27% of $T_{E_{max}}$.

Chapter 8

Conclusions and Future Directions

8.1 Conclusions

In this thesis, we have shown that it is possible to devise a highly effective local strategy (e.g., leading to immortality) without the large communication overhead incurred by global protocols, thus making scalability possible. In the proposed online strategy, **CLL** , the mobile charger decides the charging schedule on-line, communicates locally only with the node it is servicing, constantly adjust its estimates and updates its schedule while charging sensors in need. **CLL** is distributed, simple, uses small memory, and performs simple computation; at the same time, it is highly effective in maintaining the network perpetually operating, and achieves immortality or near-immortality under a large number of settings.

Furthermore, we have also shown that with **CLL** it is possible to improve upon the effectiveness of static strategies while keeping the advantages they offer. Remarkably, **CLL** outperforms the static strategies in terms of both operating size and disconnection time while still sharing the same advantages of simplicity and low communication and computations.

CLL shows high flexibility to changes in the system parameters. The success of the method is due to the ability of the mobile charger to “locally learn" the global distribution of battery discharges, which reflects the applicability of a such simple distributed strategy on a wide range of application parameters: number of sensors, sensors' battery-capacity, and mobile charger characteristics (speed, charging time, etc). The results also reveal the effectiveness and adaptiveness of **CLL** to cope with sudden changes in data rates that influence a set of sensors in the system.

8.2 Future Directions

The results of this thesis can be extended in many ways, including the following directions.

- Multi-Distribution: In the thesis, we studied various scenarios and settings, and for all of them, we had the sensors follow a Poisson distribution to generate their data rate. Thus, an open research direction is to extend the results of Chapters 6 and 7 considering different distributions and studying the influence of spikes on the performance of the system under such scenarios.

- Lifting of Assumptions: Like in most theoretical studies, the investigations carried out in this thesis have been done under several simplifying assumptions. For example, like in most literature, we did not consider the presence of obstacles in the network area, we assumed that the speed of the $\mathcal{MC}$ is constant, and we assumed that sensing and processing costs are negligible. Lifting these assumptions (e.g., studying the performance of the proposed strategy in presence of obstacles, testing the acceleration of the $\mathcal{MC}$, considering sensing and processing costs) is a clear important direction for future research.

- Multiple Chargers: In the case of extremely large networks, to maintain the operational size at a desirable level, it is necessary to employ multiple chargers

(e.g., [98, 115–119]). The quest for effective on-line recharging strategies for such a case opens promising future research directions, requiring the consideration of additional important factors, especially the coordination between the mobile chargers and the variety of related concerns (e.g., dividing the network area into clusters, fixed and non-fixed borders of the sub-areas, etc.)

- Charging multiple sensors: In this thesis, we analysed our solution assuming that the $\mathcal{MC}$ would only charge one node at a time. In reality, wireless charging occurs to all nodes within the proximity of the mobile charger at different rates. In other words, while the $\mathcal{MC}$ stands at minimal distance from a node, it might be close enough to other nodes that they can receive energy, albeit at lower recharging efficiency [105, 108–111]. Thus, an important extension of our work would be to take this factor explicitly into account; this would clearly produce a more accurate measure of the effectiveness of our strategy, showing that its performance is even better than that indicated in this thesis.

- Self-charging mobile charger: In the thesis, we made the realistic assumption that the capacity of the battery of the mobile charger is limited; thus, in order to fulfill its mission, the $\mathcal{MC}$ needs occasionally to travel back to the Service Station for battery replacement or recharging. A future research direction is to consider providing the $\mathcal{MC}$ with energy harvesting capability so to drastically reduce the time spent travelling to the service station (and being serviced there), or even to become totally self-sufficient. Since the first steps for the development of such a technology are being taken (e.g., [133–135]), it is important to start investigating how such a capability would further benefit effective strategies like **CLL**.

- Data Collection, Aggregation and Relaying: Observe that the mobile charger spends a significant amount of time near the sensor it is recharging, and that sending data over short distances consumes less energy than long distance communication. This means that, should the mobile charger have stronger equipment (i.e., larger memory, longer communication range, etc.) that we required, the $\mathcal{MC}$

could collect and relay data burst from nearby sensors to the BS, reducing in this way the overall communication overhead and the data loss (e.g., [42,44,136,137]. Studying this issue in the context of the proposed distributed solution is an open direction, which promises to effectively increase the performance of the system.

References

[1] I. Akyildiz, W. Su, Y. Sankarasubramaniam, and E. Cayirci, "A survey on sensor networks," *IEEE Communications Magazine*, vol. 40, no. 8, pp. 102–114, 2002.

[2] J. Yick, B. Mukherjee, and D. Ghosal, "Wireless sensor network survey," *Computer Networks*, vol. 52, no. 12, pp. 2292–2330, 2008.

[3] A. Pascale, M. Nicoli, F. Deflorio, B. Dalla Chiara, and U. Spagnolini, "Wireless sensor networks for traffic management and road safety," *IET Intelligent Transport Systems*, vol. 6, no. 1, pp. 67–77, 2012.

[4] F. Cirillo, D. Gómez, L. Diez, I. Elicegui Maestro, T. B. J. Gilbert, and R. Akhavan, "Smart city IoT services creation through large-scale collaboration," *IEEE Internet of Things Journal*, vol. 7, no. 6, pp. 5267–5275, 2020.

[5] A. Omara, D. Gulen, B. Kantarci, and S. Oktug, "Trajectory assisted municipal agent mobility: A sensor-driven smart waste management system," *Journal of Sensor and Actuator Networks*, vol. 7, no. 3, pp. 1–29, 2018.

[6] J. Cabra, D. Castro, J. Colorado, D. Mendez, and L. Trujillo, "An IoT approach for wireless sensor networks applied to e-health environmental monitoring," in *Proceedings of IEEE International Conference on Internet of Things (iThings) and IEEE Green Computing and Communications (GreenCom) and IEEE Cyber,*

Physical and Social Computing (CPSCom) and IEEE Smart Data (SmartData), Jun. 2017, pp. 578–583.

[7] R. S. Ransing and M. Rajput, "Smart home for elderly care, based on wireless sensor network," in *Proceedings of 1st International Conference on Nascent Technologies in the Engineering Field (ICNTE)*, Jan. 2015, pp. 1–5.

[8] M. F. Othman and K. Shazali, "Wireless sensor network applications: A study in environment monitoring system," *Procedia Engineering*, vol. 41, no. 7, pp. 1204 – 1210, 2012.

[9] A. Watt, M. Phillips, C.-A. Campbell, I. Wells, and S. Hole, "Wireless sensor networks for monitoring underwater sediment transport," *Science of The Total Environment*, vol. 667, no. 2, pp. 160 – 165, 2019.

[10] S. Ramnath, A. Javali, B. Narang, P. Mishra, and S. K. Routray, "IoT based localization and tracking(iciot)," in *Proceedings of 2nd International Conference on IoT and Application (ICIOT)*, May 2017, pp. 1–4.

[11] J. Guo, H. Zhang, Y. Sun, and R. Bie, "Square-root unscented kalman filtering-based localization and tracking in the internet of things," *Personal and Ubiquitous Computing*, vol. 18, no. 4, pp. 987–996, 2014.

[12] A. Sharma and S. Chauhan, "Detection and tracking of mobile intruder in harsh geographical terrains using surveillance wireless sensor networks," in *Handbook of Wireless Sensor Networks: Issues and Challenges in Current Scenario's*. Springer International Publishing, 2020, pp. 417–437.

[13] C. Lino, T. Navarro, C. T. Calafate, A. Diaz-Ramirez, P. Manzoni, and J. Cano, "Intruder tracking in wsns using binary detection sensors and mobile sinks," in *Proceedings of 13th IEEE Wireless Communications and Networking Conference (WCNC)*, Apr. 2012, pp. 2025–2030.

[14] C.-Y. Chang, C.-Y. Hsiao, and C.-T. Chang, "Qos guaranteed surveillance algorithms for directional wireless sensor networks," *Ad Hoc Networks*, vol. 81, no. 1, pp. 71 – 85, 2018.

[15] P. Xu, J. Wu, C. Shang, and C. Chang, "GSMS: A barrier coverage algorithm for joint surveillance quality and network lifetime in wsns," *IEEE Access*, vol. 7, no. 1, pp. 608–621, 2019.

[16] D. Punniamoorthy, V. S. Kamadal, B. Srujana Yadav, and V. S. Reddy, "Wireless sensor networks for effective environmental tracking system using IoT and sensors," in *Proceedings of 2nd International Conference on I-SMAC (IoT in Social, Mobile, Analytics and Cloud) (I-SMAC)I-SMAC (IoT in Social, Mobile, Analytics and Cloud) (I-SMAC)*, Aug. 2018, pp. 66–69.

[17] G. Anastasi, M. Conti, M. D. Francesco, and A. Passarella, "Energy conservation in wireless sensor networks: A survey," *Ad Hoc Networks*, vol. 7, no. 3, pp. 537 – 568, 2009.

[18] S. Sendra Compte, J. Lloret, M. García Pineda, and J. F. Toledo Alarcón, "Power saving and energy optimization techniques for wireless sensor networks," *Journal of communications*, vol. 6, no. 6, pp. 439–459, 2011.

[19] F. Akhtar and M. H. Rehmani, "Energy replenishment using renewable and traditional energy resources for sustainable wireless sensor networks: A review," *Renewable and Sustainable Energy Reviews*, vol. 45, no. 1, pp. 769 – 784, 2015.

[20] H. Sharma, A. Haque, and Z. A. Jaffery, "Solar energy harvesting wireless sensor network nodes: A survey," *Journal of Renewable and Sustainable Energy*, vol. 10, no. 2, pp. 1–19, 2018.

[21] N. Santoro and E. Velazquez, "*Energy Restoration in Mobile Sensor Networks*," in *Wireless Sensor and Robot Networks*. World Scientific, 2014, pp. 113–142.

[22] S. Soni and M. Shrivastava, "Novel wireless charging algorithms to charge mobile wireless sensor network by using reinforcement learning," *SN Applied Sciences*, vol. 1, no. 9, pp. 1052–1070, 2019.

[23] S. L. Ho, J. Wang, W. N. Fu, and M. Sun, "A comparative study between novel witricity and traditional inductive magnetic coupling in wireless charging," *IEEE Transactions on Magnetics*, vol. 47, no. 5, pp. 1522–1525, 2011.

[24] A. Kurs, A. Karalis, R. Moffatt, J. D. Joannopoulos, P. Fisher, and M. Soljačić, "Wireless power transfer via strongly coupled magnetic resonances," *Science*, vol. 317, no. 5834, pp. 83–86, 2007.

[25] A. Kurs, R. Moffatt, and M. Soljačić, "Simultaneous mid-range power transfer to multiple devices," *Applied Physics Letters*, vol. 96, no. 4, pp. 1–3, 2010.

[26] F. Lu, H. Zhang, and C. Mi, "A review on the recent development of capacitive wireless power transfer technology," *Energies*, vol. 10, no. 11, pp. 1752–1782, 2017.

[27] Y. Yang and C. Wang, *Wireless Rechargeable Sensor Networks*. Springer International Publishing, 2015.

[28] C. M. Angelopoulos, S. Nikoletseas, and T. P. Raptis, "Wireless energy transfer in sensor networks with adaptive, limited knowledge protocols," *Computer Networks*, vol. 70, no. 1, pp. 113 – 141, 2014.

[29] C. M. Angelopoulos, S. Nikoletseas, T. P. Raptis, C. Raptopoulos, and F. Vasilakis, "Improving sensor network performance with wireless energy transfer," *International Journal of Ad Hoc and Ubiquitous Computing*, vol. 20, no. 3, pp. 159–171, 2015.

[30] Y. Shi, L. Xie, T. Hou, and H. Sherali, "On renewable sensor networks with wireless energy transfer," in *Proceedings of 30th IEEE Conference on Computer Communications (INFOCOM)*, Jun. 2011, pp. 1350–1358.

[31] L. Jiang, X. Wu, G. Chen, and Y. Li, "Effective on-demand mobile charger scheduling for maximizing coverage in wireless rechargeable sensor networks," *Mobile Networks and Applications*, vol. 19, no. 4, pp. 543–551, 2014.

[32] M. Zhao, J. Li, and Y. Yang, "Joint mobile energy replenishment and data gathering in wireless rechargeable sensor networks," in *Proceedings of 23rd IEEE International Teletraffic Congress (ITC)*, Sep. 2011.

[33] L. Xie, Y. Shi, Y. T. Hou, and H. D. Sherali, "Making sensor networks immortal: An energy-renewal approach with wireless power transfer," *IEEE/ACM Transactions on Networking*, vol. 20, no. 6, pp. 1748–1761, 2012.

[34] Q. Zhang, R. Cheng, and Z. Zheng, "Energy-efficient renewable scheme for rechargeable sensor networks," *EURASIP Journal on Wireless Communications and Networking*, vol. 1, no. 4, pp. 74–87, 2020.

[35] E. Omar, P. Flocchini, and N. Santoro, "Perpetual energy restoration by multiple mobile robots in circular sensor networks," in *Proceedings of 16th IEEE/ACS International Conference on Computer Systems and Applications (AICCSA)*, 2019, pp. 1–8.

[36] L. Xie, Y. Shi, Y. T. Hou, W. Lou, H. D. Sherali, and S. F. Midkiff, "Bundling mobile base station and wireless energy transfer: Modeling and optimization," in *Proceedings of 32nd IEEE Conference on Computer Communications(INFOCOM)*, Jul. 2013, pp. 1636–1644.

[37] Y. Dong, Y. Wang, S. Li, M. Cui, and H. Wu, "Demand-based charging strategy for wireless rechargeable sensor networks," *ETRI Journal*, vol. 1, no. 1, pp. 326–336, 2019.

[38] W. Liang, Z. Xu, W. Xu, J. Shi, G. Mao, and S. K. Das, "Approximation algorithms for charging reward maximization in rechargeable sensor networks via a mobile charger," *IEEE/ACM Transactions on Networking*, vol. 25, no. 5, pp. 3161–3174, 2017.

[39] Z. Li, Peng, W. Zhang, and D. Qiao, "J-roc: A joint routing and charging scheme to prolong sensor network lifetime," in *Proceedings of 19th IEEE International Conference on Network Protocols (ICNP)*, Apr 2011, pp. 373–382.

[40] C. Lin, D. Han, J. Deng, and G. Wu, "P^2S: A primary and passer-by scheduling algorithm for on-demand charging architecture in wireless rechargeable sensor networks," *IEEE Transactions on Vehicular Technology*, vol. 66, no. 9, pp. 8047–8058, 2017.

[41] X. Ren, W. Liang, and W. Xu, "Maximizing charging throughput in rechargeable sensor networks," in *Proceedings of 23rd International Conference on Computer Communication and Networks (ICCCN)*, Aug 2014, pp. 1–8.

[42] S. Guo, C. Wang, and Y. Yang, "Joint mobile data gathering and energy provisioning in wireless rechargeable sensor networks," *IEEE Transactions on Mobile Computing*, vol. 13, no. 12, pp. 2836–2852, 2014.

[43] S. Guo, C. Wang, and Y. Yang, "Mobile data gathering with wireless energy replenishment in rechargeable sensor networks," in *Proceedings of 32nd IEEE Conference on Computer Communications(INFOCOM)*, Apr 2013, pp. 1932–1940.

[44] M. Zhao, J. Li, and Y. Yang, "A framework of joint mobile energy replenishment and data gathering in wireless rechargeable sensor networks," *IEEE Transactions on Mobile Computing*, vol. 13, no. 12, pp. 2689–2705, 2014.

[45] C. Wang, S. Guo, and Y. Yang, "An optimization framework for mobile data collection in energy-harvesting wireless sensor networks," *IEEE Transactions on Mobile Computing*, vol. 15, no. 12, pp. 2969–2986, 2016.

[46] L. He, Y. Gu, J. Pan, and T. Zhu, "On-demand charging in wireless sensor networks: Theories and applications'," in *Proceedings of 10th IEEE International Conference on Mobile Ad-Hoc and Sensor Systems (MASS)*, Oct. 2012, pp. 28–36.

[47] L. He, L. Kong, Y. Gu, J. Pan, and T. Zhu, "Evaluating the on-demand mobile charging in wireless sensor networks," *IEEE Transactions on Mobile Computing*, vol. 14, no. 9, pp. 1861–1875, 2015.

[48] Y. Peng, Z. Li, W. Zhang, and D. Qiao, "Prolonging sensor network lifetime through wireless charging," in *Proceedings of 31st IEEE Real-Time Systems Symposium(RTSS)*, Nov. 2010, pp. 129–139.

[49] Z. Qin, C. Zhou, Y. Yu, L. Wang, L. Sun, and Y. Zhang, "A practical solution to wireless energy transfer in wsns," in *Proceedings of 4th International Conference on ICT Convergence (ICTC)*, 2013, pp. 660–665.

[50] S. Suman, S. Kumar, and S. De, "Uav-assisted rfet: A novel framework for sustainable wsn," *IEEE Transactions on Green Communications and Networking*, vol. 3, no. 4, pp. 1117–1131, 2019.

[51] H. Liu, Q. Deng, S. Tian, X. Peng, and T. Pei, "Recharging schedule for mitigating data loss in wireless rechargeable sensor network," *MDPI Sensors*, vol. 18, no. 7, pp. 141–158, 2018.

[52] W. Na, J. Park, C. Lee, K. Park, J. Kim, and S. Cho, "Energy-efficient mobile charging for wireless power transfer in internet of things networks," *IEEE Internet of Things Journal*, vol. 5, no. 1, pp. 79–92, 2018.

[53] X. Lu, P. Wang, D. Niyato, D. I. Kim, and Z. Han, "Wireless charging technologies: Fundamentals, standards, and network applications," *IEEE Communications Surveys Tutorials*, vol. 18, no. 2, pp. 1413–1452, 2016.

[54] C. M. Angelopoulos, S. Nikoletseas, T. P. Raptis, C. Raptopoulos, and F. Vasilakis, "Efficient energy management in wireless rechargeable sensor networks," in *Proceedings of 15th ACM International Conference on Modeling, Analysis and Simulation of Wireless and Mobile Systems(MSWIM)*, Oct. 2012, p. 309–316.

[55] R. Du, A. Özçelikkale, C. Fischione, and M. Xiao, "Towards immortal wireless sensor networks by optimal energy beamforming and data routing," *IEEE Transactions on Wireless Communications*, vol. 17, no. 8, pp. 5338–5352, 2018.

[56] C. Lin, Z. Wang, D. Han, Y. Wu, C. W. Yu, and G. Wu, "Tadp: Enabling temporal and distantial priority scheduling for on-demand charging architecture in wireless rechargeable sensor networks," *Journal of Systems Architecture*, vol. 70, no. 5, pp. 26–38, 2016.

[57] Y. Feng, L. Guo, X. Fu, and N. Liu, "Efficient mobile energy replenishment scheme based on hybrid mode for wireless rechargeable sensor networks," *IEEE Sensors Journal*, vol. 19, no. 21, pp. 10 131–10 143, 2019.

[58] A. Kaswan, A. Tomar, and P. K. Jana, "An efficient scheduling scheme for mobile charger in on-demand wireless rechargeable sensor networks," *Journal of Network and Computer Applications*, vol. 114, no. 1, pp. 123 – 134, 2018.

[59] L. Khelladia, D. Djenouria, M. Rossib, and N. Badache, "Efficient on-demand multi-node charging techniques for wireless sensor networks," *Computer Communications*, vol. 101, no. 1, pp. 44– 56, 2017.

[60] S. Zhan, J. Wu, L. Qu, and D. Xin, "Efficient scheduling strategy for mobile charger in wireless rechargeable sensor networks," in *Proceedings of 17th International Conference on Parallel and Distributed Computing, Applications and Technologies (PDCAT)*, Dec. 2016, pp. 36–39.

[61] C. Lin, J. Zhou, C. Guo, H. Song, G. Wu, and M. S. Obaidat, "TSCA: a temporal-spatial real-time charging scheduling algorithm for on-demand architecture in wireless rechargeable sensor networks," *IEEE Transactions on Mobile Computing*, vol. 17, no. 1, pp. 211–224, 2018.

[62] E. L. Souza, E. F. Nakamura, and R. W. Pazzi, "Target tracking for sensor networks: A survey," *ACM Comput. Surv.*, vol. 49, no. 2, pp. 1–31, 2016.

[63] L. Militano, M. Erdelj, A. Molinaro, N. Mitton, and A. Iera, "Recharging versus replacing sensor nodes using mobile robots for network maintenance," *Telecommunication Systems*, vol. 63, no. 4, pp. 625–642, 2016.

[64] E. Omar, P. Flocchini, and N. Santoro, "Energy restoration in a linear sensor network," in *Proceedings of 15th IEEE/ACS International Conference on Computer Systems and Applications (AICCSA)*, Nov. 2018, pp. 1–8.

[65] P. Flocchini, E. Omar, and N. Santoro, "Effective energy restoration of wireless sensor networks by a mobile robot," *International Journal of Networking and Computing*, vol. 10, no. 2, pp. 62–83, 2020.

[66] O. Aloqaily, P. Flocchini, and N. Santoro, "Achieving immortality in wireless rechargeable sensor networks using local learning," in *Proceedings of 7th IEEE International Symposium on Networks, Computers and Communications (ISNCC)*, Oct. 2020, pp. 1–6.

[67] O. I. Aloqaily, "Flexibility of decentralized energy restoration in WSNs," in *Proceedings of 12th EAI International Conference on Ad Hoc Networks (ADHOCNETS)*, 2020, pp. 1–16.

[68] W. R. Heinzelman, A. Chandrakasan, and H. Balakrishnan, "Energy-efficient communication protocol for wireless microsensor networks," in *Proceedings of 33rd Annual Hawaii International Conference on System Sciences(HICSS)*, Jan. 2000, pp. 1–10.

[69] O. Younis and S. Fahmy, "HEED: a hybrid, energy-efficient, distributed clustering approach for ad hoc sensor networks," *IEEE Transactions on Mobile Computing*, vol. 3, no. 4, pp. 366–379, 2004.

[70] X. Wu, J. Cho, B. J. D'Auriol, and S. Lee, "Sleep nodes scheduling in cluster-based heterogeneous sensor networks using ahp," in *Proceedings of 3rd International Conference on Embedded Software and Systems(ICESS)*, May 2007, p. 437–444.

[71] Y. Wu, S. Fahmy, and N. Shroff, "Optimal sleep/wake scheduling for time-synchronized sensor networks with qos guarantees," *IEEE/ACM Transactions on Networking.*, vol. 17, no. 5, pp. 1508–1521, 2009.

[72] S. Wang, K. Shih, Y. Chen, and H. Ku, "Preserving target area coverage in wireless sensor networks by using computational geometry," in *Proceedings of 11th IEEE Wireless Communication and Networking Conference(WCNC)*, Apr. 2010, pp. 1–6.

[73] R. Wan, N. Xiong, and N. T. Loc, "An energy-efficient sleep scheduling mechanism with similarity measure for wireless sensor networks," *Human-centric Computing and Information Sciences*, vol. 8, no. 141, pp. 1–22, 2018.

[74] N. M. A. Latiff, C. C. Tsimenidis, and B. S. Sharif, "Energy-aware clustering for wireless sensor networks using particle swarm optimization," in *Proceedings of 18th IEEE International Symposium on Personal, Indoor and Mobile Radio Communications(PIMRC)*, Sep. 2007, pp. 1–5.

[75] S. Lindsey and C. S. Raghavendra, "PEGASIS: Power-efficient gathering in sensor information systems," in *Proceedings of 6th IEEE Aerospace Conference(IAC)*, Mar. 2002, pp. 1–6.

[76] K. Huang, Y. Yen, and H. Chao, "Tree-clustered data gathering protocol (TCDGP) for wireless sensor networks," in *Proceedings of 1st Future Generation Communication and Networking (FGCN 2007)*, Dec. 2007, pp. 31–36.

[77] F. Kiyani, R. Babazadeh-razi, B. Talebzadeh, and S. Alizadeh, "Prolonging life time of wireless sensor network," in *Proceedings of 2nd International Conference on Advanced Computer Control (ICACC)*, vol. 2, Mar. 2010, pp. 102–105.

[78] Dan Liu, Qian Zhou, Zhi Zhang, and Baoling Liu, "Cluster-based energy-efficient transmission using a new hybrid compressed sensing in WSN," in *Proceedings of 35th IEEE Conference on Computer Communications Workshops (INFOCOM WKSHPS)*, Apr. 2016, pp. 372–376.

[79] Nguyen Duy Tan and Nguyen Dinh Viet, "SSTBC: Sleep scheduled and tree-based clustering routing protocol for energy-efficient in wireless sensor networks," in *Proceedings of 12th IEEE International Conference on Computing Communication Technologies - Research, Innovation, and Vision for Future (RIVF)*, Jan. 2015, pp. 180–185.

[80] S. Akbari, "Energy harvesting for wireless sensor networks review," in *Proceedings of 4th Federated Conference on Computer Science and Information Systems (FedCSIS)*, Sep. 2014, pp. 987–992.

[81] Haowei Bai, M. Atiquzzaman, and D. Lilja, "Wireless sensor network for aircraft health monitoring," in *Proceedings of 1st International Conference on Broadband Networks (BroadNets)*, Oct. 2004, pp. 748–750.

[82] X. Wang, V. S. Rao, R. V. Prasad, and I. Niemegeers, "Choose wisely: Topology control in energy-harvesting wireless sensor networks," in *Proceedings of 13th IEEE Annual Consumer Communications Networking Conference (CCNC)*, Jan. 2016, pp. 1054–1059.

[83] Z. Mihajlovic, A. Joza, V. Milosavljevic, V. Rajs, and M. Zivanov, "Energy harvesting wireless sensor node for monitoring of surface water," in *Proceedings of 21st International Conference on Automation and Computing (ICAC)*, Sep. 2015, pp. 1–6.

[84] S. Basagni, V. Di Valerio, G. Koutsandria, and C. Petrioli, "Wake-up radio-enabled routing for green wireless sensor networks," in *Proceedings of 86th IEEE Vehicular Technology Conference (VTC)*, Sep. 2017, pp. 1–6.

[85] X. Liu, Z. Li, and J. Wang, "How many hops are needed in multi-hop energy harvesting wireless networks," in *Proceedings of 86th IEEE Vehicular Technology Conference (VTC)*, Sep. 2017, pp. 1–6.

[86] D. Djenouri, M. Bagaa, A. Chelli, and I. Balasingham, "Energy harvesting aware minimum spanning tree for survivable wsn with minimum relay node addition,"

in *Proceedings of 17th IEEE Global Communications Workshops (GC Wkshps)*, Dec. 2016, pp. 1–6.

[87] P. Zhou, C. Wang, and Y. Yang, "Self-sustainable sensor networks with multi-source energy harvesting and wireless charging," in *Proceedings of 38th IEEE Conference on Computer Communications (INFOCOM)*, Apr. 2019, pp. 1828–1836.

[88] C. Wang, J. Li, Y. Yang, and F. Ye, "Combining solar energy harvesting with wireless charging for hybrid wireless sensor networks," *IEEE Transactions on Mobile Computing*, vol. 17, no. 3, pp. 560–576, 2018.

[89] M. S. N. Shahzad Hassan and H.-B. Jiang, "*Mobile multi-node recharging in heterogeneous wireless sensor networks*," in *Computer Science, Technology and Application*. World Scientific, 2016, pp. 234–240.

[90] Z. Mi, Y. Yang, and J. Y. Yang, "Restoring connectivity of mobile robotic sensor networks while avoiding obstacles," *IEEE Sensors Journal*, vol. 15, no. 8, pp. 4640–4650, 2015.

[91] L. He, P. Cheng, Y. Gu, J. Pan, T. Zhu, and C. Liu, "Mobile-to-mobile energy replenishment in mission-critical robotic sensor networks," in *Proceedings of 33th IEEE Conference on Computer Communications (INFOCOM)*, Apr. 2014, pp. 1195–1203.

[92] Y. Mei, C. Xian, S. Das, Y. C. Hu, and Y.-H. Lu, "Sensor replacement using mobile robots," *Computer Communications*, vol. 30, no. 13, pp. 2615 – 2626, 2007.

[93] B. Tong, G. Wang, W. Zhang, and C. Wang, "Node reclamation and replacement for long-lived sensor networks," *IEEE Transactions on Parallel Distributed Systems*, vol. 22, no. 9, pp. 1550–1563, 2011.

[94] R. Falcon, X. Li, A. Nayak, and I. Stojmenovic, "The one-commodity traveling salesman problem with selective pickup and delivery: An ant colony approach," in *Proceedings of 9th IEEE Congress on Evolutionary Computation(CEC)*, Jul. 2010, pp. 1–8.

[95] H. Dai, L. Jiang, X. Wu, D. K. Y. Yau, G. Chen, and S. Tang, "Near optimal charging and scheduling scheme for stochastic event capture with rechargeable sensors," in *Proceedings of 10th IEEE International Conference on Mobile Ad-Hoc and Sensor Systems(MASS)*, Oct. 2013, pp. 10–18.

[96] W. Xu, W. Liang, X. Lin, G. Mao, and X. Ren, "Towards perpetual sensor networks via deploying multiple mobile wireless chargers," in *Proceedings of 43rd International Conference on Parallel Processing(ICCP)*, Sep. 2014, pp. 80–89.

[97] R. Beigel, J. Wu, and H. Zheng, "On optimal scheduling of multiple mobile chargers in wireless sensor networks," in *Proceedings of the 1st International Workshop on Mobile Sensing, Computing and Communication(MSCC)*, Aug. 2014, p. 1–6.

[98] W. Liang, W. Xu, X. Ren, X. Jia, and X. Lin, "Maintaining large-scale rechargeable sensor networks perpetually via multiple mobile charging vehicles," *ACM Transactions on Sensor Networks*, vol. 12, no. 2, pp. 1–26, 2016.

[99] C. Hu and Y. Wang, "Schedulability decision of charging missions in wireless rechargeable sensor networks," in *Proceedings of 11th Annual IEEE International Conference on Sensing, Communication, and Networking (SECON)*, Jun. 2014, pp. 450–458.

[100] L. Li, Y. Xu, Z. Zhang, J. Yin, W. Chen, and Z. Han, "A prediction-based charging policy and interference mitigation approach in the wireless powered internet of things," *IEEE Journal on Selected Areas in Communications*, vol. 37, no. 2, pp. 439–451, 2019.

[101] Y. Yang, H. Li, X. Qiu, S. Guo, X. Zeng, K. Zhao, and H. Xin, "Research on lifetime prediction-based recharging scheme in rechargeable wsns," in *Proceedings*

of 14th IEEE/IFIP Network Operations and Management Symposium(NOMS), 2018, pp. 1–4.

[102] P. Flocchini, E. Omar, and N. Santoro, "Effective decentralized energy restoration by a mobile robot," in *Proceedings of 7th International Symposium on Computing and Networking (CANDAR)*, Nov. 2019, pp. 73–81.

[103] L. Xie, Y. Shi, Y. T. Hou, W. Lou, H. D. Sherali, and S. F. Midkiff, "On renewable sensor networks with wireless energy transfer: The multi-node case," in *Proceeding of 9th Annual IEEE Communications Society Conference on Sensor, Mesh and Ad Hoc Communications and Networks (SECON)*, Jun. 2012, pp. 10–18.

[104] L. Xie, Y. Shi, Y. T. Hou, W. Lou, H. D. Sherali, and S. F. Midkiff, "Multi-node wireless energy charging in sensor networks," *IEEE/ACM Transactions on Networking*, vol. 23, no. 2, pp. 437–450, 2015.

[105] N. Wang, J. Wu, and H. Dai, "Bundle charging: Wireless charging energy minimization in dense wireless sensor networks," in *Proceedings of 39th IEEE International Conference on Distributed Computing Systems (ICDCS)*, Jul. 2019, pp. 810–820.

[106] Y. Ma, W. Liang, and W. Xu, "Charging utility maximization in wireless rechargeable sensor networks by charging multiple sensors simultaneously," *IEEE/ACM Transactions on Networking*, vol. 26, no. 4, pp. 1591–1604, 2018.

[107] L. Fu, P. Cheng, Y. Gu, J. Chen, and T. He, "Minimizing charging delay in wireless rechargeable sensor networks," in *Proceedings of 32nd IEEE Conference on Computer Communications(INFOCOM)*, Jul. 2013, pp. 2922–2930.

[108] L. Fu, P. Cheng, Y. Gu, J. Chen, and T.He, "Optimal charging in wireless rechargeable sensor networks," *IEEE Transactions on Vehicular Technology*, vol. 65, no. 1, pp. 278–291, 2016.

[109] W.-Y. Lai and T.-R. Hsiang, "Wireless charging deployment in sensor networks," *MDPI Sensors*, vol. 19, no. 1, pp. 201–220, 2019.

[110] P. Chanak, I. Banerjee, and R. S. Sherratt, "Energy-aware distributed routing algorithm to tolerate network failure in wireless sensor networks," *Ad Hoc Networks*, vol. 56, no. 1, pp. 158 – 172, 2017.

[111] K.-P. Shih and C.-M. Yang, "A coverage-aware energy replenishment scheme for wireless rechargeable sensor networks," *EURASIP Journal on Wireless Communications and Networking*, vol. 2017, no. 1, pp. 217–228, 2017.

[112] W. Xu, W. Liang, X. Jia, and Z. Xu, "Maximizing sensor lifetime in a rechargeable sensor network via partial energy charging on sensors," in *Proceedings of 13th Annual IEEE International Conference on Sensing, Communication, and Networking (SECON)*, Jun. 2016, pp. 1–9.

[113] W. Xu, W. Liang, X. Jia, Z. Xu, Z. Li, and Y. Liu, "Maximizing sensor lifetime with the minimal service cost of a mobile charger in wireless sensor networks," *IEEE Transactions on Mobile Computing*, vol. 17, no. 11, pp. 2564–2577, 2018.

[114] K. Wang, L. Wang, M. S. Obaidat, C. Lin, and M. Alam, "Extending network lifetime for wireless rechargeable sensor network systems through partial charge," *IEEE Systems Journal*, vol. 15, no. 1, pp. 1–11, 2021.

[115] C. Wang, J. Li, F. Ye, and Y. Yang, "Multi-vehicle coordination for wireless energy replenishment in sensor networks," in *Proceedings of 27th IEEE International Symposium on Parallel and Distributed Processing(IPDPS)*, May 2013, pp. 1101–1111.

[116] C. Wang, J. Li, F. Ye, and Y. Yang, "NETWRAP: An NDN based real-time wireless recharging framework for wireless sensor networks," *IEEE Transactions on Mobile Computing*, vol. 13, no. 6, pp. 1283–1297, 2014.

[117] C. Hu and Y. Wang, "Minimizing the number of mobile chargers to keep large-scale wrsns working perpetually," *International Journal of Distributed Sensor Networks*, vol. 11, no. 6, pp. 1–15, 2015.

[118] C. Lin, Z. Wang, J. Deng, L. Wang, J. Ren, and G. Wu, "mTS: Temporal- and spatial-collaborative charging for wireless rechargeable sensor networks with multiple vehicles," in *Proceedings of 37th IEEE Conference on Computer Communications(INFOCOM)*, Apr. 2018, pp. 99–107.

[119] C. Xu, R.-H. Cheng, and T.-K. Wu, "Wireless rechargeable sensor networks with separable charger array," *International Journal of Distributed Sensor Networks*, vol. 14, no. 4, pp. 1–14, 2018.

[120] C. Wang, J. Li, F. Ye, and Y. Yang, "Recharging schedules for wireless sensor networks with vehicle movement costs and capacity constraints," in *Proceedings of 11th Annual IEEE International Conference on Sensing, Communication, and Networking (SECON)*, Jun. 2014, pp. 468–476.

[121] A. Madhja, S. Nikoletseas, and T. Raptis, "Distributed wireless power transfer in sensor networks with multiple mobile chargers," *Computer Networks*, vol. 80, no. 1, pp. 89–108, 2015.

[122] J. Chang and L. Tassiulas, "Maximum lifetime routing in wireless sensor networks," *IEEE/ACM Transactions on Networking*, vol. 12, no. 4, pp. 609–619, 2004.

[123] Y. Hou, Y. Shi, and H. Sherali, "Rate allocation and network lifetime problems for wireless sensor networks," *IEEE/ACM Transactions on Networking*, vol. 16, no. 2, pp. 321–334, 2008.

[124] M. Yang, N. Liu, L. Zuo, Y. Feng, M. Liu, H. Gong, and M. Liu, "Dynamic charging scheme problem with actor–critic reinforcement learning," *IEEE Internet of Things Journal*, vol. 8, no. 1, pp. 370–380, 2021.

[125] "Li-Ion rechargeable battery," Technical Handbook, p. 17, 2021. [Online]. Available: https://cdn.sparkfun.com/datasheets/Prototyping/Lithium%20Ion%20Battery%20MSDS.pdf

[126] "Panasonic Ni-MH rechargeable battery," Technical Handbook, p. 8, 2021. [Online]. Available: https://eu.industrial.panasonic.com/sites/default/pidseu/files/downloads/files/id_ni-mh_1104_e.pdf

[127] L. Xie, Y. Shi, Y. T. Hou, and A. Lou, "Wireless power transfer and applications to sensor networks," *IEEE Wireless Communications*, vol. 20, no. 4, pp. 140–145, 2013.

[128] H. Dai, X. Wu, L. Xu, G. Chen, and S. Lin, "Using minimum mobile chargers to keep large-scale wireless rechargeable sensor networks running forever," in *Proceedings of 22nd International Conference on Computer Communication and Networks (ICCCN)*, 2013, pp. 1–7.

[129] C. Lee, W. Na, G. Jang, C. Lee, and S. Cho, "Energy-efficient and delay-minimizing charging method with a multiple directional mobile charger," *IEEE Internet of Things Journal*, vol. 8, no. 10, pp. 8291–8303, 2021.

[130] J. Wang, M. Hu, C. Cai, Z. Lin, L. Li, and Z. Fang, "Optimization design of wireless charging system for autonomous robots based on magnetic resonance coupling," *AIP Advances*, vol. 8, no. 5, 2018.

[131] C. Jiang, F. Liu, J. Li, P. LV, and W. Xiao, "Mobile energy replenishment scheduling based on quantum-behavior particle swarm optimization," in *Proceedings of 39th Chinese Control Conference (CCC)*, Jul. 2020, pp. 5253–5258.

[132] S. Tabibi and A. Ghaffari, "Energy-efficient routing mechanism for mobile sink in wireless sensor networks using particle swarm optimization algorithm," *Wireless Personal Communications*, vol. 104, no. 1, pp. 199–216, 2019.

[133] Y. Fei and H. Lv, "Design of the solar-driven module on modular mobile robot," in *Proceedings of 19th International Conference on Mechatronics and Machine Vision in Practice (M2VIP)*, 2012, pp. 470–473.

[134] R. Mukherjee, P. Ganguly, and R. Dahiya, "Bioinspired distributed energy in robotics and enabling technologies," *Advanced Intelligent Systems*, vol. 3, 2021.

[135] N. Ramsaroop, O. Olugbara, and E. Joubert, "Exploring energy harvesting technology for wireless charging of mobile device batteries," in *Proceedings of 1st Conference on Information Communication Technology and Society (ICTAS)*, Mar. 2017, pp. 1–5.

[136] H. Huang, C. Li, F. Liu, H. Lu, and L. Li, "Mobile data gathering and charging in wireless rechargeable sensor networks," in *Proceedings of 8th International Conference on Cyber-Enabled Distributed Computing and Knowledge Discovery*, Oct. 2018, pp. 378–3786.

[137] T. D. Nguyen, S. Chu, B. Liu, C. Chen, H. S. Dang, and T. Perumal, "Mobile charging and data gathering in multiple sink wireless sensor networks: How and why," in *Proceedings of 7th International Conference on System Science and Engineering (ICSSE)*, Jul. 2017, pp. 550–553.